

ACCELERATOR LABORATORY
ADVANCED RESEARCH CENTER FOR BEAM SCIENCE
INSTITUTE FOR CHEMICAL RESEARCH
KYOTO UNIVERSITY



High-resolution Surface Inspection Camera for Sc Cavities (with introduction of recent activities)

Y. Iwashita, et al., Kyoto U.



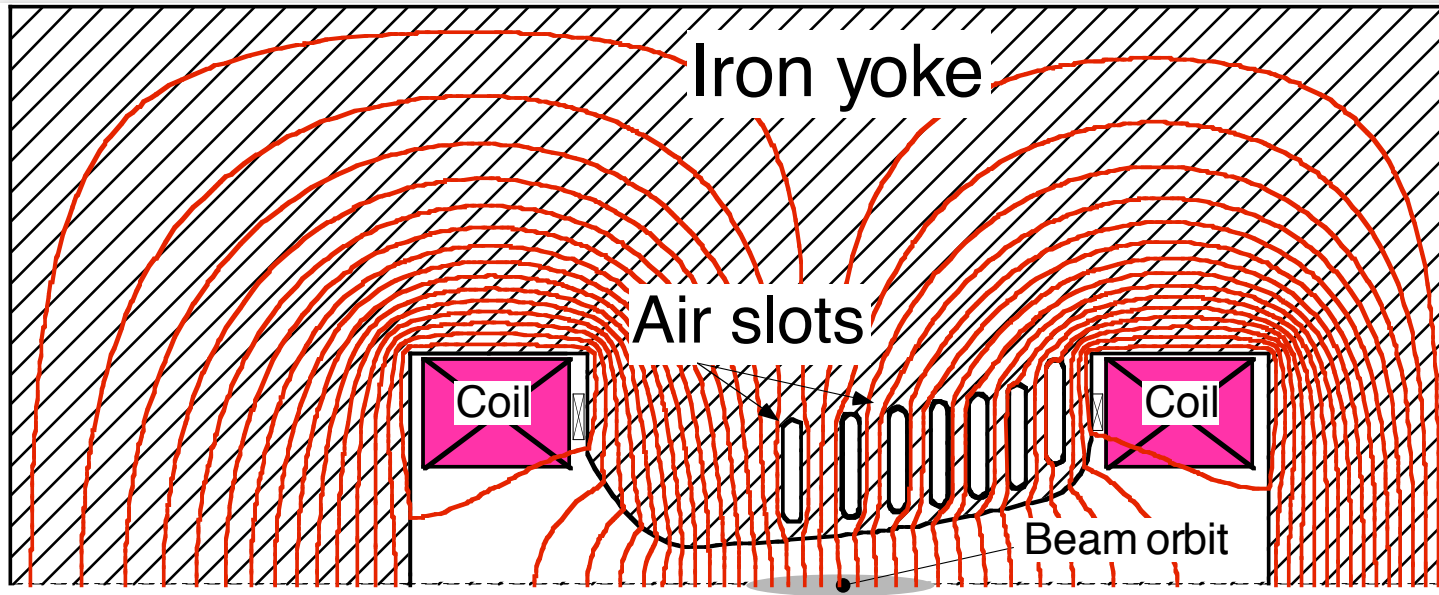
Introduction of Recent Activities

	ILC	JPARC	Small Neutron Source	Misc.
RF	Cavity Inspection	Untuned Cavity (Start of FINEMET)	ECR Ion Source, RFQ	Skin Effect PISCES-II (2.5D-RF code)
Permanent Magnets/ Magnets	PMQ – Final Focus, PMO – Tail Folding, QEX1		ECR PM, LEBT	Flux Density Equalizer for Gradient Dipoles, InterPole

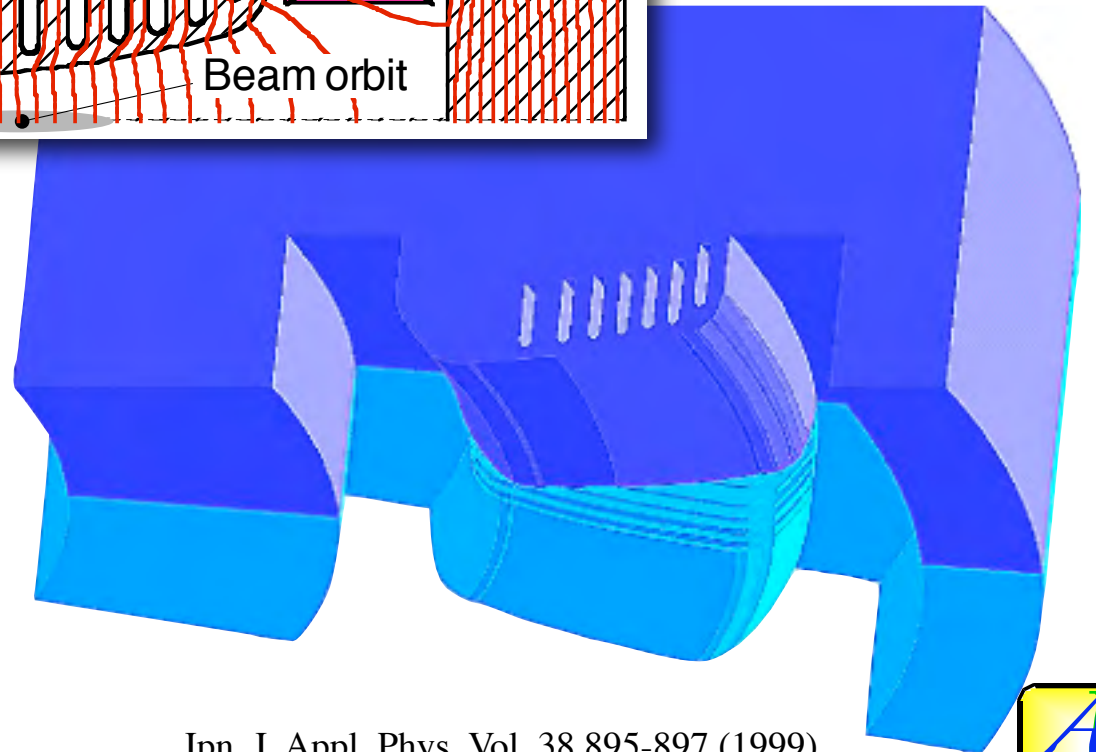
Introduction of Recent Activities

	ILC	JPARC	Small Neutron Source	Misc.
RF	Cavity Inspection	Untuned Cavity (Start of FINEMET)	ECR Ion Source, RFQ	Skin Effect PISCES-II (2.5D-RF code)
Permanent Magnets/ Magnets	PMQ – Final Focus, PMO – Tail Folding, QEX1		ECR PM, LEBT	Flux Density Equalizer for Gradient Dipoles, InterPole

Flux Density Equalizer



Combined
Function Triplet
Magnet
(1997)



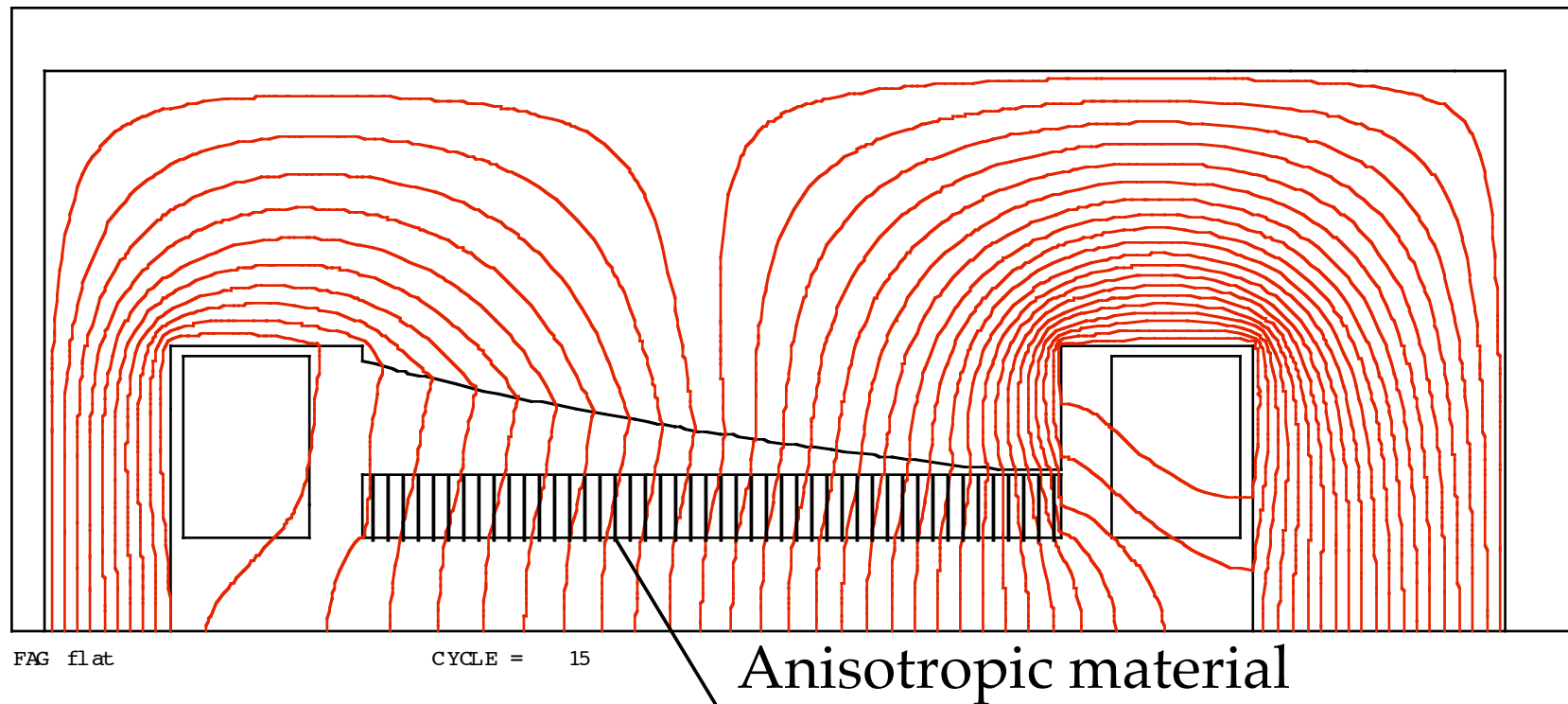
Flux Density Equalizer



Equal Operation Point.

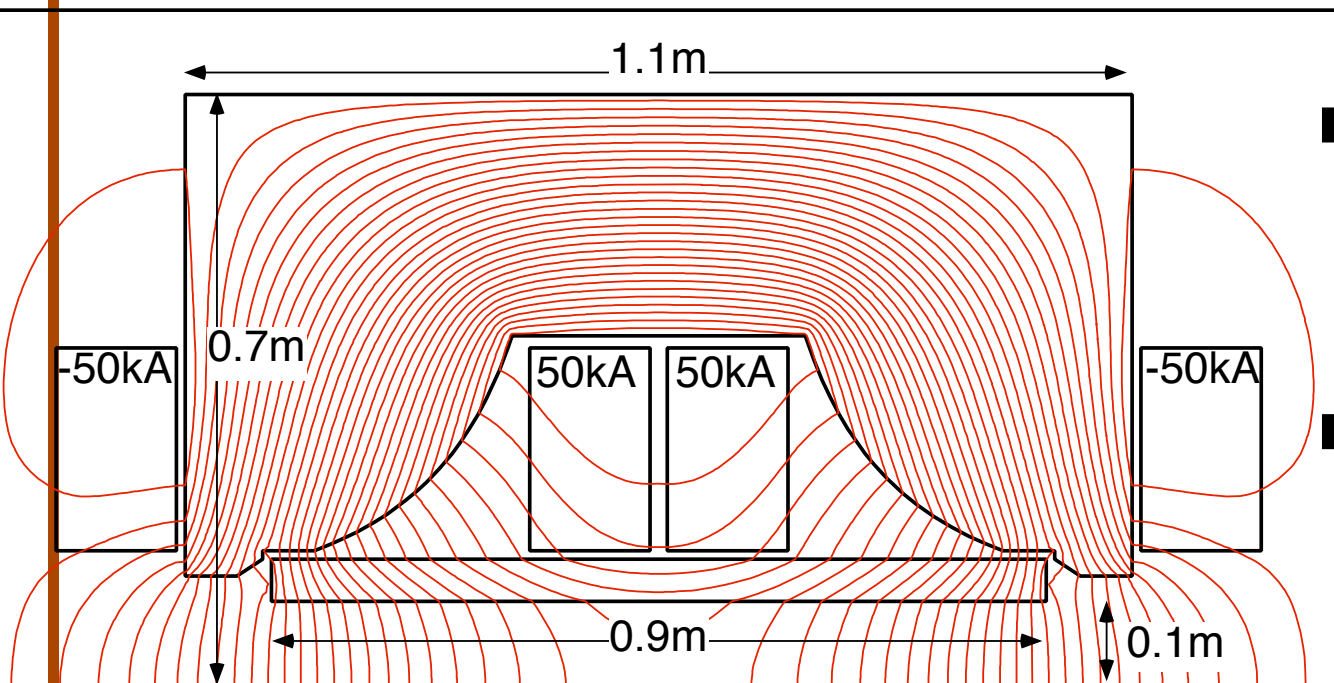


Wide Excitation Range.



Stack Si steel sheets.
packing factor=0.5 $\rightarrow \mu_r=2$

Flat Gapped Q-magnet

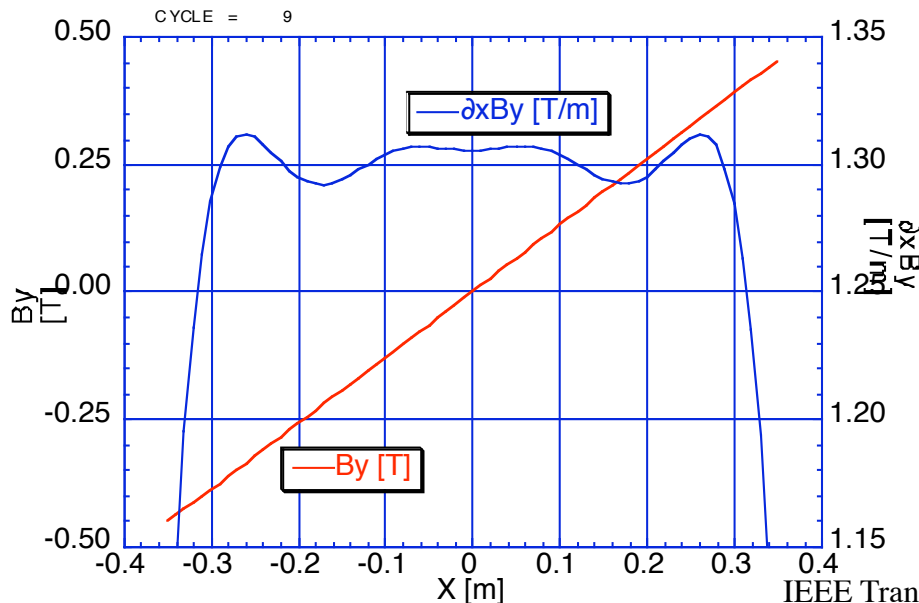


➔ Extreme application

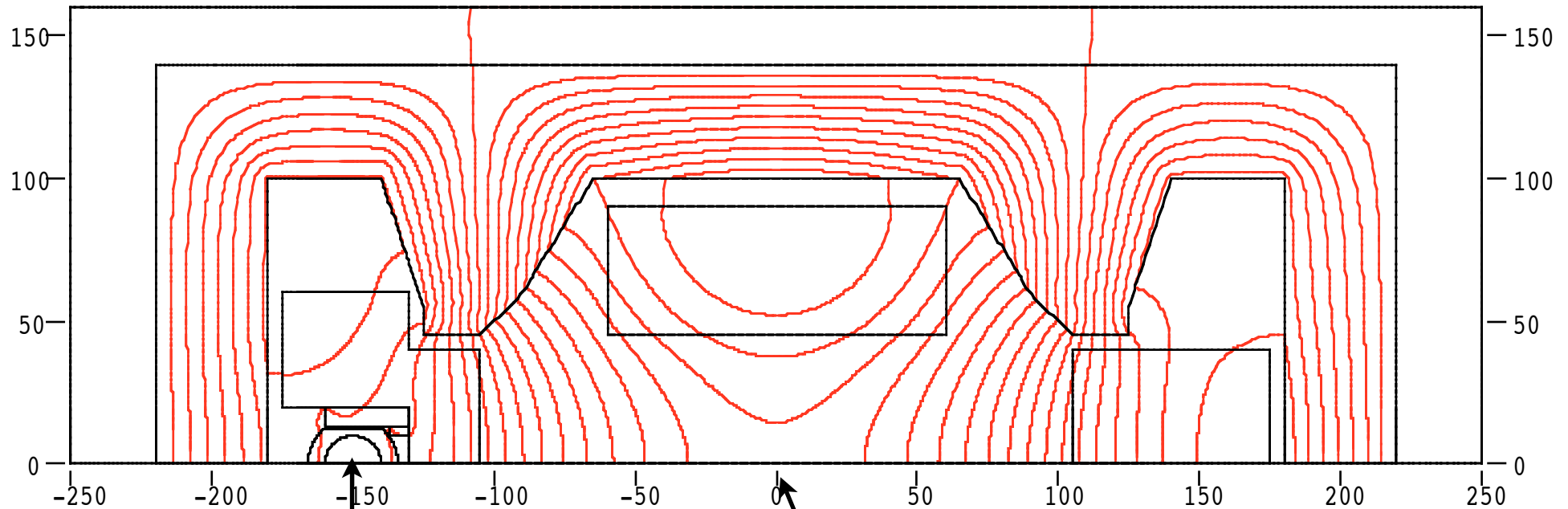
➔ Uniform (short) Fringe Effect

➔ Suitable for short Qauds

➔ Short fringing region



QEX1 for 2mrad X'ing Angle



Incoming Beam

Outgoing Beam
position

Introduction of Recent Activities

	ILC	JPARC	Small Neutron Source	Misc.
RF	Cavity Inspection	Untuned Cavity (Start of FINEMET)	ECR Ion Source, RFQ	Skin Effect PISCES-II (2.5D-RF code)
Permanent Magnets/ Magnets	PMQ – Final Focus, PMO – Tail Folding, QEX1		ECR PM, LEBT	Flux Density Equalizer for Gradient Dipoles, InterPole



Introduction of Recent Activities

	ILC	JPARC	Small Neutron Source	Misc.
RF	Cavity Inspection	Untuned Cavity (Start of FINEMET)	ECR Ion Source, RFQ	Skin Effect <i>PISCES-II</i> (2.5D-RF code)
Permanent Magnets/ Magnets	PMQ – Final Focus, PMO – Tail Folding, QEX1		ECR PM, LEBT	Flux Density Equalizer for Gradient Dipoles, InterPole



Mitigation of Power Loss due to Skin Effect

A. M. Clogston, Reduction of Skin-Effect Losses by the Use of Laminated Conductors, Proc. of the IRE, 39-7, July 1951, pp.767-782

Reduction of Skin-Effect Losses by the Use of Laminated Conductors*

A. M. CLOGSTON†, SENIOR MEMBER, IRE

(Copyright 1951, American Telephone & Telegraph Company)

Summary—It has recently been discovered that it is possible to reduce skin effect losses in transmission lines by properly laminating the conductors and adjusting the velocity of transmission of the waves. The theory for such laminated transmission lines is presented in the case of planar systems for both infinitesimally thin laminae and laminae of finite thickness. A transmission line completely filled with laminated material is discussed. An analysis is given of the modes of transmission in a laminated line, and of the problem of terminating such a line.

I. INTRODUCTION

IT HAS LONG been recognized that an electromagnetic wave propagating in the vicinity of an electrical conductor can penetrate only a limited distance into the interior of the material. This phenomenon is known as "skin effect" and is usually measured by a so-called "skin depth" δ . If y is measured from the surface of a conductor into its depth, the amplitude of the electromagnetic wave and the accompanying current density decreases as $e^{-y/\delta}$, provided the conductor is several times δ in thickness, so that for $y=\delta$ the amplitude has fallen to $1/e=0.367$ times its value at the surface. The skin depth δ is given by

$$\delta = \sqrt{\frac{2}{\omega\mu\sigma}}, \quad (1)$$

* This is one of a class of papers published through arrangements with certain other journals. It is appearing also in the July, 1951, issue of the *Bell System Technical Journal*.

† Bell Telephone Laboratories, Inc., Murray Hill, N. J.

where σ is the conductivity of the material, μ is its permeability, and ω is 2π times the frequency f under consideration. Throughout this paper rationalized mks units are used.

From one point of view, skin effect serves a most useful purpose; for instance, in shielding electrical equipment or reducing cross talk between communication circuits. On the other hand, the effect severely limits the high-frequency performance of many types of electrical apparatus, including in particular the various kinds of transmission lines.

Surprisingly enough, it has been discovered that it is possible, within limits, to increase the distance to which an electromagnetic wave penetrates into a conducting material. This is done essentially by fabricating the conductor of many insulated laminae or filaments of conducting material arranged parallel to the direction of current flow. If the transverse dimensions of the laminae or filaments are small compared to the skin depth δ at the frequency under consideration, and if the velocity of the electromagnetic wave along the conductor is close to a certain critical value, the wave will penetrate into the composite conductor a distance great enough to include a thickness of conducting material many skin depths deep. Physically speaking, the lateral change of the wave through the conducting regions is very nearly cancelled by the change through the insulating regions.

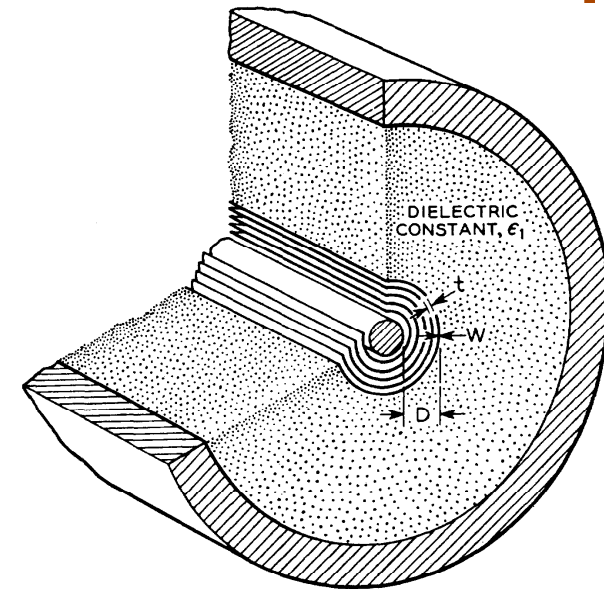
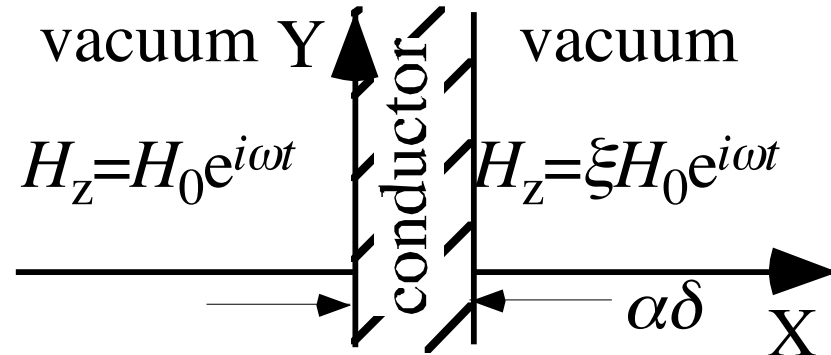


Fig. 1—Laminated transmission line.

EM Field in a Thin Foil Conductor

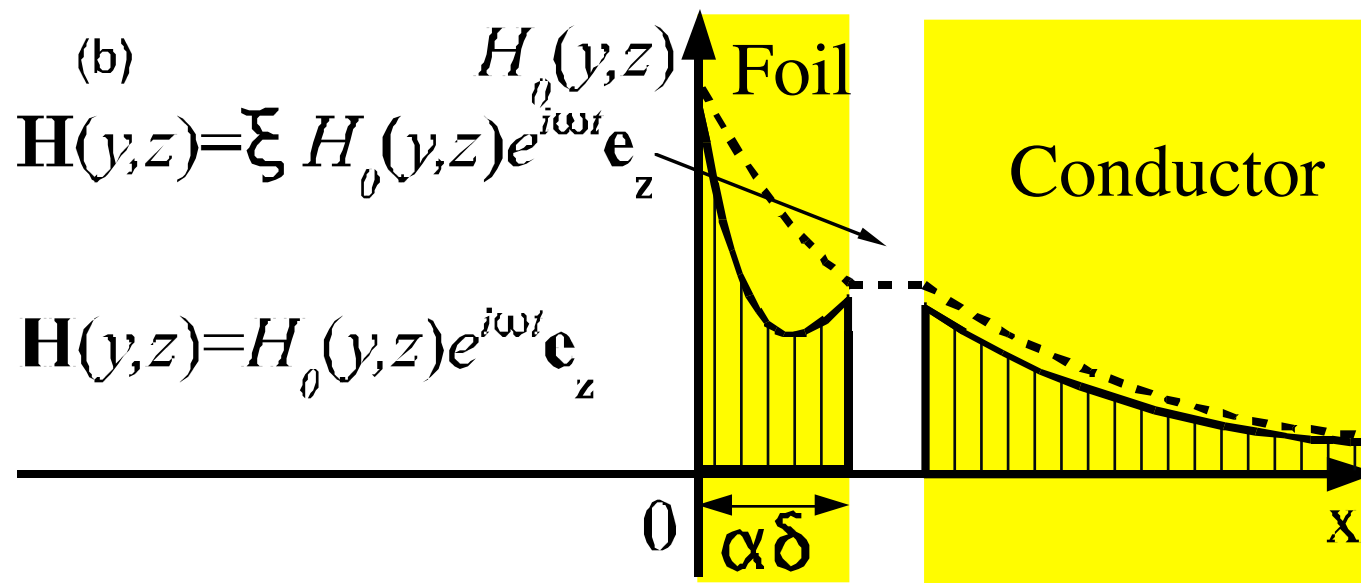
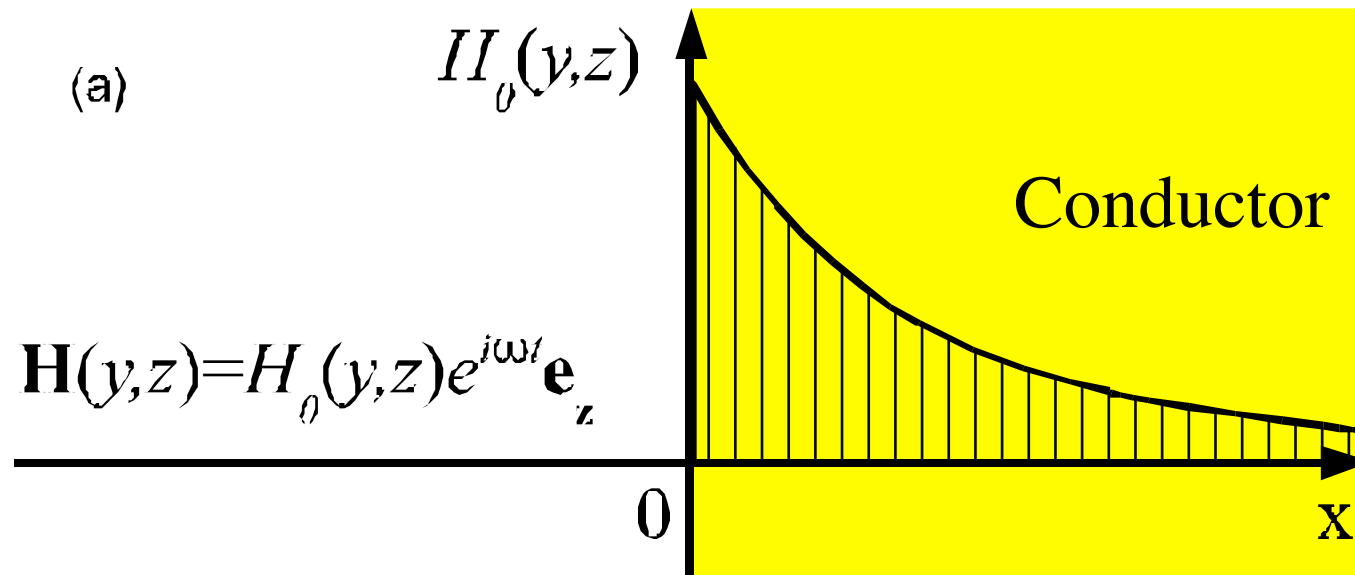


$$j(x) = H_z(0) \left(j_f e^{-(1+i)x/\delta} + j_b e^{-(1+i)(\alpha\delta - x)/\delta} \right)$$

$$j_f = \frac{(1+i)e^{(1+i)\alpha} \left(e^{(1+i)\alpha} - \xi \right)}{\delta \left(e^{2(1+i)\alpha} - 1 \right)}, \quad j_b = \frac{(1+i)e^{(1+i)\alpha} \left(\xi e^{(1+i)\alpha} - 1 \right)}{\delta \left(e^{2(1+i)\alpha} - 1 \right)}.$$

Superposition of left and right traveling waves.

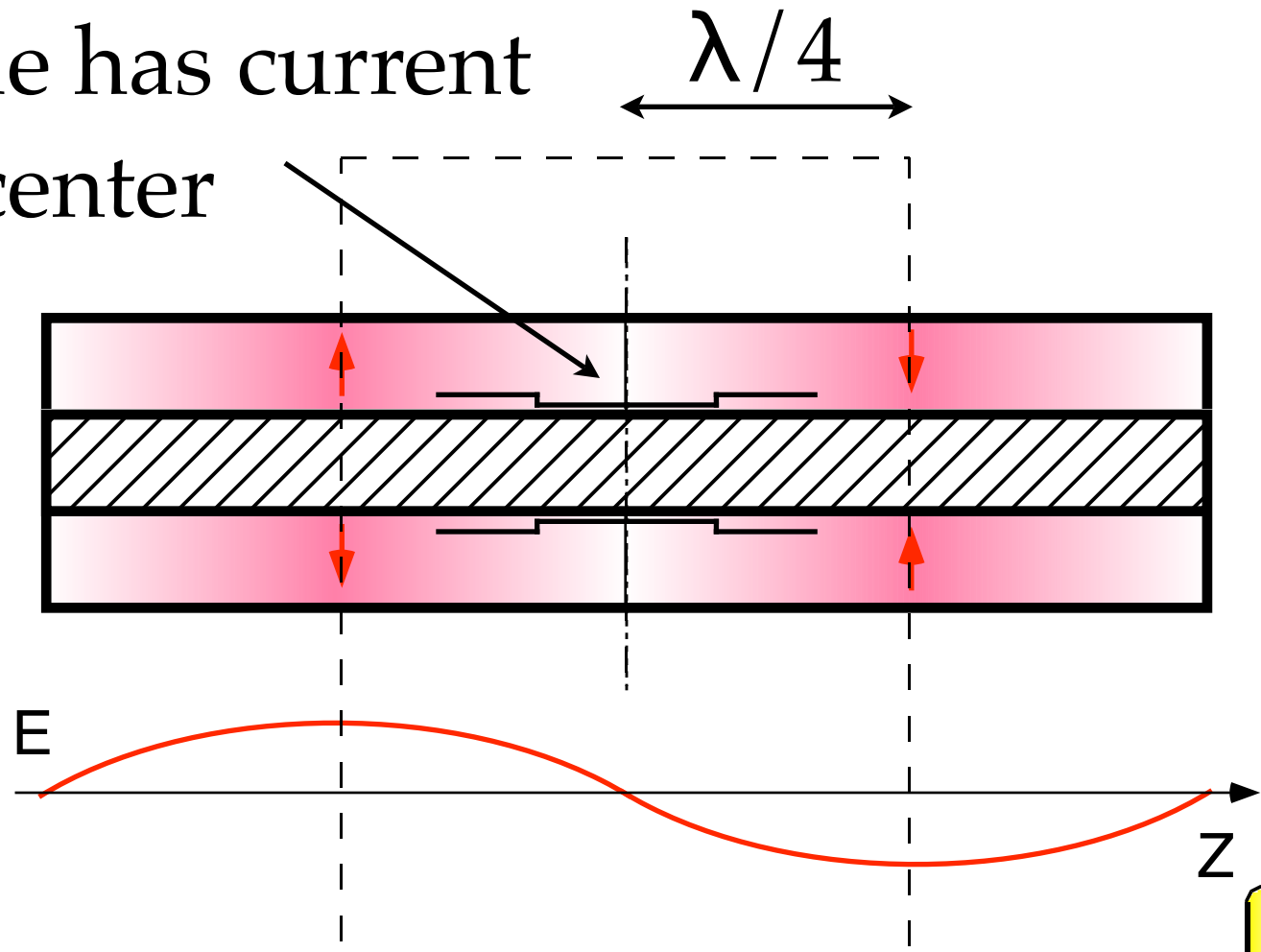
Magnetic Field(current)distribution



How to re-distribute the currents?

Experiment with coaxial cavity (Simple Cavity Structure)

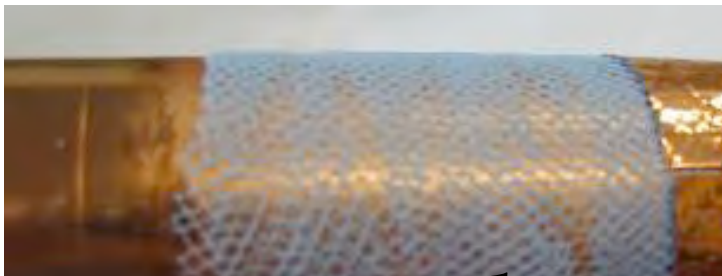
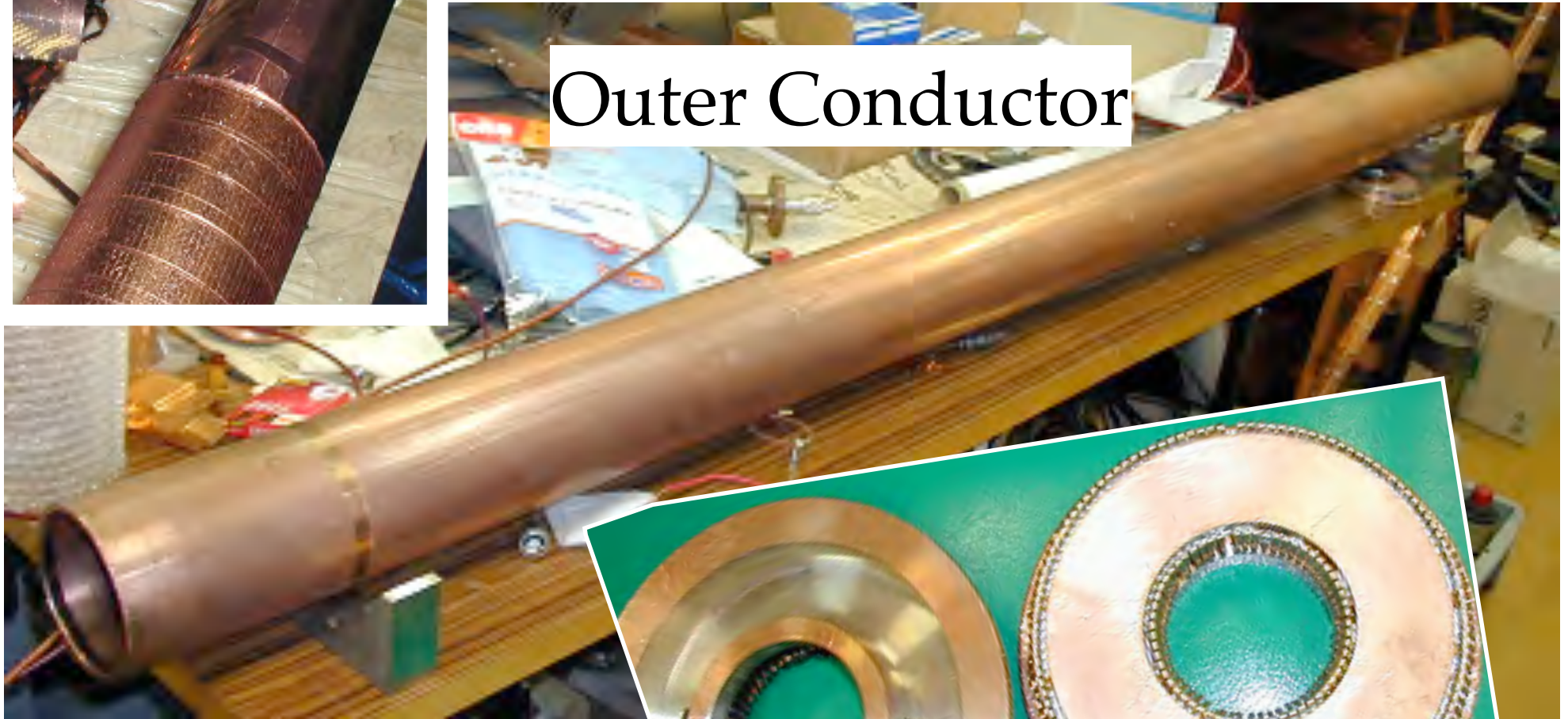
Second Mode has current
peak at the center



Inner Conductor



Outer Conductor

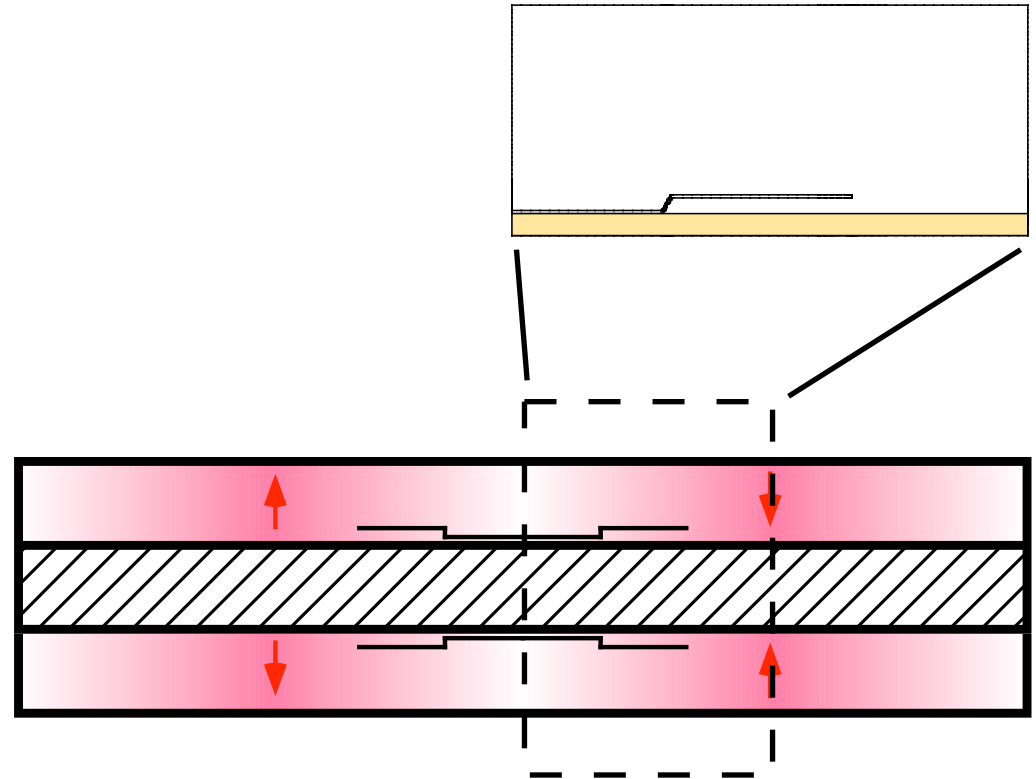
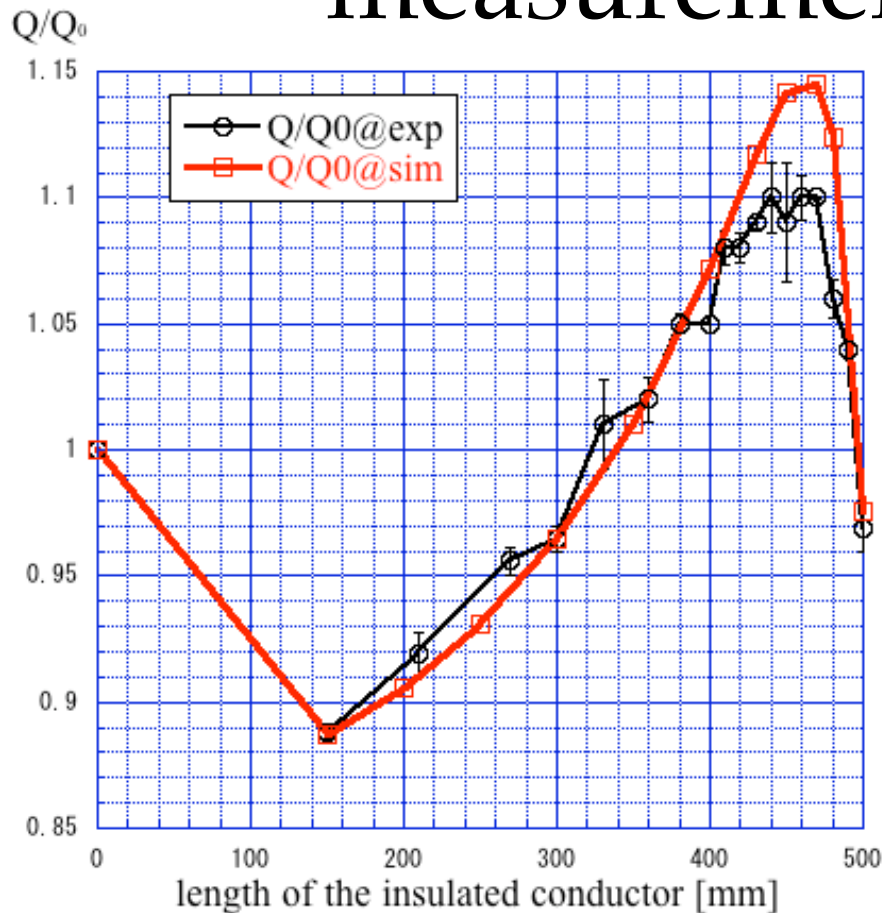


PE mesh



End Plates

Comparison between measurements and CFISH

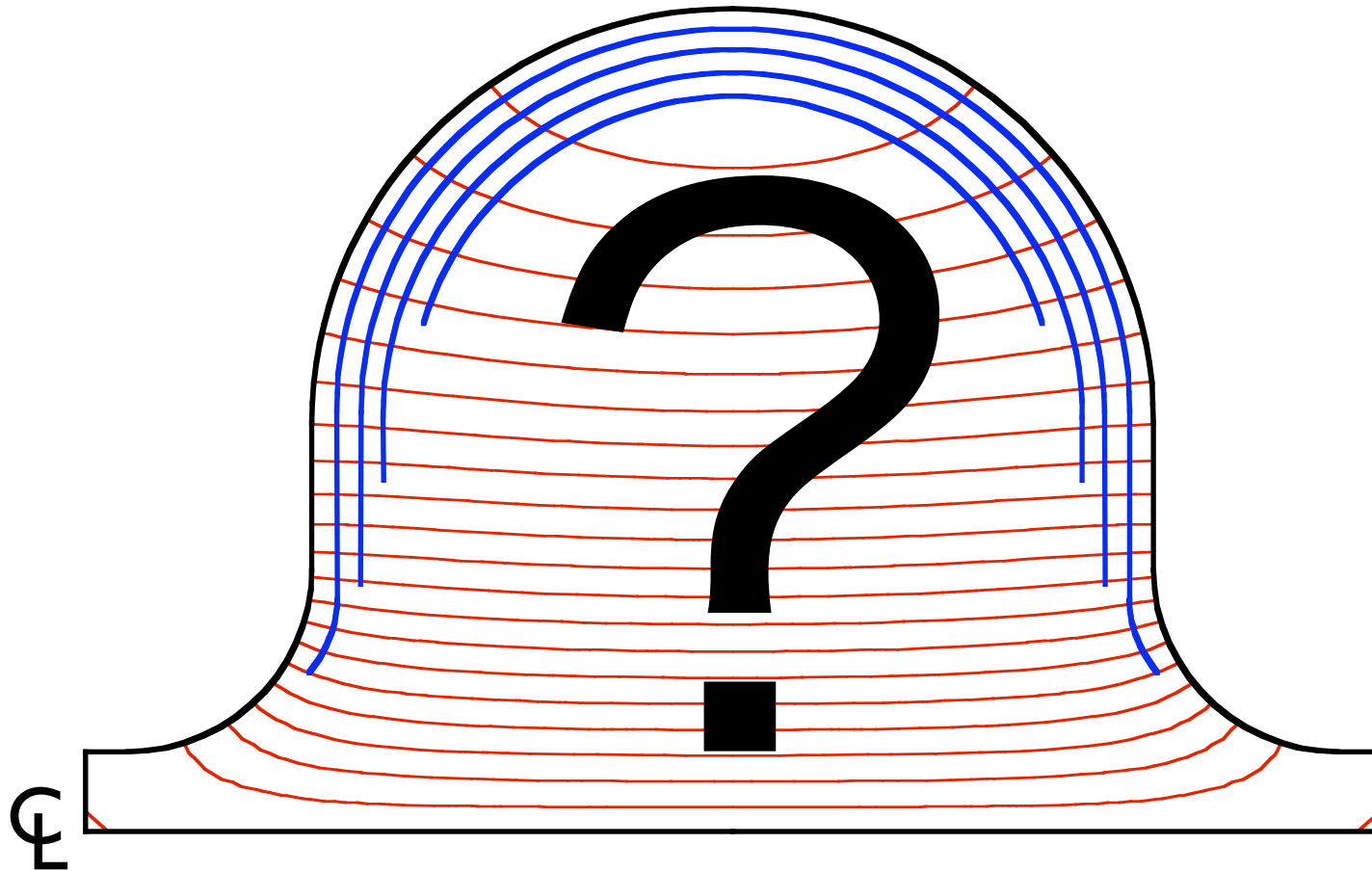


CFISH : Complex version of SUPERFISH

Agrees within a few %.

Future Target

But needs $\epsilon < 1$ material ...



Multi-layer Coated Cavity

Introduction of Recent Activities

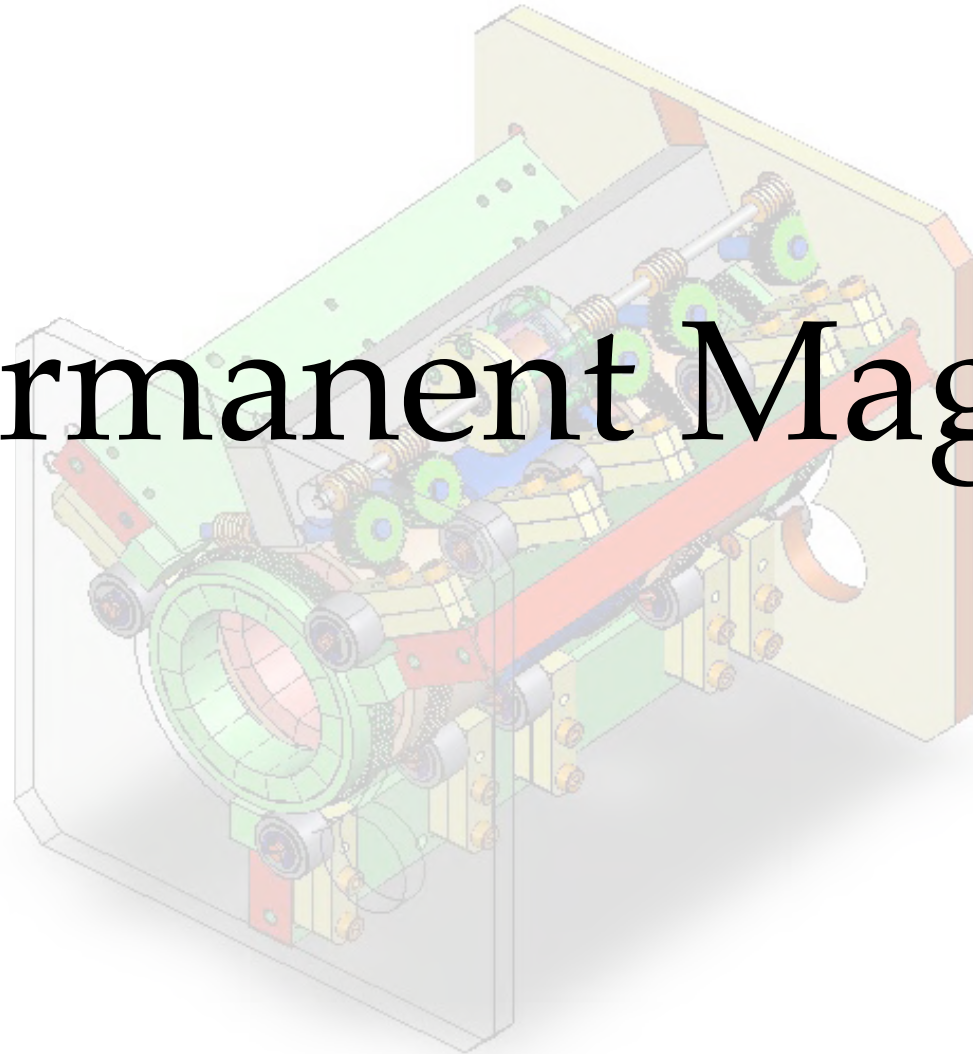
	ILC	JPARC	Small Neutron Source	Misc.
RF	Cavity Inspection	Untuned Cavity (Start of FINEMET)	ECR Ion Source, RFQ	Skin Effect PISCES-II (2.5D-RF code)
Permanent Magnets/ Magnets	PMQ – Final Focus, PMO – Tail Folding, QEX1		ECR PM, LEBT	Flux Density Equalizer for Gradient Dipoles, InterPole

Introduction of Recent Activities

	ILC	JPARC	Small Neutron Source	Misc.
RF	Cavity Inspection	Untuned Cavity (Start of FINEMET)	ECR Ion Source, RFQ	Skin Effect PISCES-II (2.5D-RF code)
Permanent Magnets/ Magnets	PMQ – Final Focus, PMO – Tail Folding, QEX1		ECR PM, LEBT	Flux Density Equalizer for Gradient Dipoles, InterPole



Permanent Magnets



Permanent Magnet Study Short History

2002~2005 First R&D program for FFQ

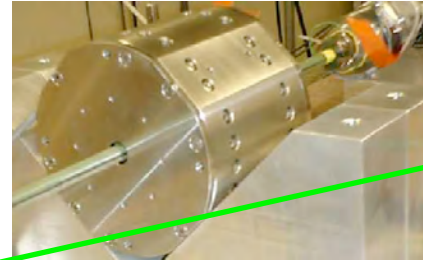
Permanent Magnet Quadrupole for Final Focus
Lens in a Linear Collider

2002 Fixed strength PMQ

2003 Adjustable PMQ (double ring)

2004 Measurement and fine tuning

2005 Higher gradient at small bore



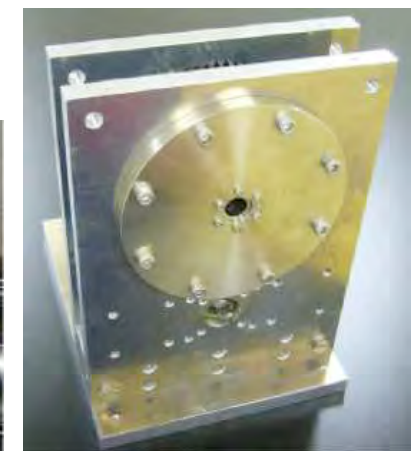
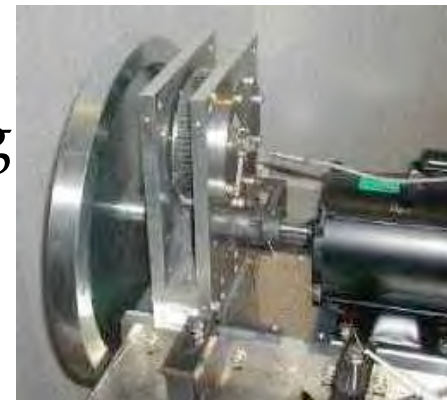
2006~2009 Second R&D program

Development and Application of PMQ for Linear
Collider and Neutron optics

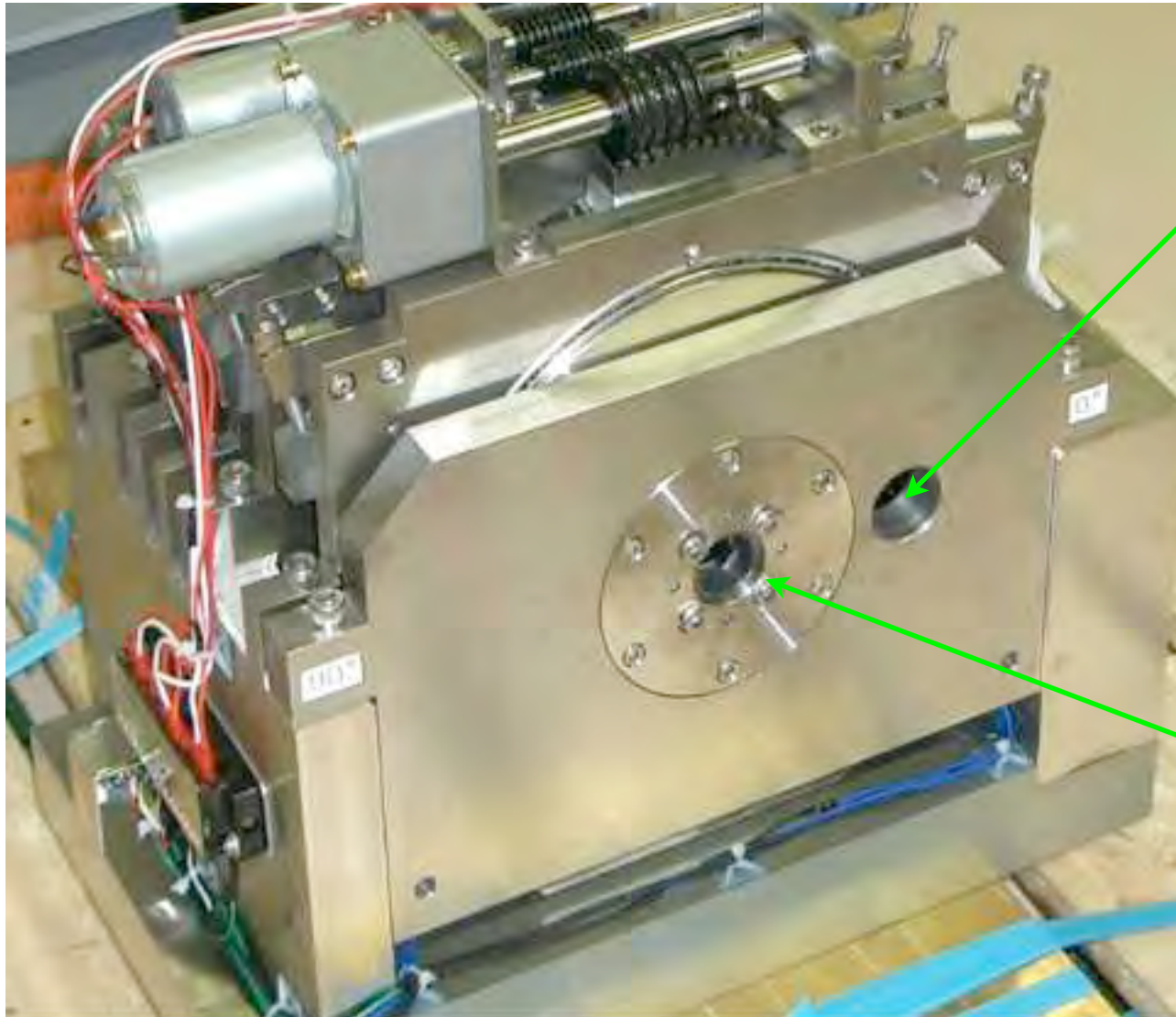
2006 Half scale Model of Rapid Cycling
Sextupole

2007~Adjustable PMQ (2nd model)

2008 ...



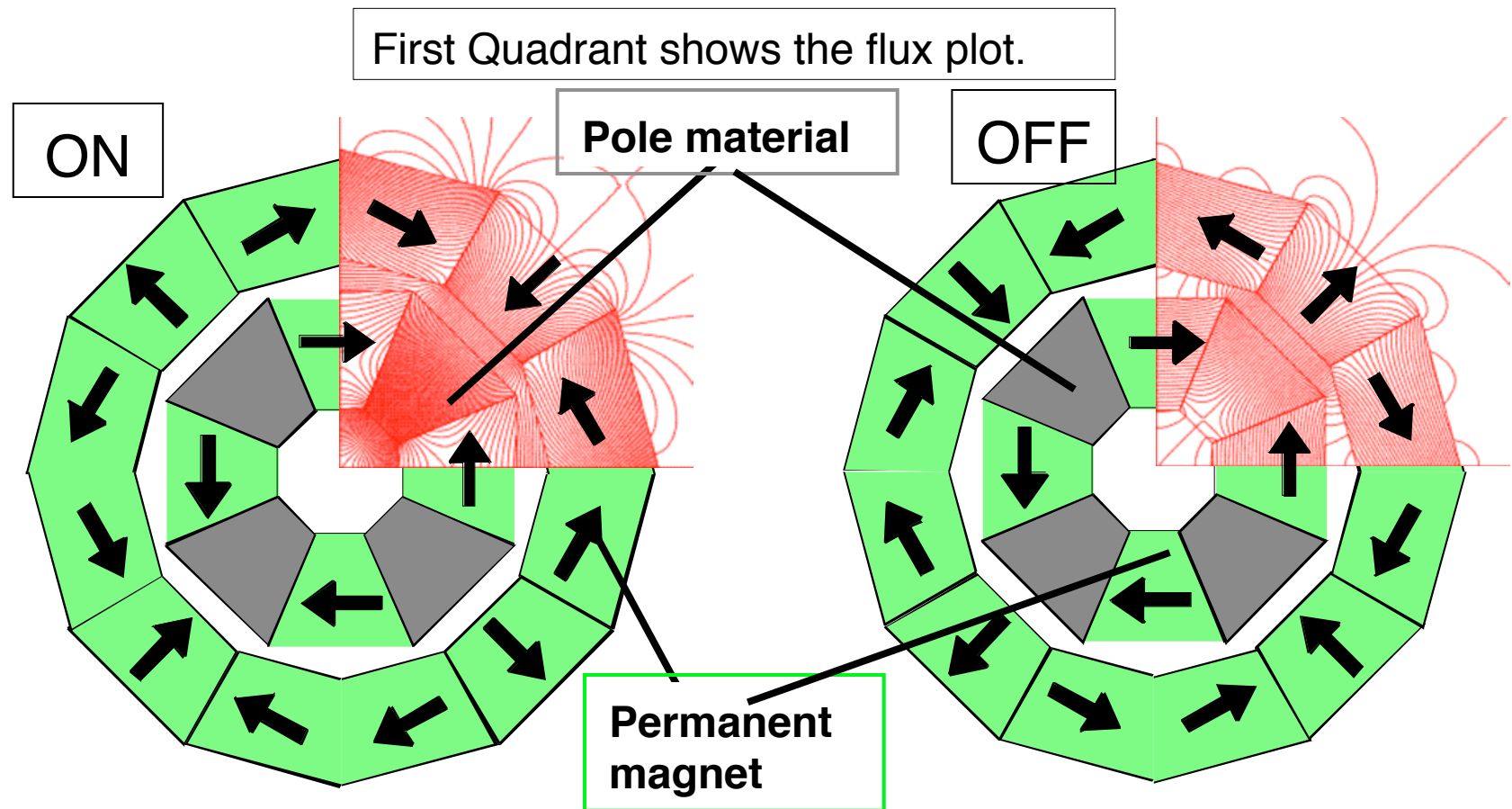
The 20mr Variable FFQ Magnet



hole for
outgoing
beam

hole for
incoming
beam

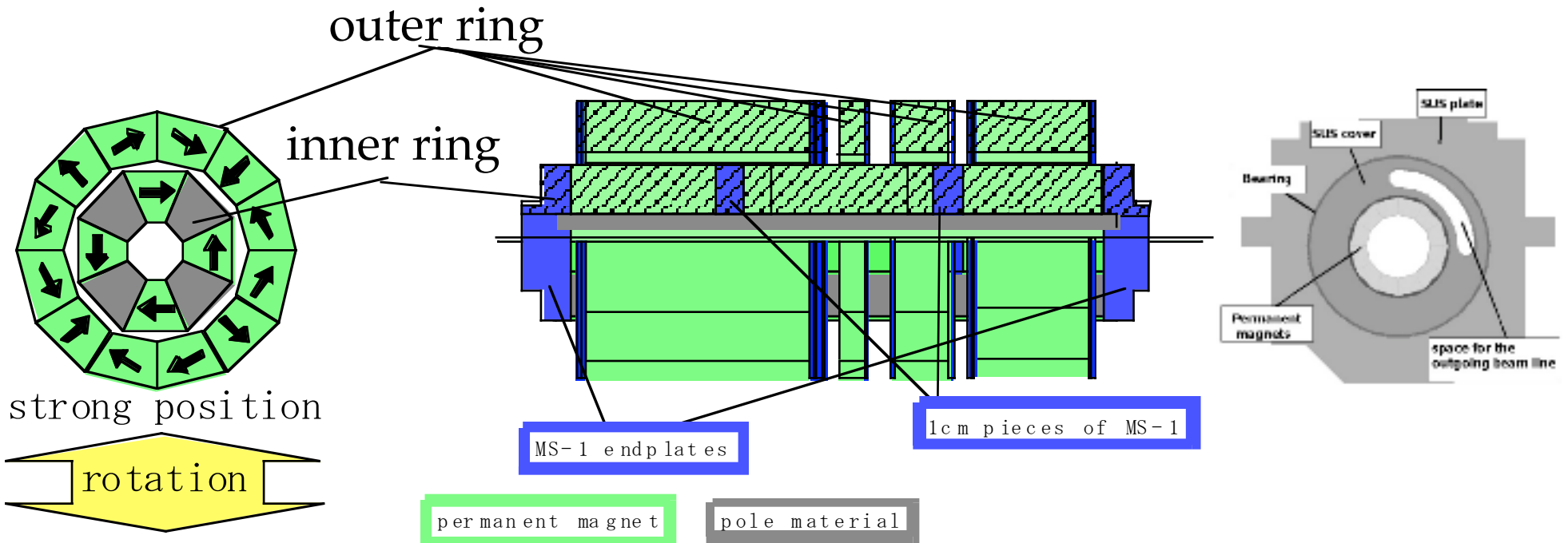
Double Ring Structure



The double ring structure

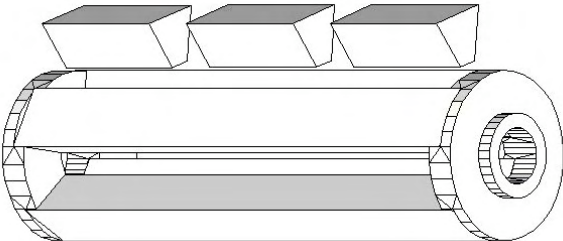
PMQ is split into inner ring and outer ring. Only the outer ring is rotated 90° around the beam axis to vary the focal strength.

Adjustable Permanent Magnet Quadrupole

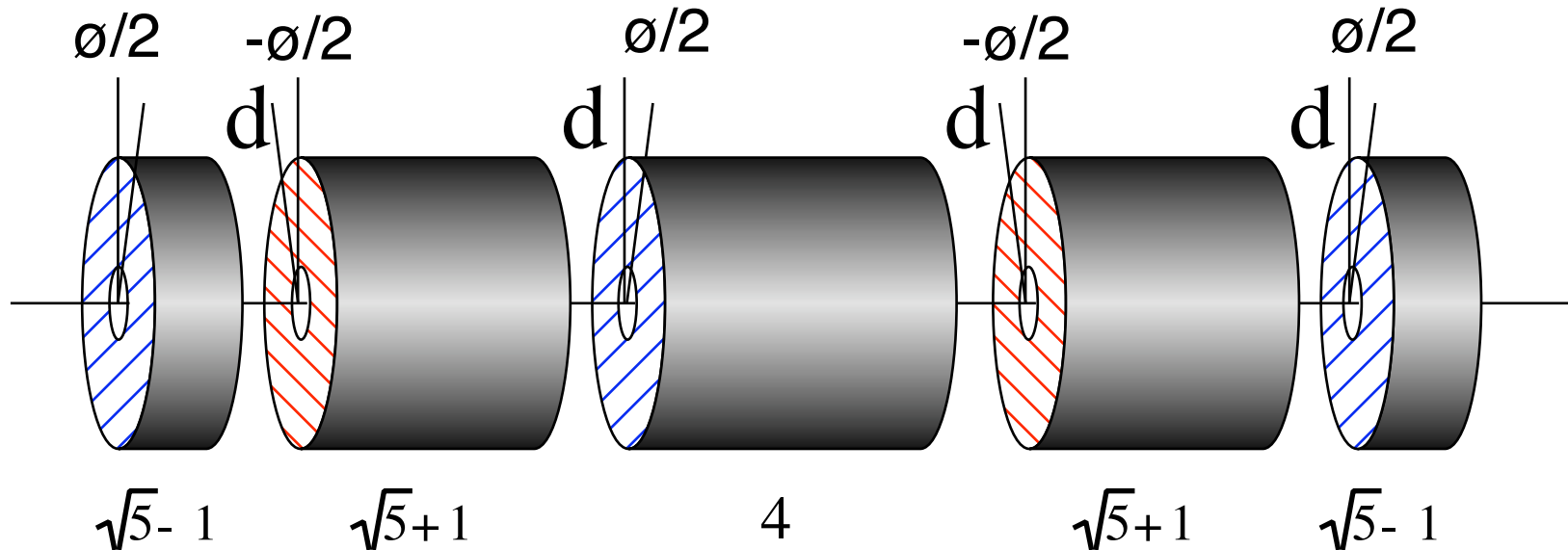


The PMQ is composed of an inner ring and four outer rings (Double Ring Structure). Only the outer rings are rotated in order to change the integrated gradient. The fixed inner ring suppresses any errors caused by rotation of outer rings.

Permanent Magnet (NEOMAX38AH)



Gluckstern's skewless variable PMQ

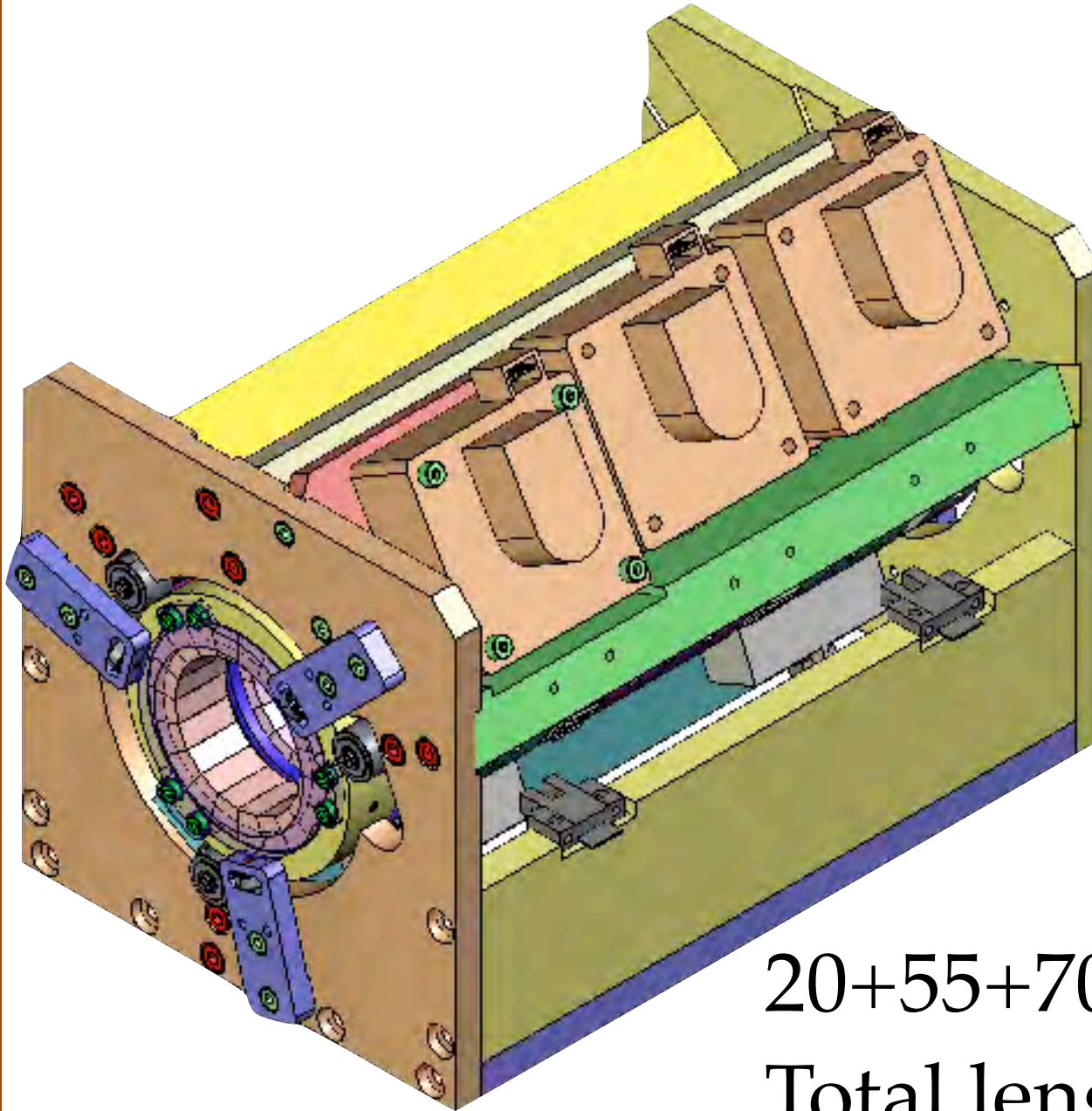


$$M = R \cdot M_2 \cdot R^{-2} \cdot M_1 \cdot R^2 \cdot M_0 \cdot R^{-2} \cdot M_1 \cdot R^2 \cdot M_2 \cdot R^{-1}$$

$$4 \times 4 \text{ matrix: } M = \begin{pmatrix} M_{xx} & O^5 \\ O^5 & M_{yy} \end{pmatrix} \text{ when } d=0.$$

R.L. Gluckstern and R.F. Holsinger: Adjustable Strength REC Quadrupoles, IEEE Trans. Nucl. Sci., Vol. NS-30, NO. 4, August 1983, http://epaper.kek.jp/p83/PDF/PAC1983_3326.PDF

One Module

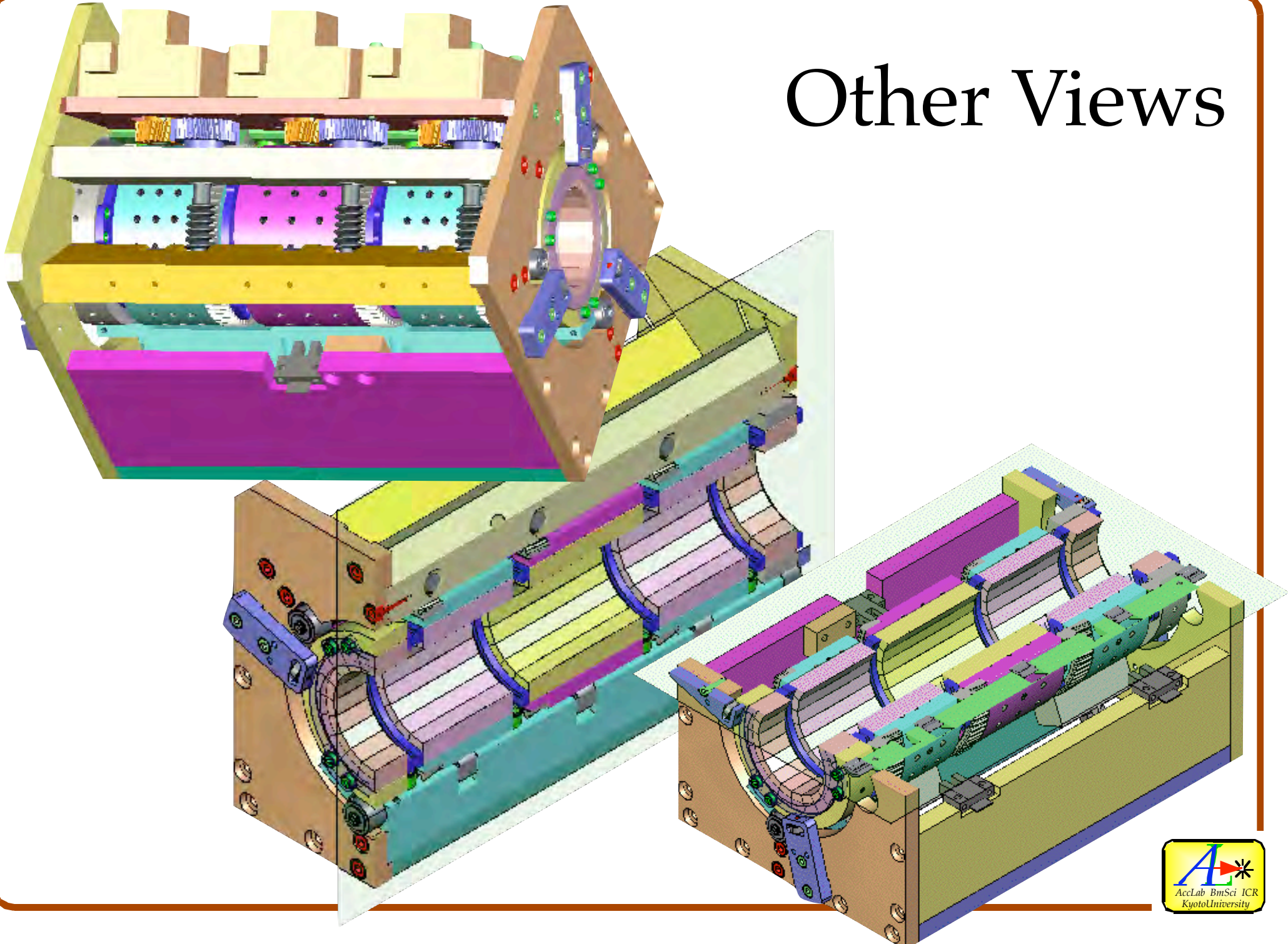


Supersonic
Motor
(nonmagnetic)

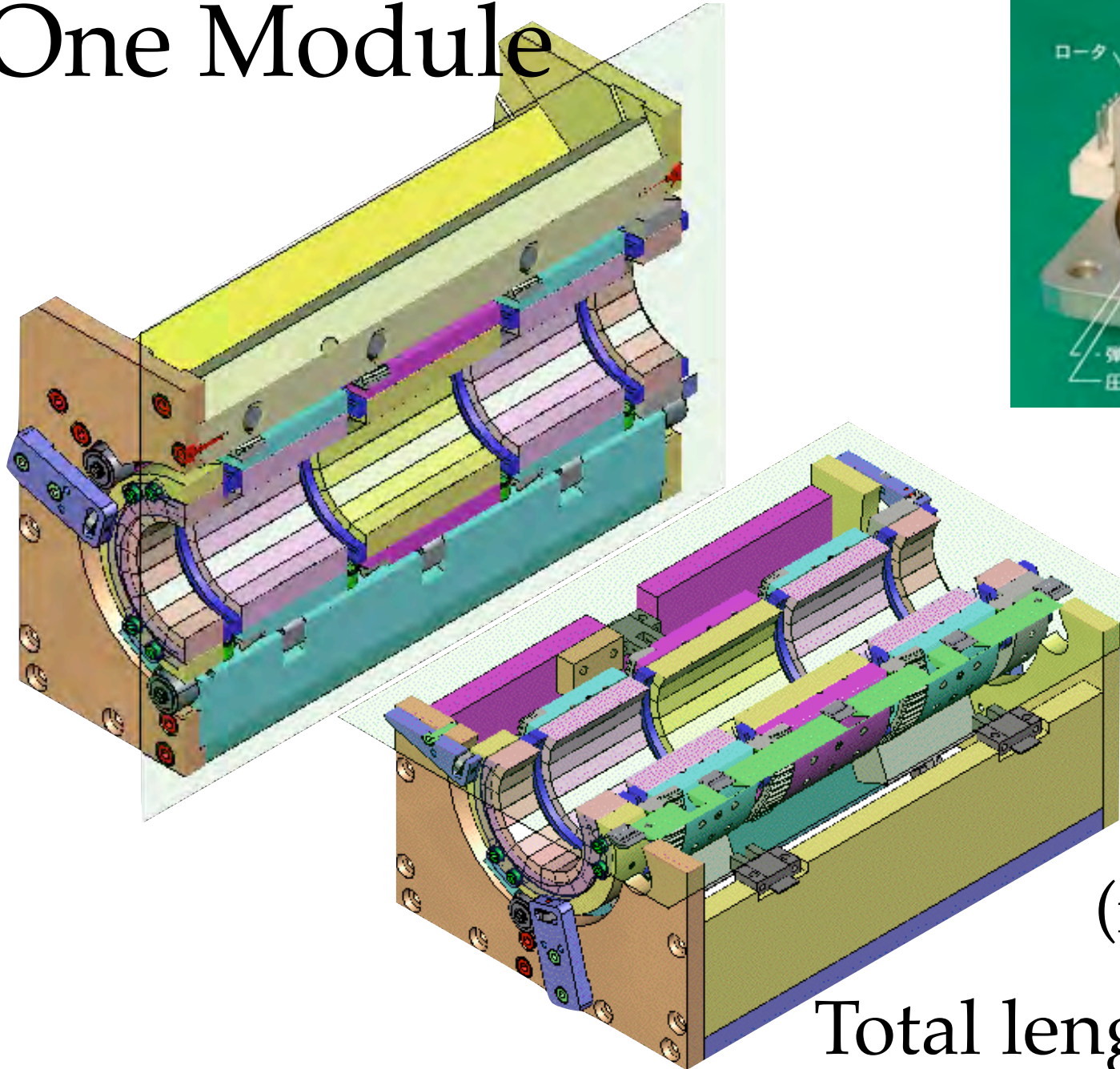
$$20+55+70+55+20 = 220\text{mm}$$

Total length is 260mm

Other Views



One Module

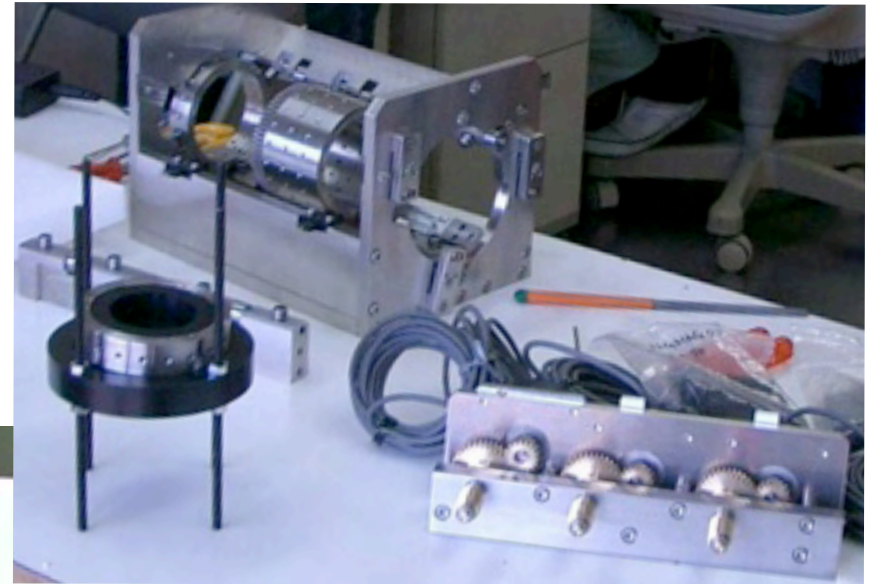
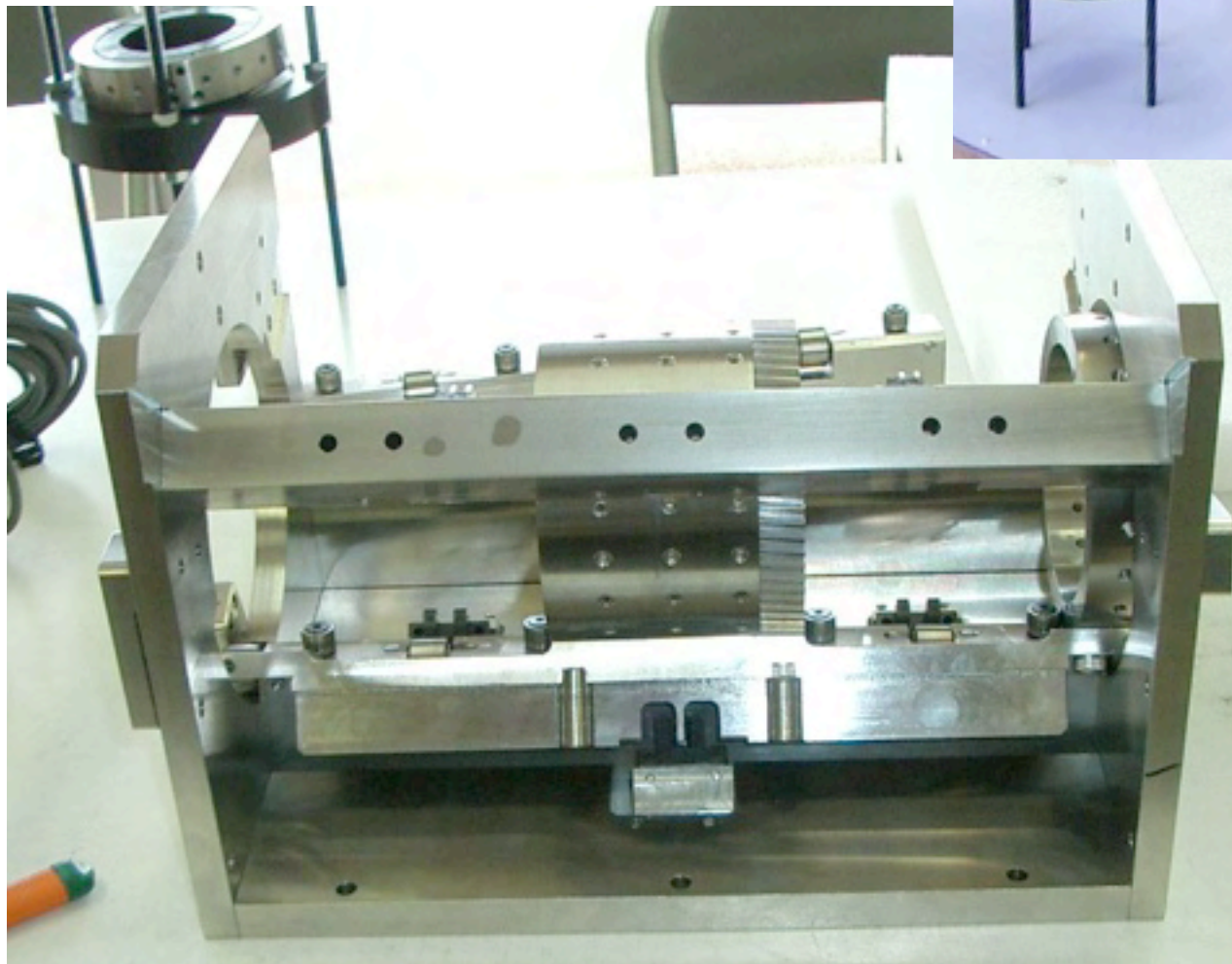


Supersonic
Motor
(non-magnetic)

Total length: 260mm

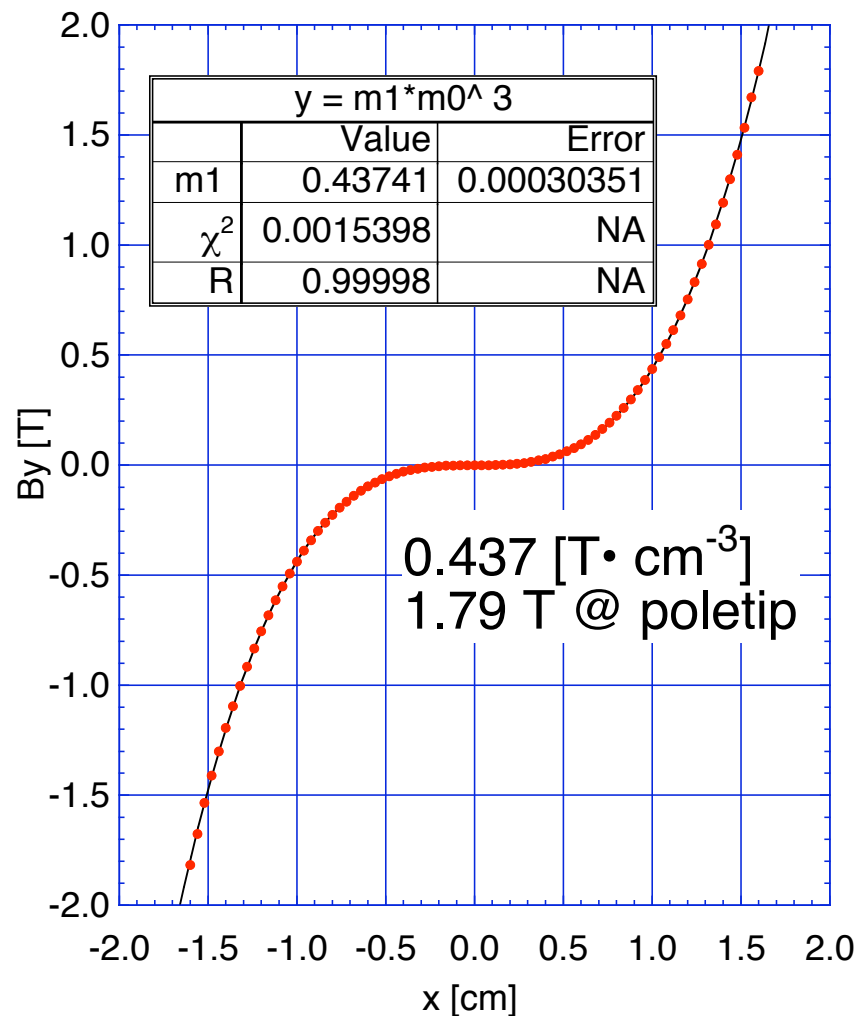
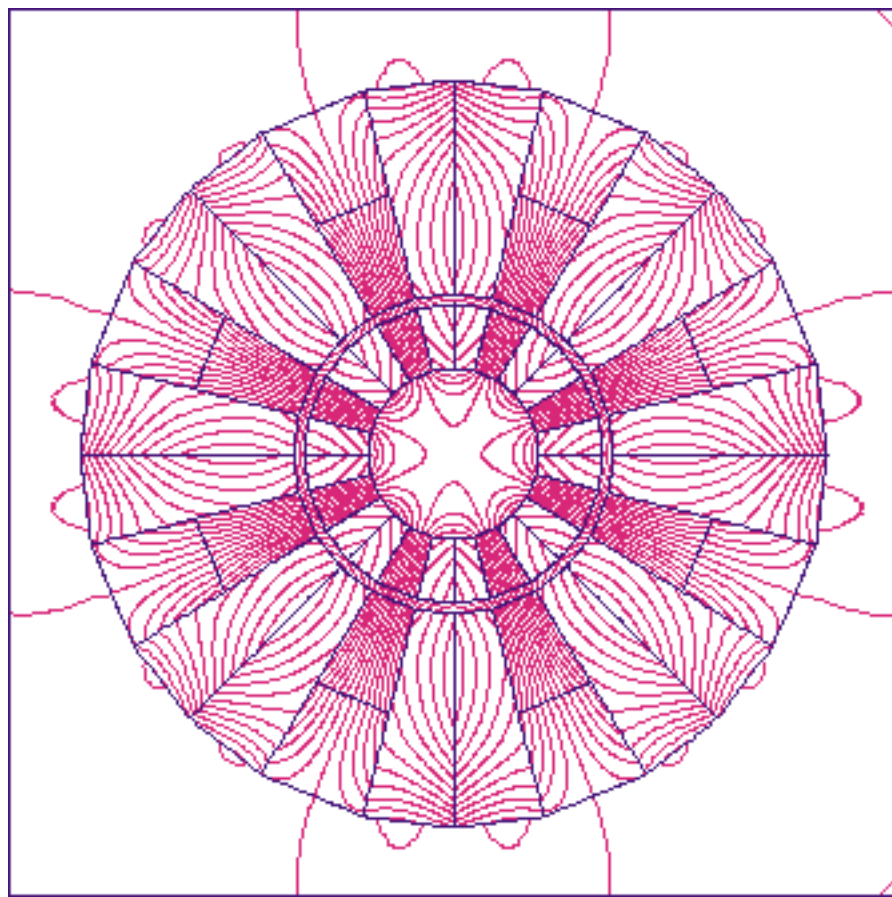
$$20+55+70+55+20 = 220$$

The Parts



PM-Octupole for Tail Folding

PM-Octupole for tail-folding

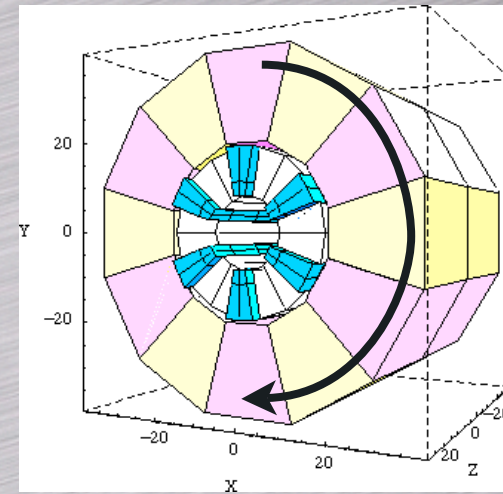
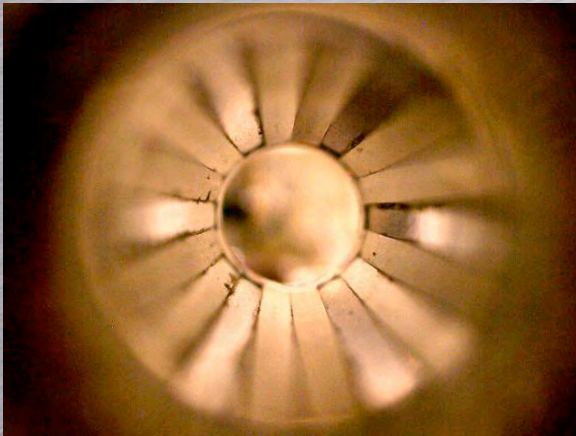


Bore $\varnothing 32$, Size $\varnothing 150$ for **ATF2**

ILC: Baseline Sc design: 0.5T@pole tip, 1TeVCM

PMO can be strong; shorter in length.

Rapid Cycling Variable Permanent Magnet Sextupole Lens for Pulsed Cold Neutrons

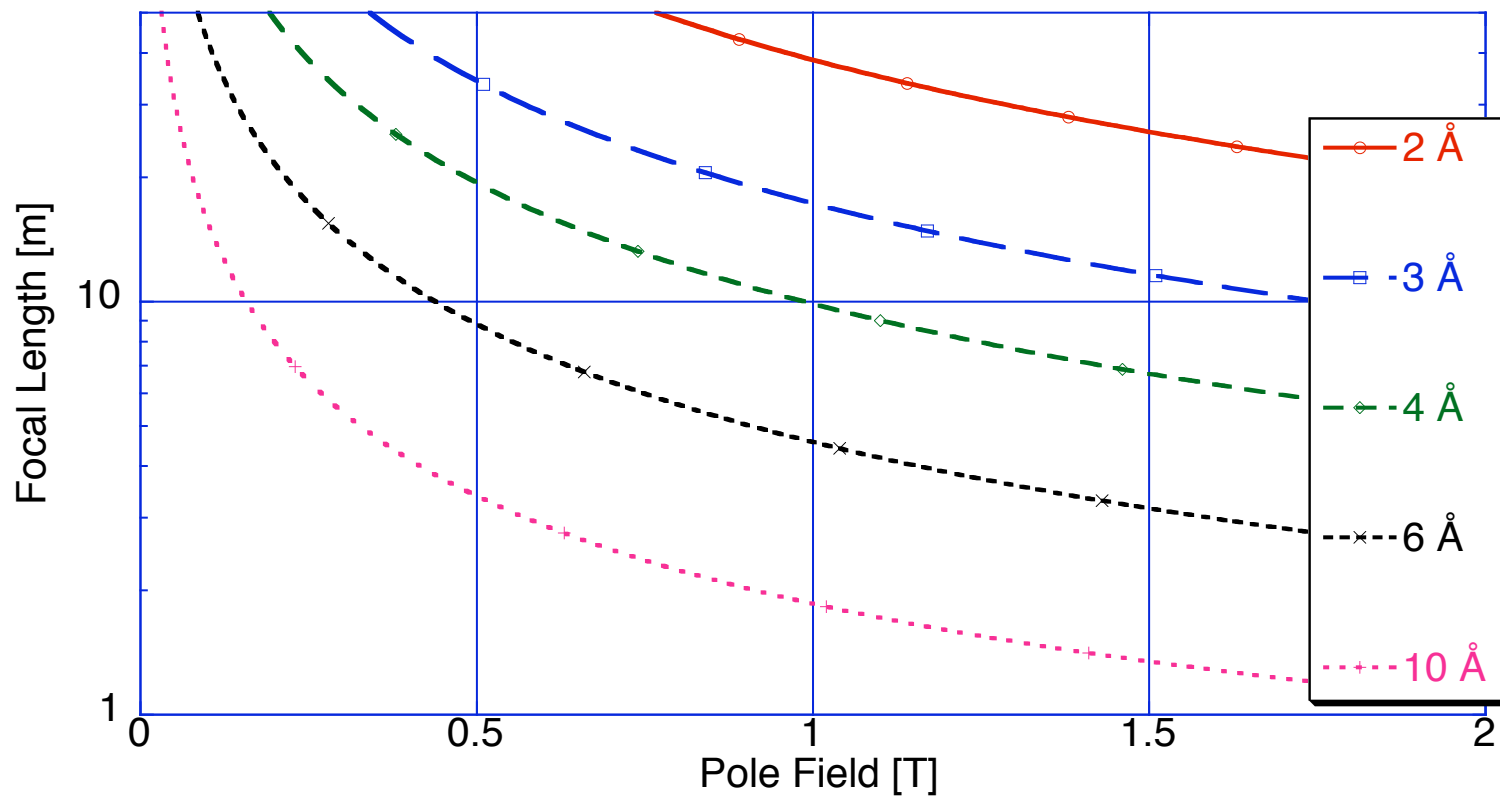
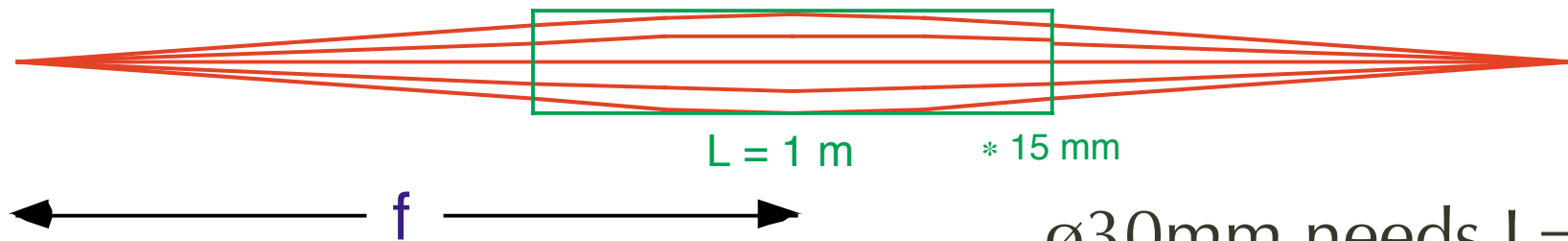


Y. Iwashita, Y. Tajima, M. Ichikawa, S. Nakamura
Kyoto Univ., Uji, Kyoto, Japan

T. Ino, S. Muto and H.M. Shimizu
KEK, Tsukuba, Ibaraki, Japan

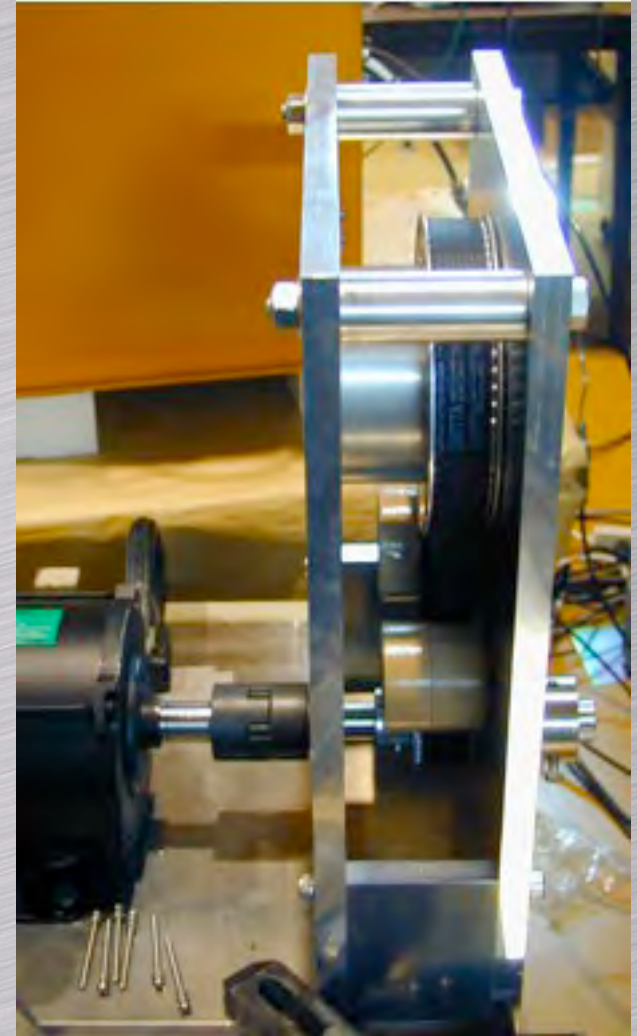
Focal Length

Sextupole



Second 1/2 Scale Model

uses a belt instead of gears.



Introduction of Recent Activities

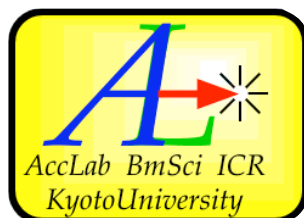
	ILC	JPARC	Small Neutron Source	Misc.
RF	Cavity Inspection	Untuned Cavity (Start of FINEMET)	ECR Ion Source, RFQ	Skin Effect PISCES-II (2.5D-RF code)
Permanent Magnets/ Magnets	PMQ – Final Focus, PMO – Tail Folding, QEX1		ECR PM, LEBT	Flux Density Equalizer for Gradient Dipoles, InterPole



Introduction of Recent Activities

	ILC	JPARC	Small Neutron Source	Misc.
RF	Cavity Inspection	Untuned Cavity (Start of FINEMET)	ECR Ion Source, RFQ	Skin Effect PISCES-II (2.5D-RF code)
Permanent Magnets/ Magnets	PMQ – Final Focus, PMO – Tail Folding, QEX1		ECR PM, LEBT	Flux Density Equalizer for Gradient Dipoles, InterPole





ACCELERATOR LABORATORY
ADVANCED RESEARCH CENTER FOR BEAM SCIENCE
INSTITUTE FOR CHEMICAL RESEARCH
KYOTO UNIVERSITY

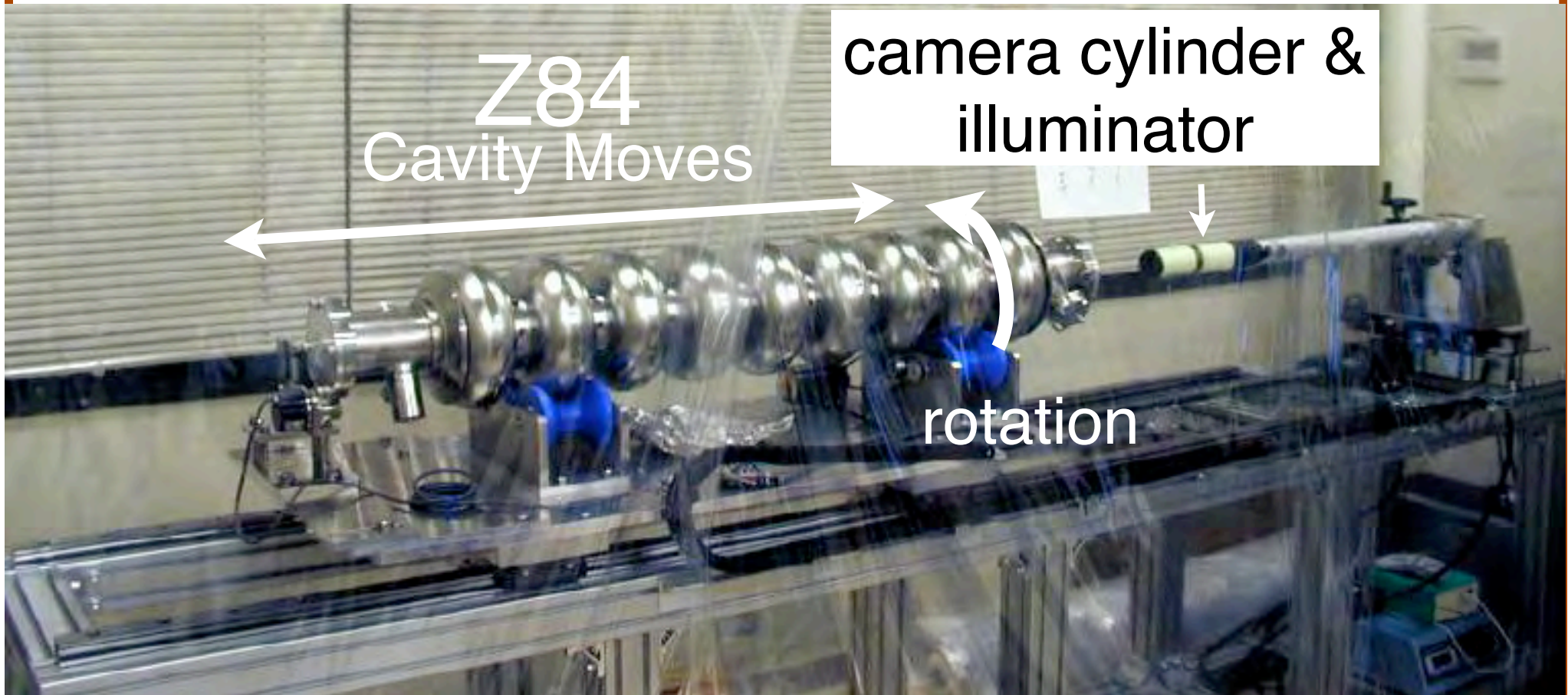


Development of High Resolution Camera and Observations in TESLA Cavities

Y. Iwashita, Y. Tajima and H. Hayano

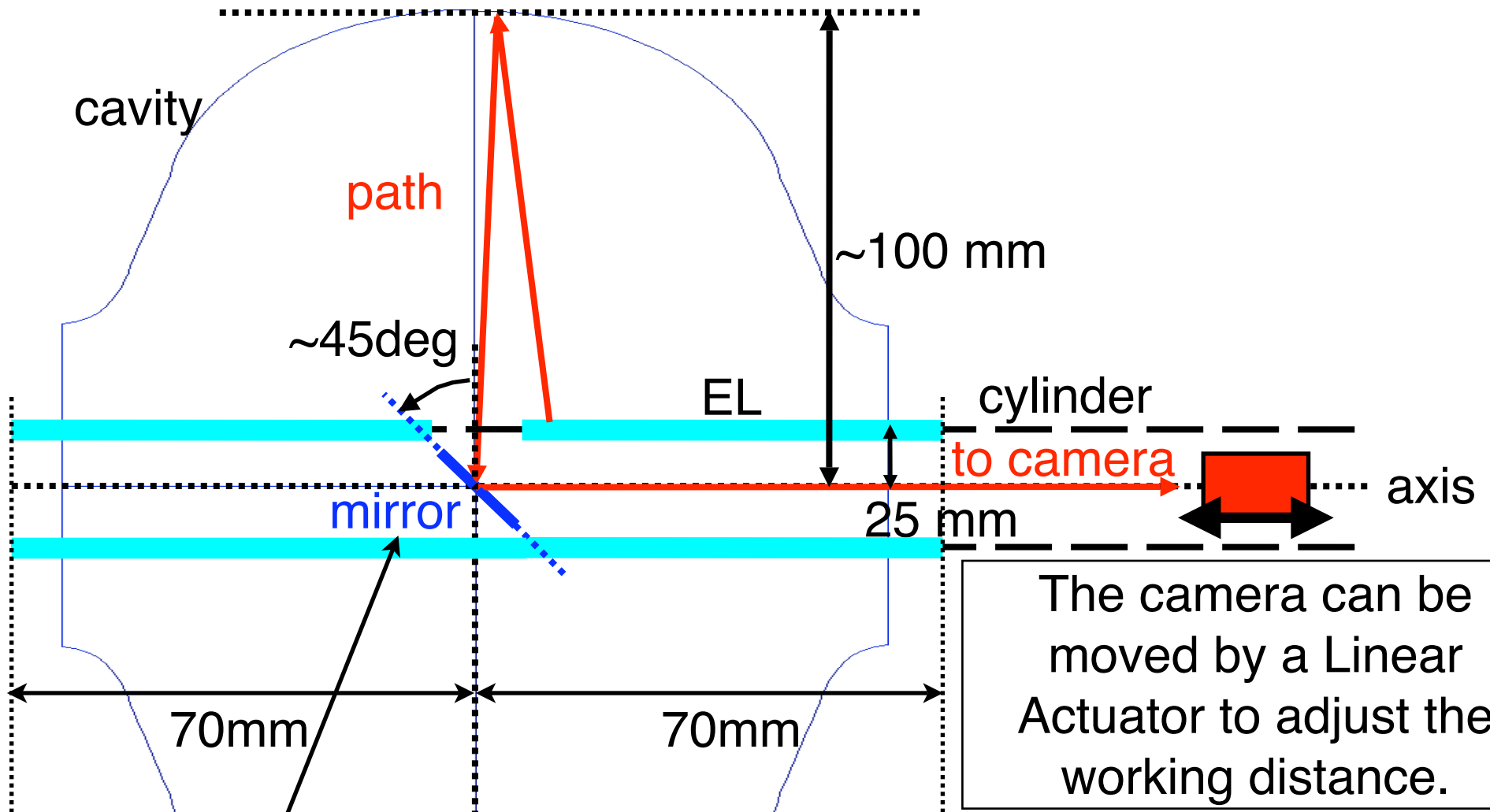


Early System



Cavity is rotated and moved longitudinally.
The cavity moves to swallow the camera cylinder.

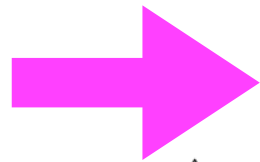
Inside the Cylinder



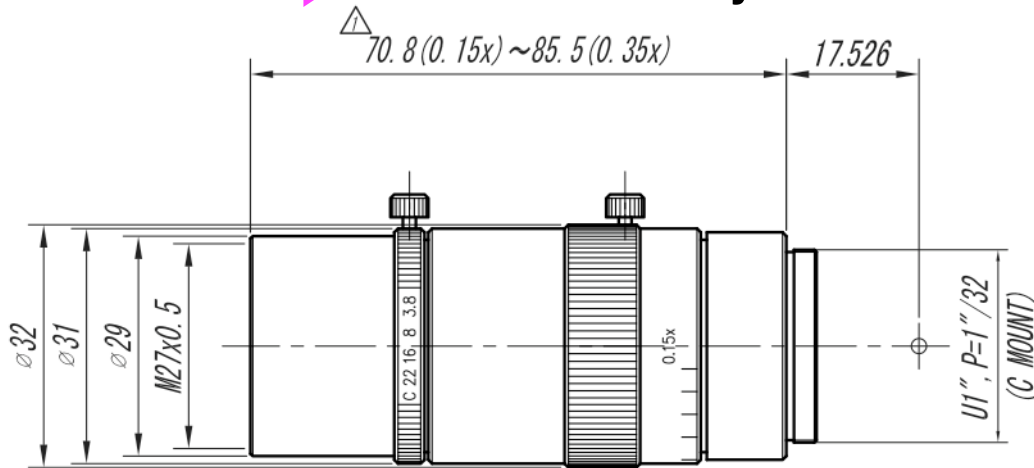
Mirror can be tilted by a Pulse Motor.

Camera Specification

- 1.5M-pixel CMOS Color Camera
1400px X1000 px: 5.0 μ m/px
Toshiba teli CSF5M7C3L18NR
- Distortionless Lens(0.15x ~ 0.35x, f75mm)
V.S. Technology Corp. VS-LD75
- 40mm Extension Tube (later)



Maximum resolution: ~0.70x, ~7 μ m/px (~15 μ m/px)
Limited by the Working Distance~120mm



VS-LD75



CSF5M7C3L18NR

Setup of Illumination

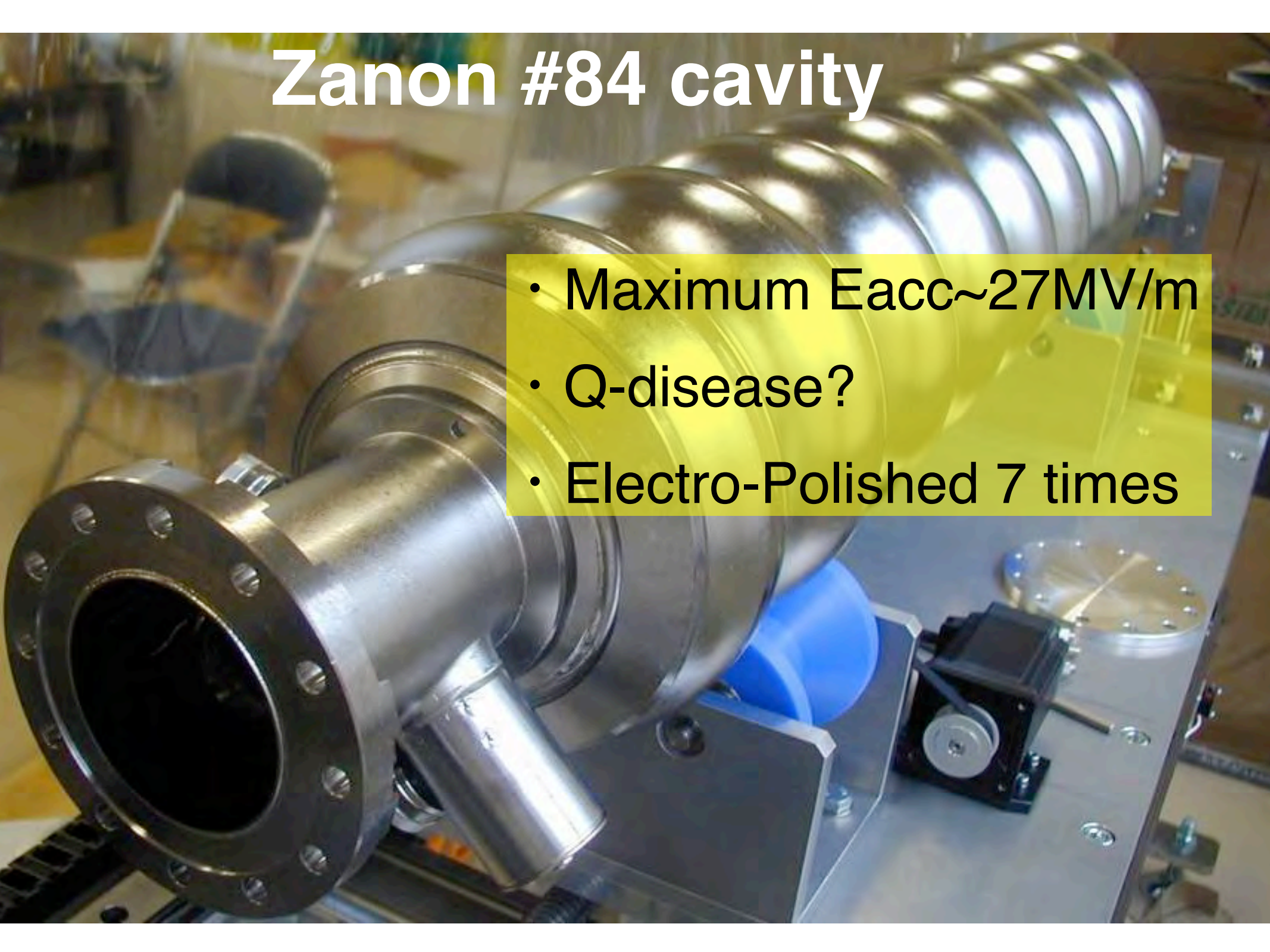
Blue Electro-Luminescence (EL) sheet



mirror: $\sim 40\text{deg}$

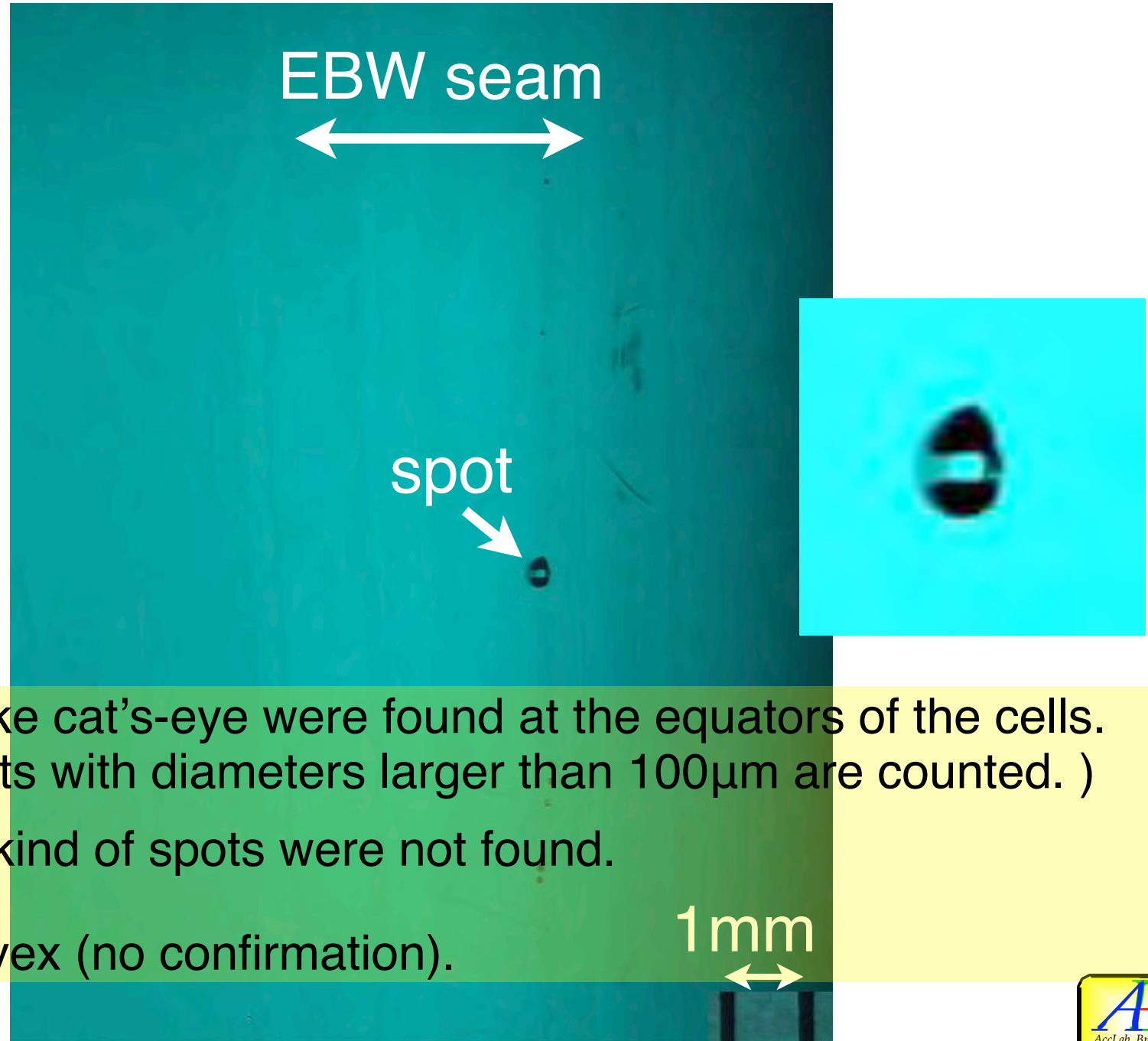
Blue EL sheet

Zanon #84 cavity



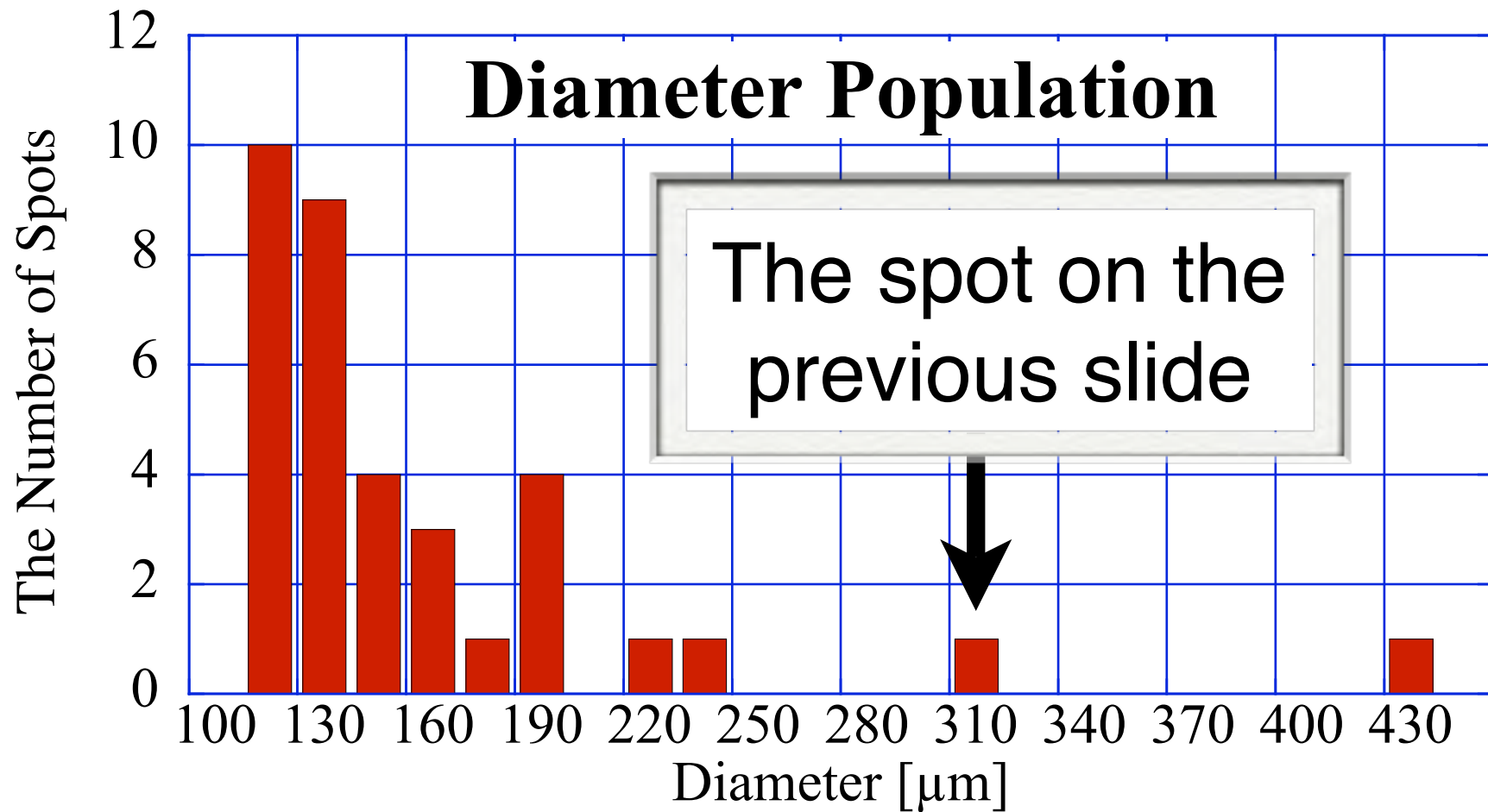
- Maximum $E_{acc} \sim 27 \text{ MV/m}$
- Q-disease?
- Electro-Polished 7 times

Interior Surface of Zanon #84



- 28 spots like cat's-eye were found at the equators of the cells. (only the spots with diameters larger than $100\mu\text{m}$ are counted.)
- Any other kind of spots were not found.
- Likely convex (no confirmation).

Statistics of spots(>100 μm) in Z84



REMARK: All the spots were found at the input coupler side of the EBW seam.

Modification

● Zanon #84: by the first inspection system.
Only sizes of spots were observed.

- ➔ Rebuilt the tube after this observation,
1. New drive mechanism for better positioning
 2. The extension tube for 2X magnification
 3. New illumination system
 4. A height estimation method was also established after this.

● AES001: will be explained ...

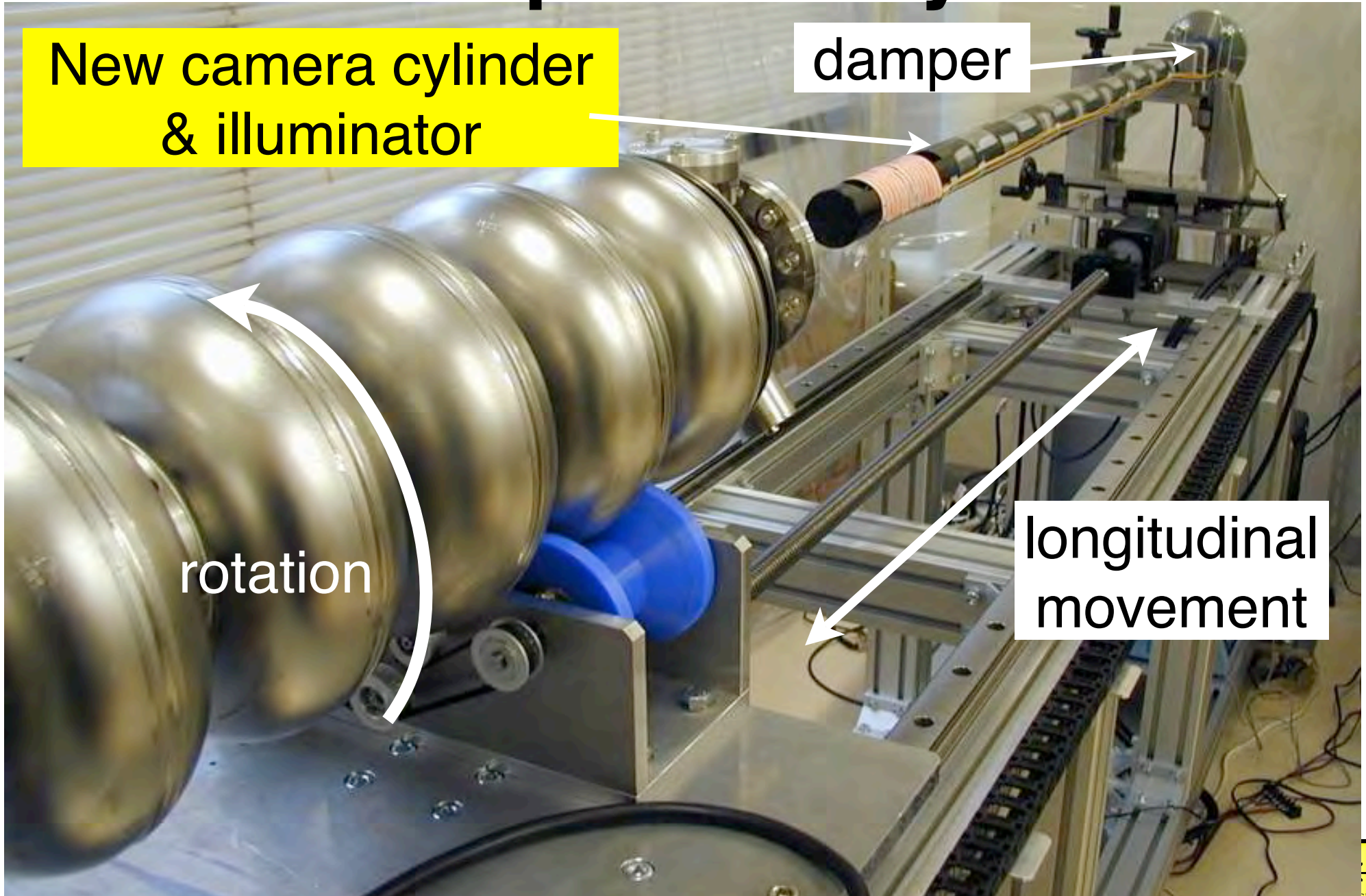
New Inspection System

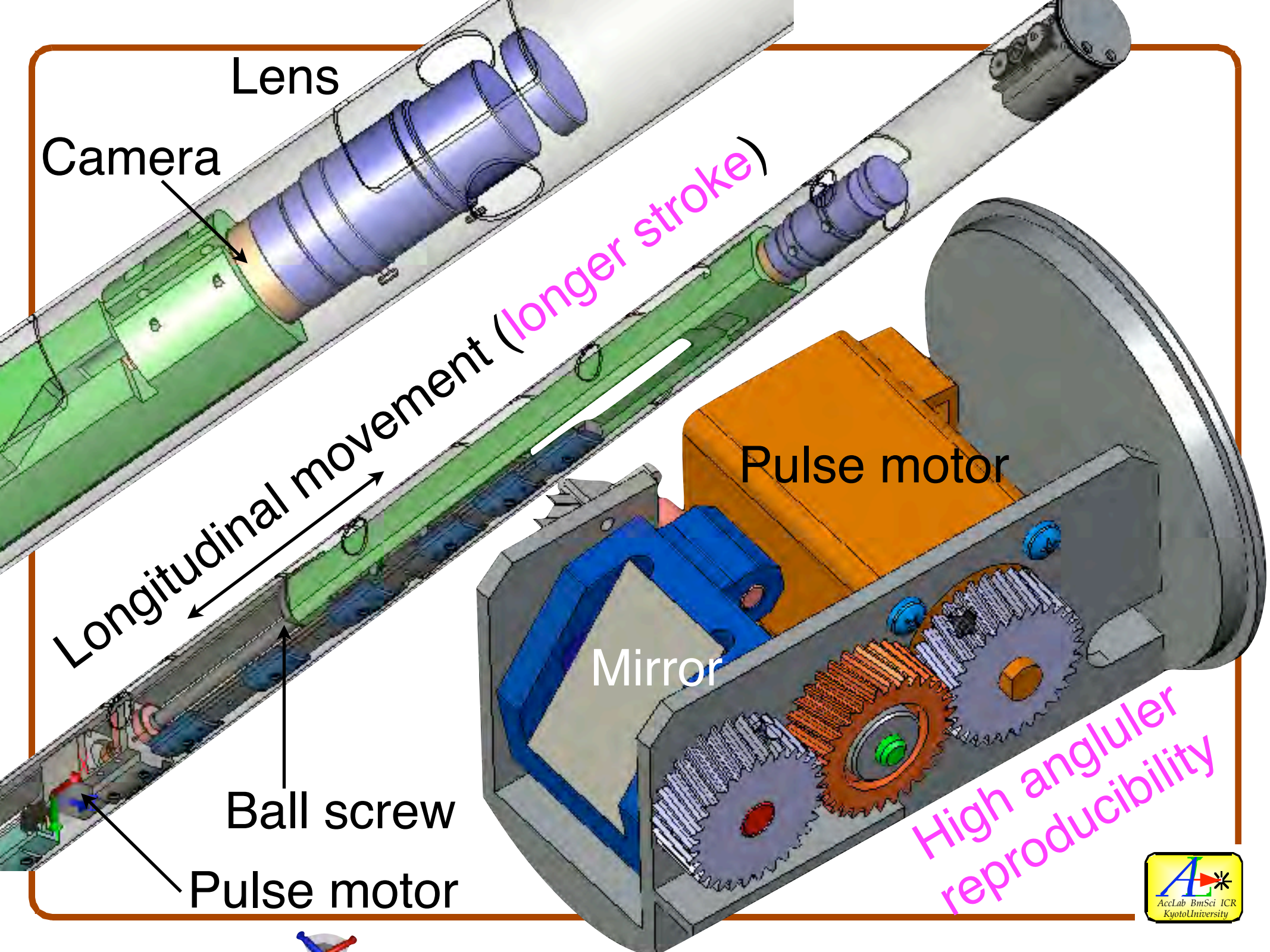
New camera cylinder
& illuminator

damper

rotation

longitudinal
movement





Lens

Camera

Longitudinal movement (longer stroke)

Pulse motor

Mirror

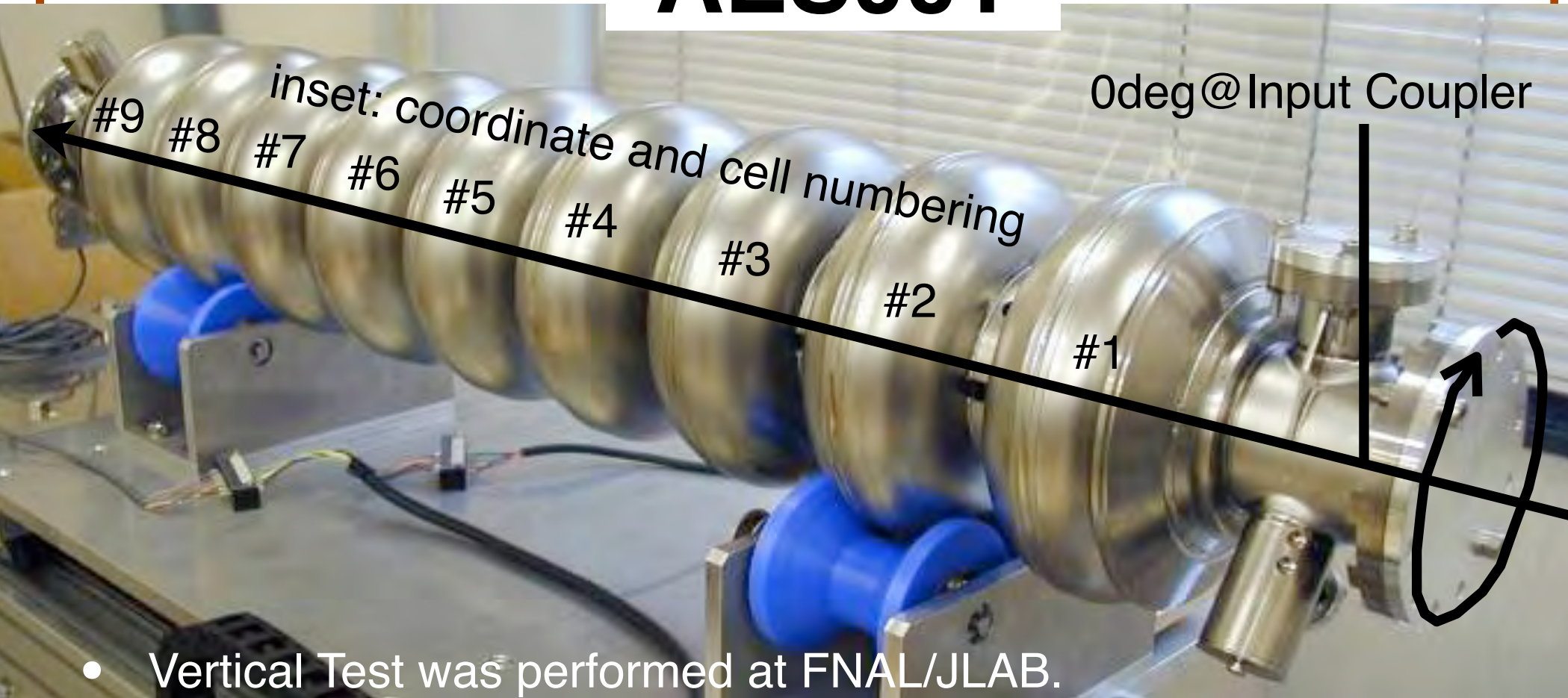
Ball screw

Pulse motor

High angular reproducibility

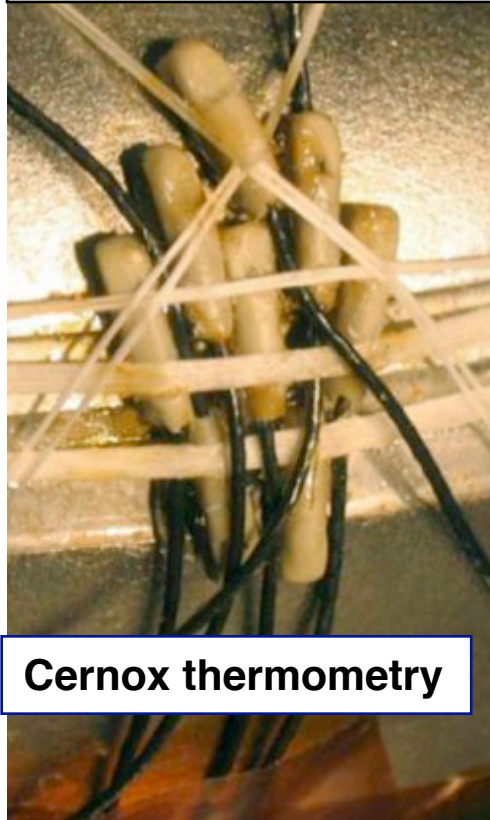
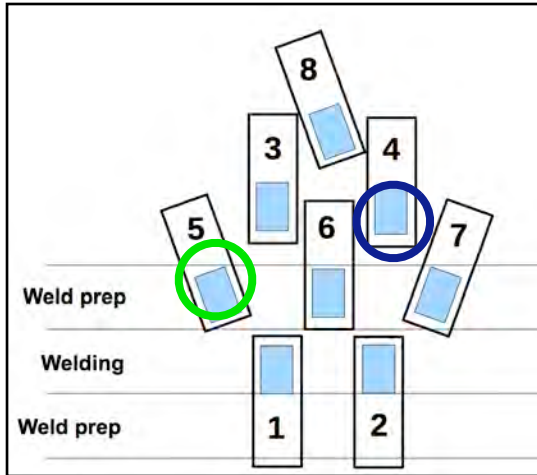


AES001



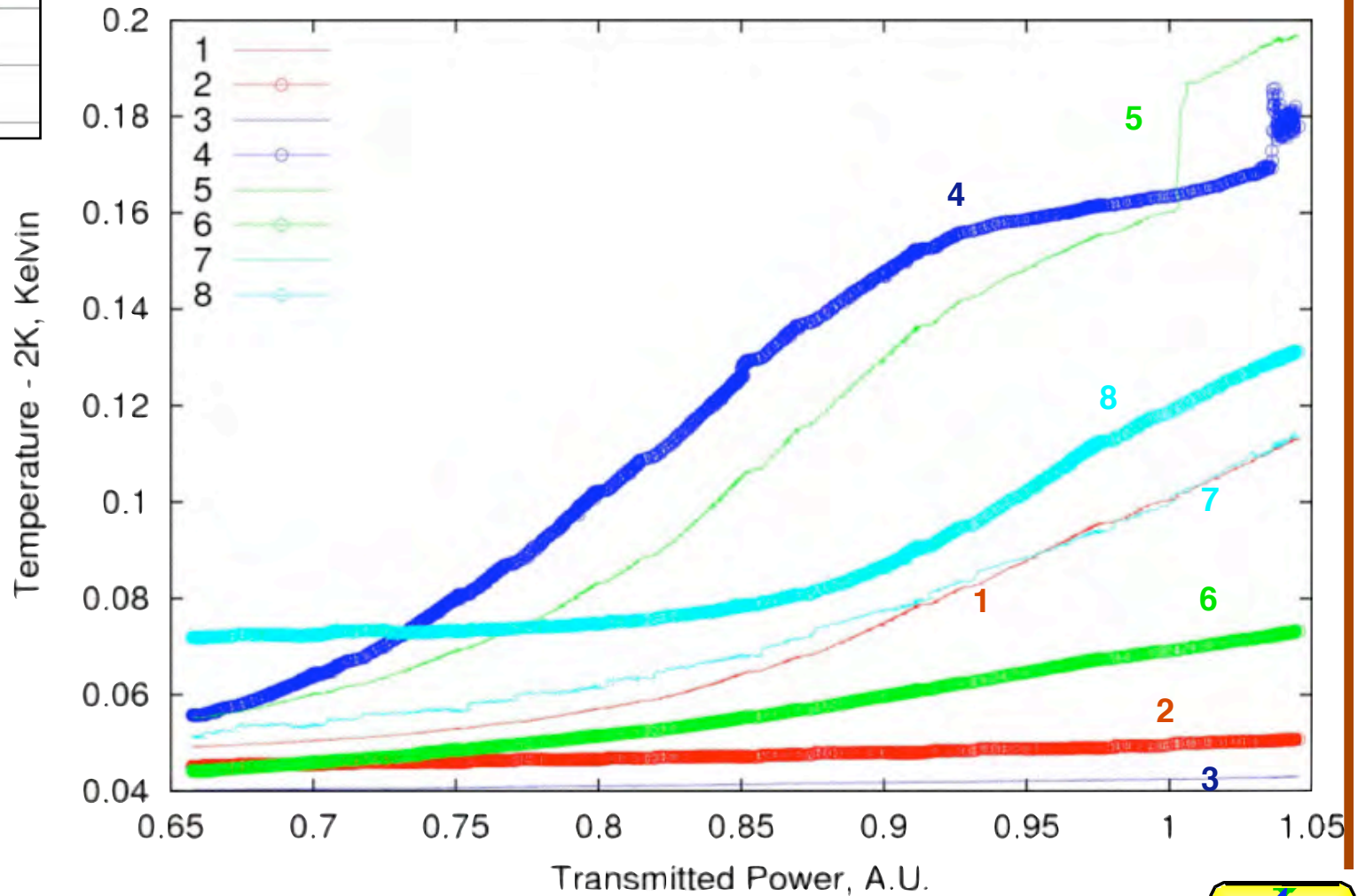
- Vertical Test was performed at FNAL/JLAB.
- Quenched at $E_{acc} \sim 15 \text{ MV/m}$ without field emission (no Xray).
- Passband mode measurements shows that #3 and #7 cell are suspicious.
- In CERNOX measurements two hot spots were found at the equator region of #3 cell.

AES001 has hard quench at 15MV/m, where its location was identified by Cernox at FNAL.



Cernox thermometry

aes01 11-08-07-10-52-59



AES001 #3 cell 169°

Larger grains

Fine grains

EBW area: Larger Grain

Twins

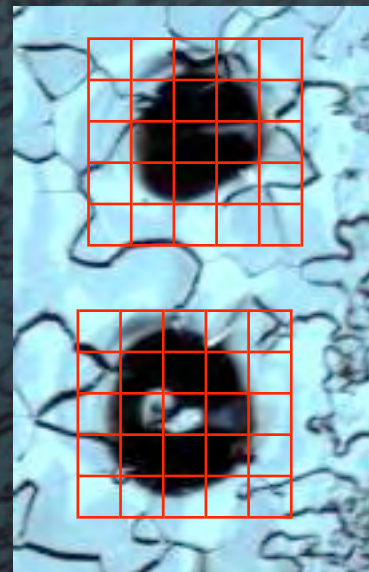
spot(a) @ 168°

spot(b) @ 169°

to Equator
and #2 cell



200 $\mu\text{m}/\text{div}$



z
1 mm
 θ

AES001 #3 cell 181°



EBW affected area

Larger grains Transition?

Fine grains



200 μ m/div

↑
spot

←
to Equator
and #2 cell



1mm

AES001 #7 cell 325°

EBW affected area

Largest grains

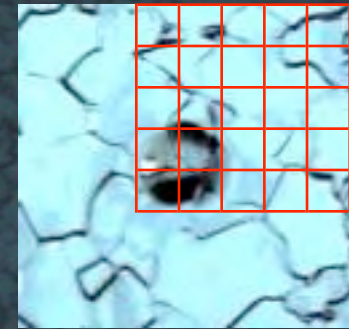
spot

Larger grains

Transition?

to Equator
and #6 cell

Fine grains

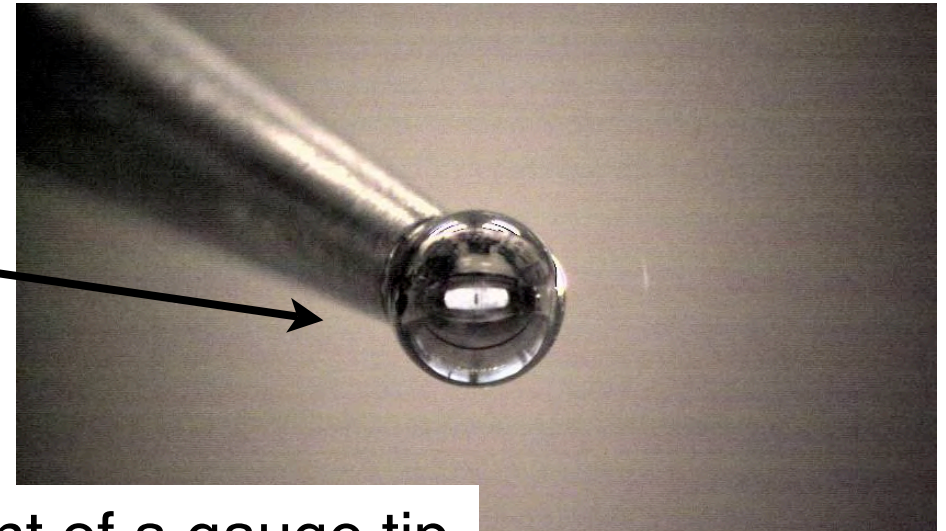
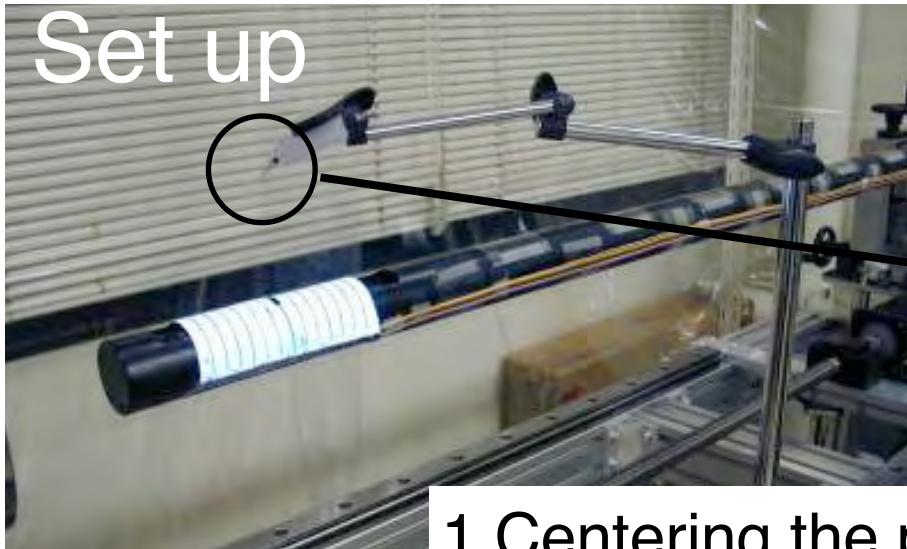


200 μ m/div

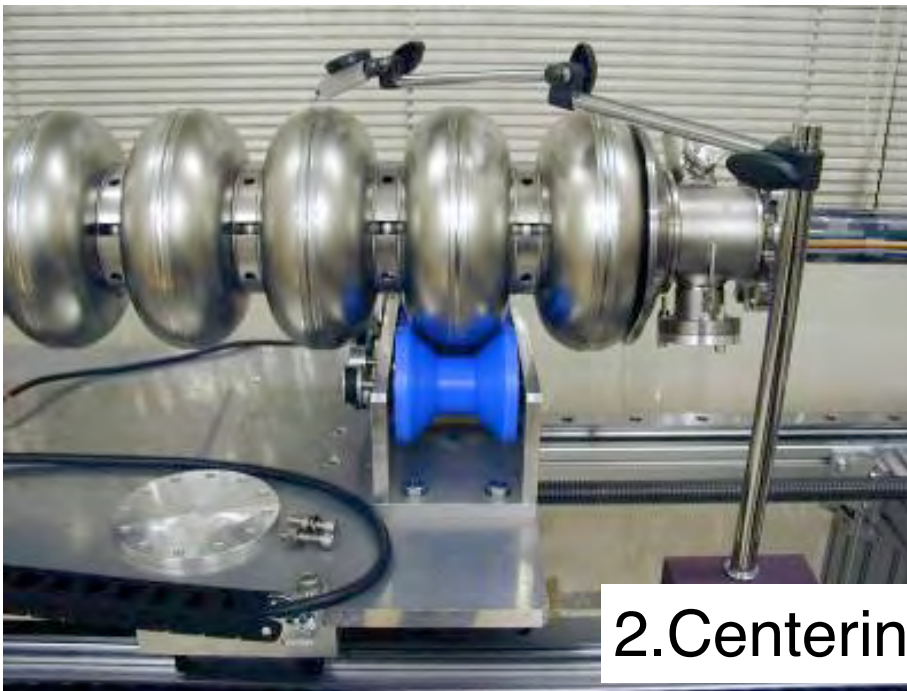


1mm

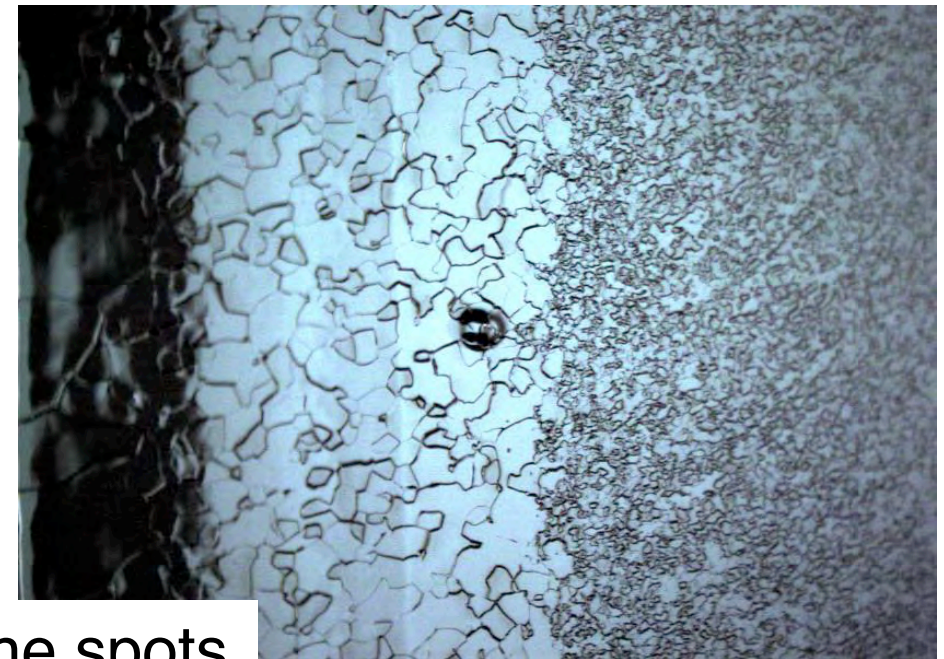
Determination of Spot Positions



1.Centering the point of a gauge tip.



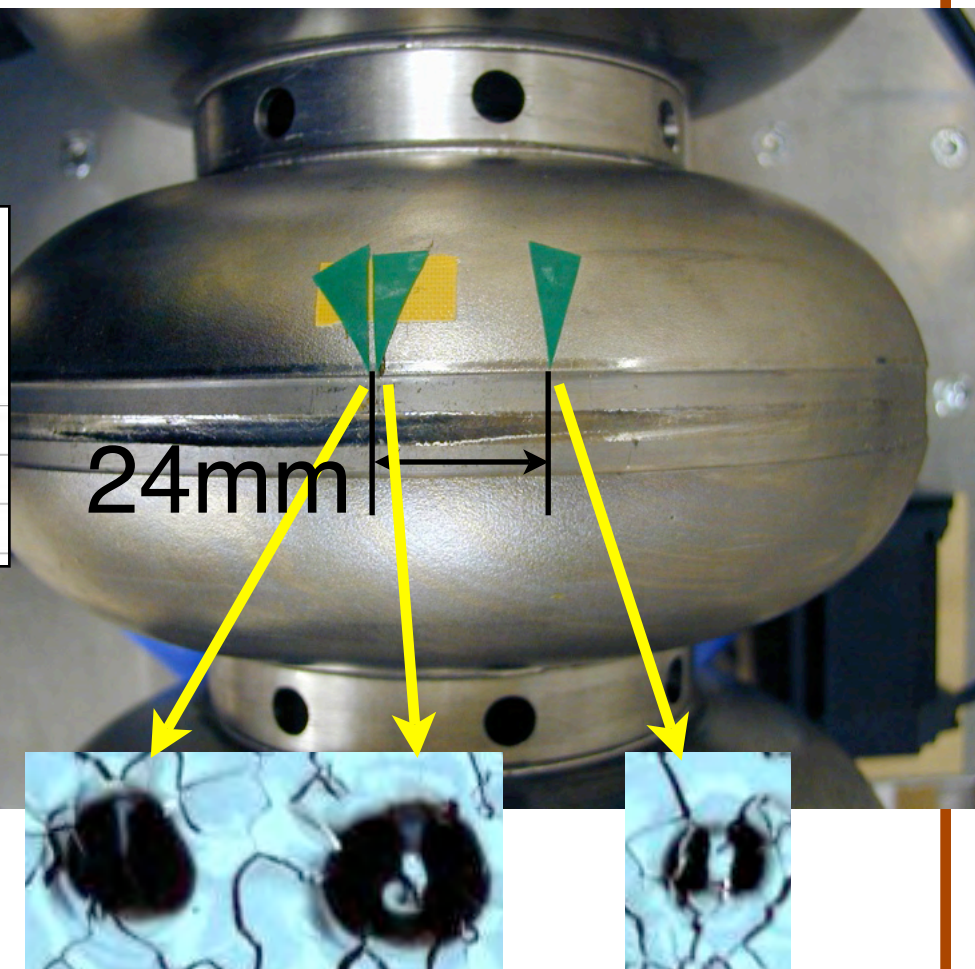
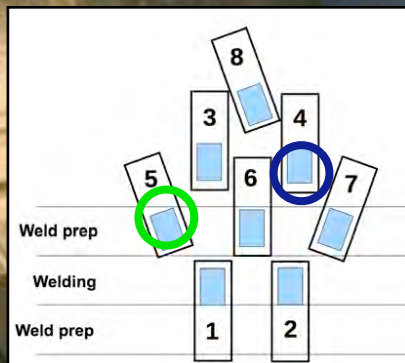
2.Centering the spots.



Correlation with Thermometry

Two thermometers shows the temperature rise.

24mm?
The width of the thermometers are about 5mm.

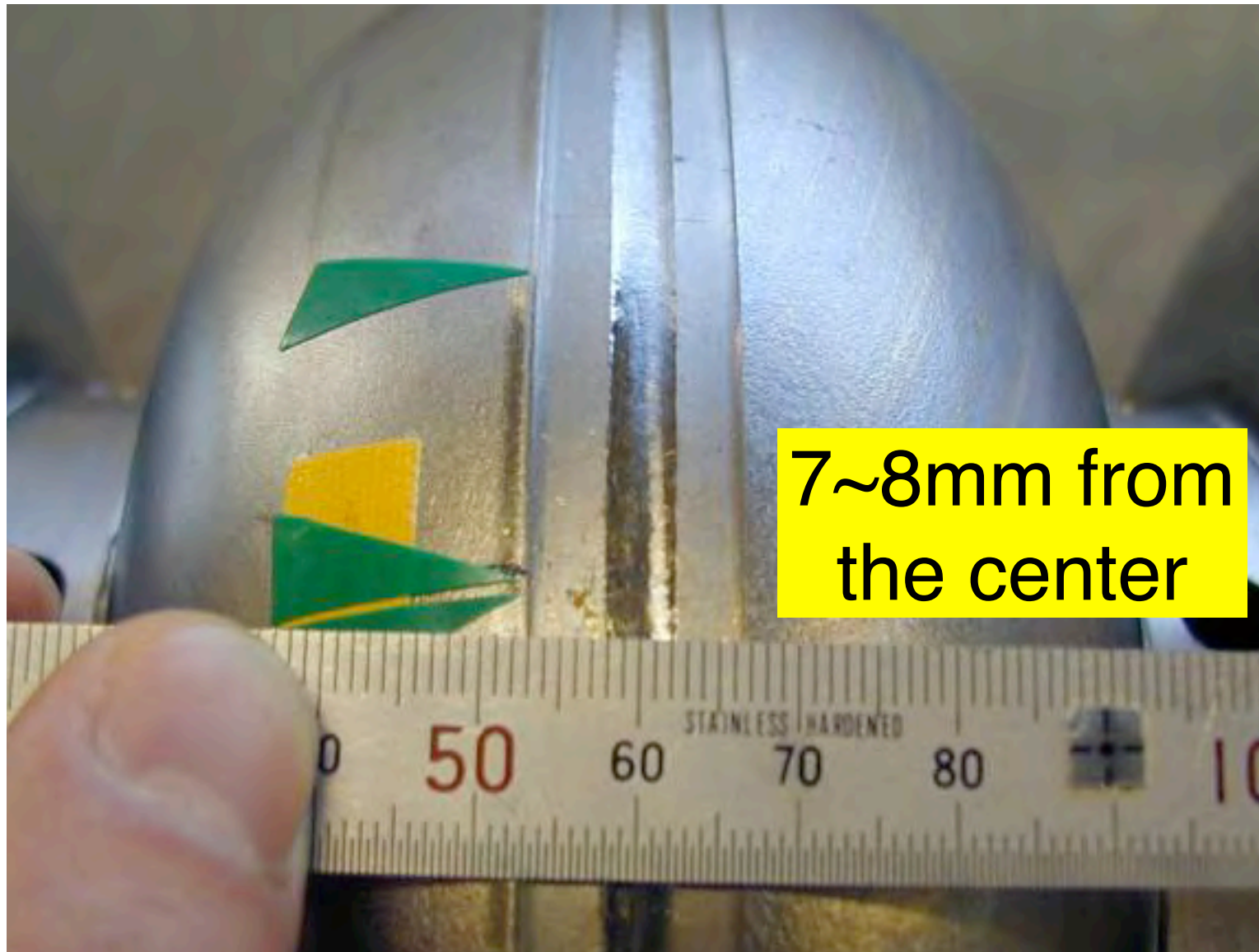


Dmitri A. Sergatskov: Thermometry on AES01 cavity at Fermilab
@webex20071204

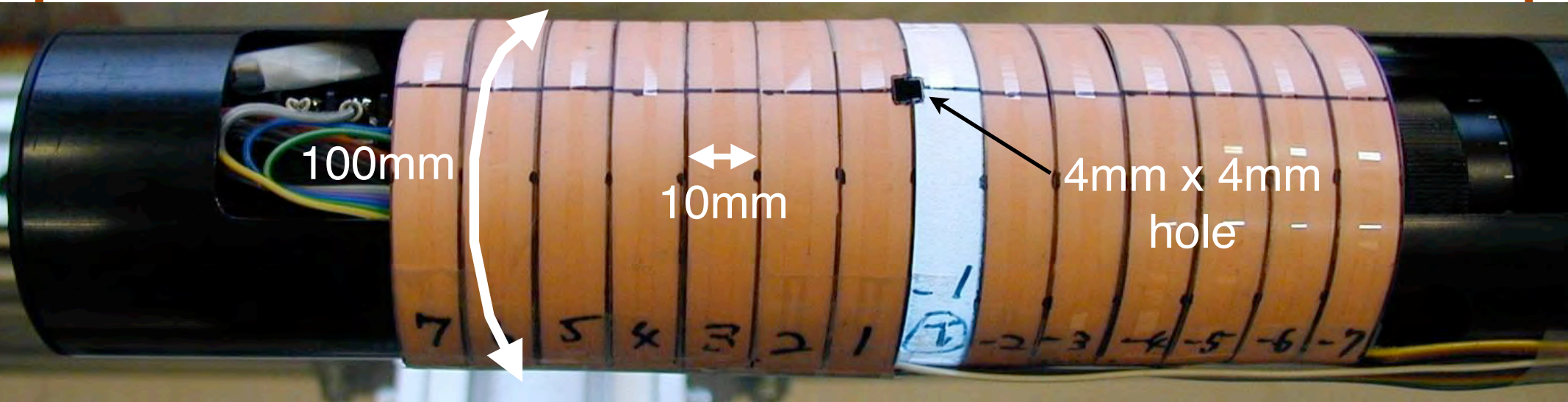
Two hot spots@FNAL/JLAB

Three spots found@Kyoto

The location

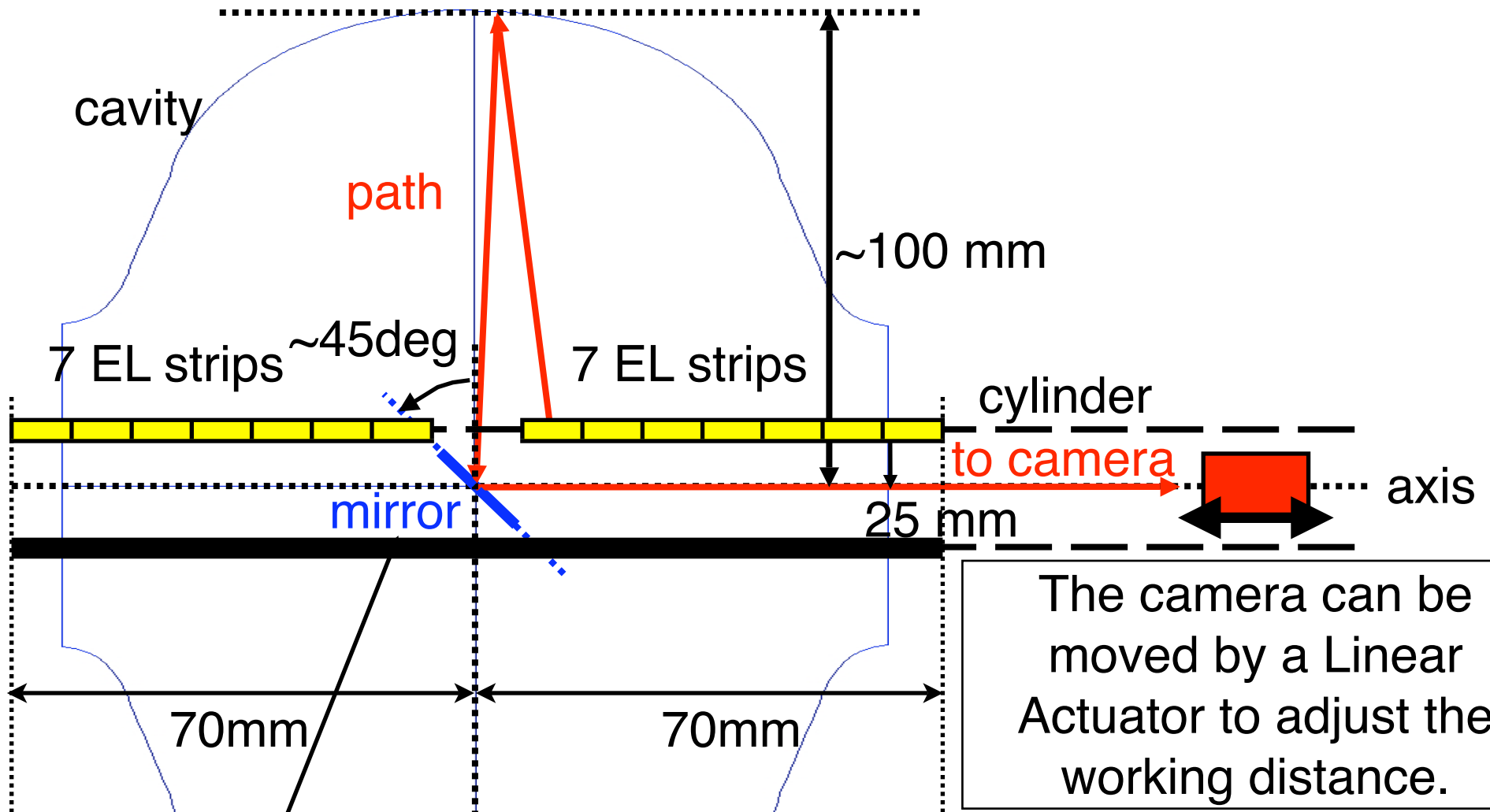


Stripe Illumination(SI)



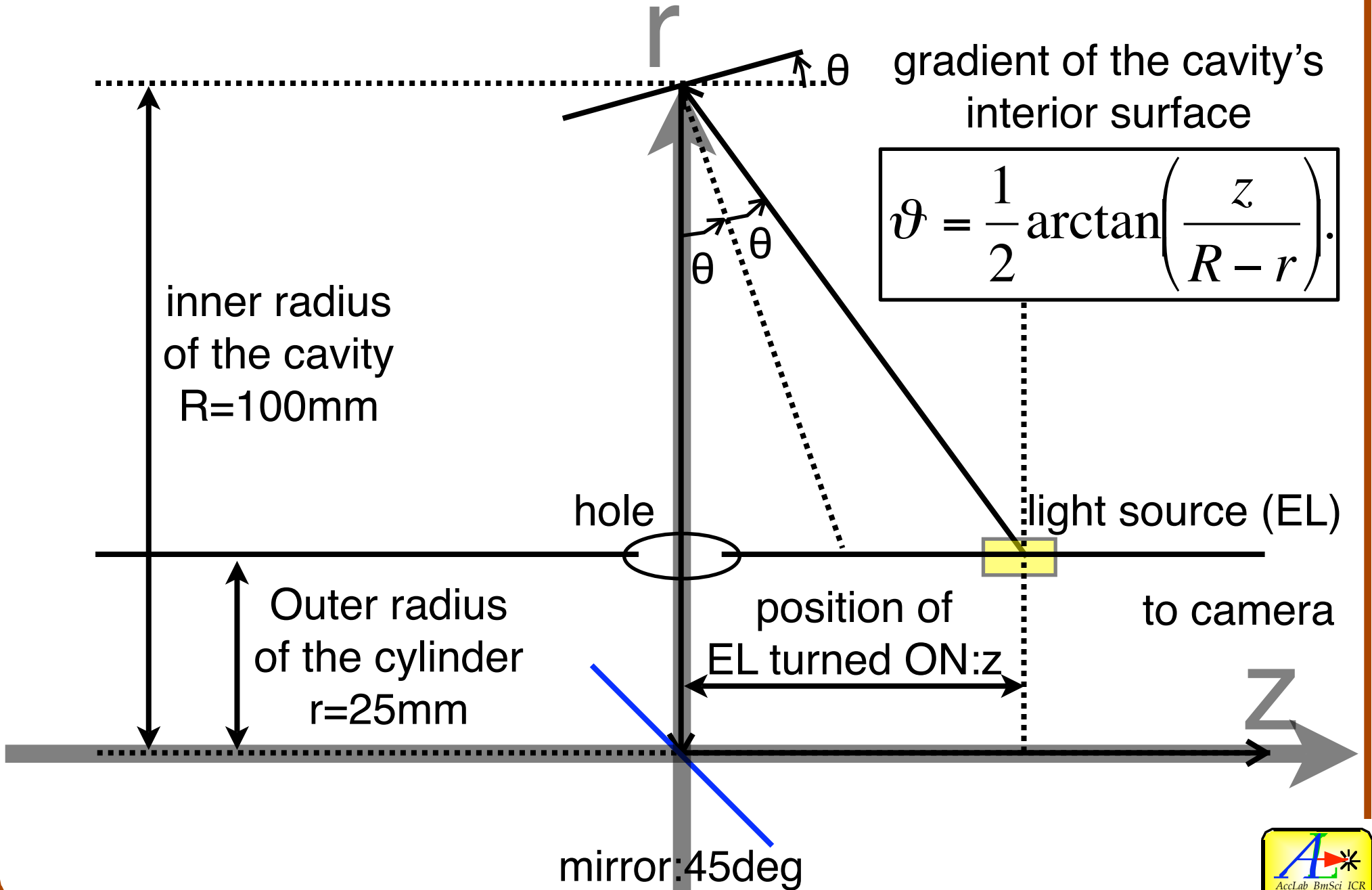
- Fourteen Electro-Luminescence(EL) strip sheets are 10mm in axial direction and cover 100mm in azimuthal direction.
- These fourteen strips can be turned ON/OFF one by one.
- Assuming that cavity's interior surface is a complete mirror, we can measure wall gradients of the cavity's interior surface with these ELs.

Inside the Cylinder



Mirror can be tilted by a Pulse Motor.

Wall Gradient Measurement

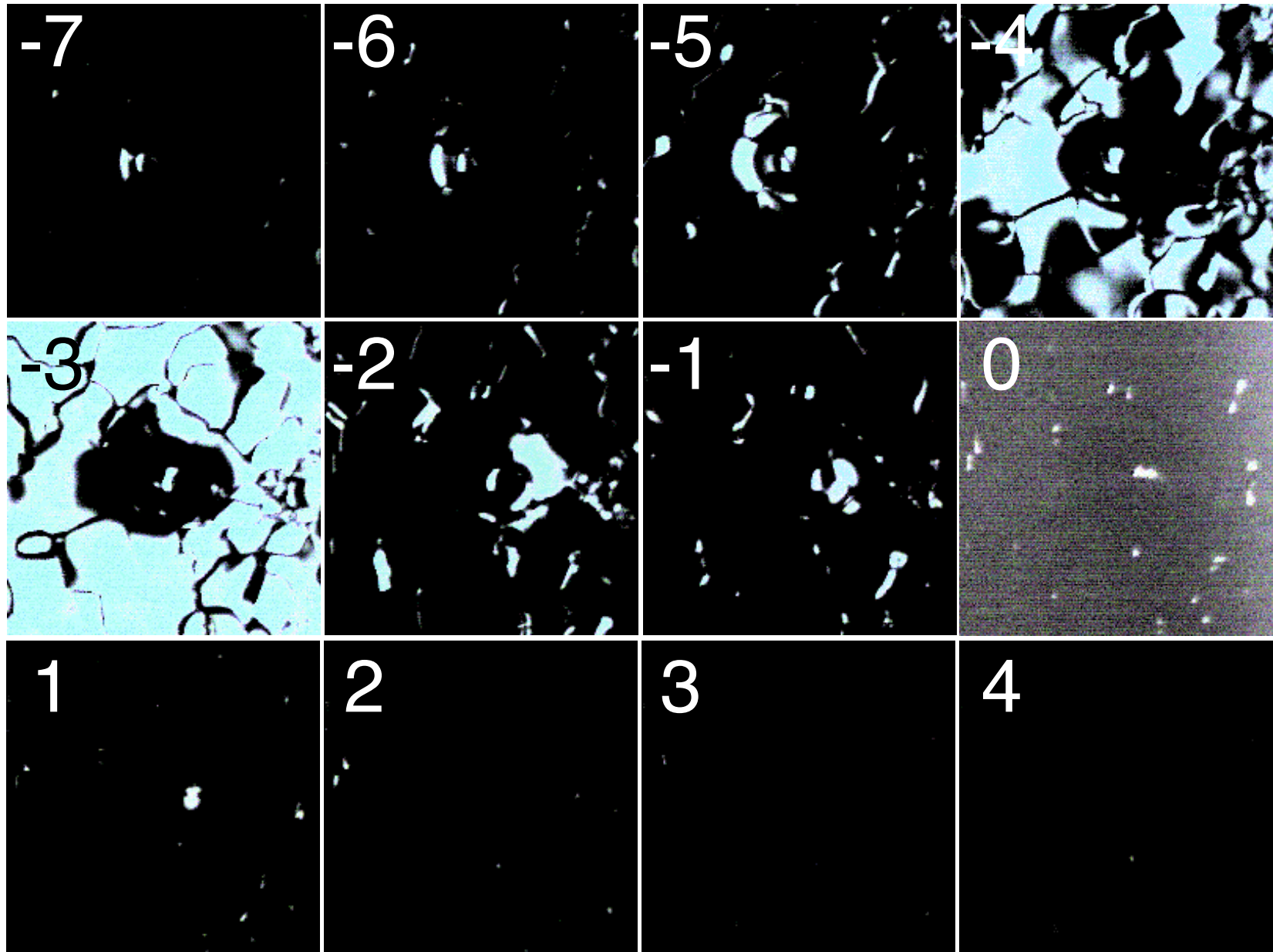


Wall Gradient Measurement

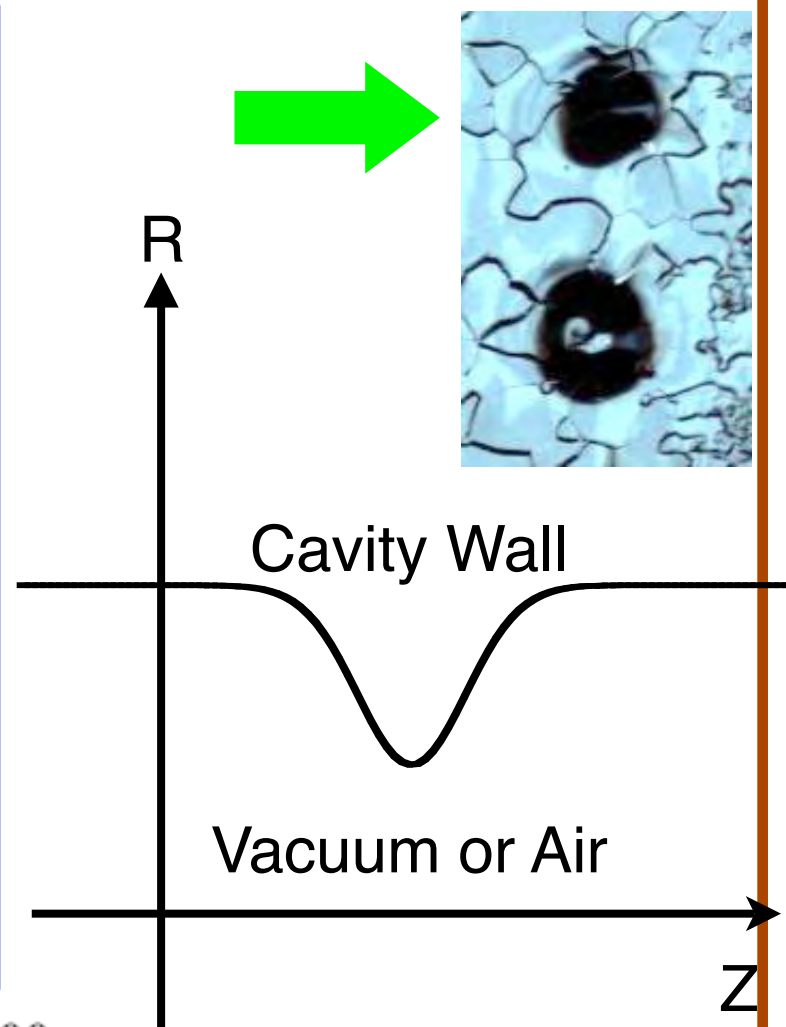
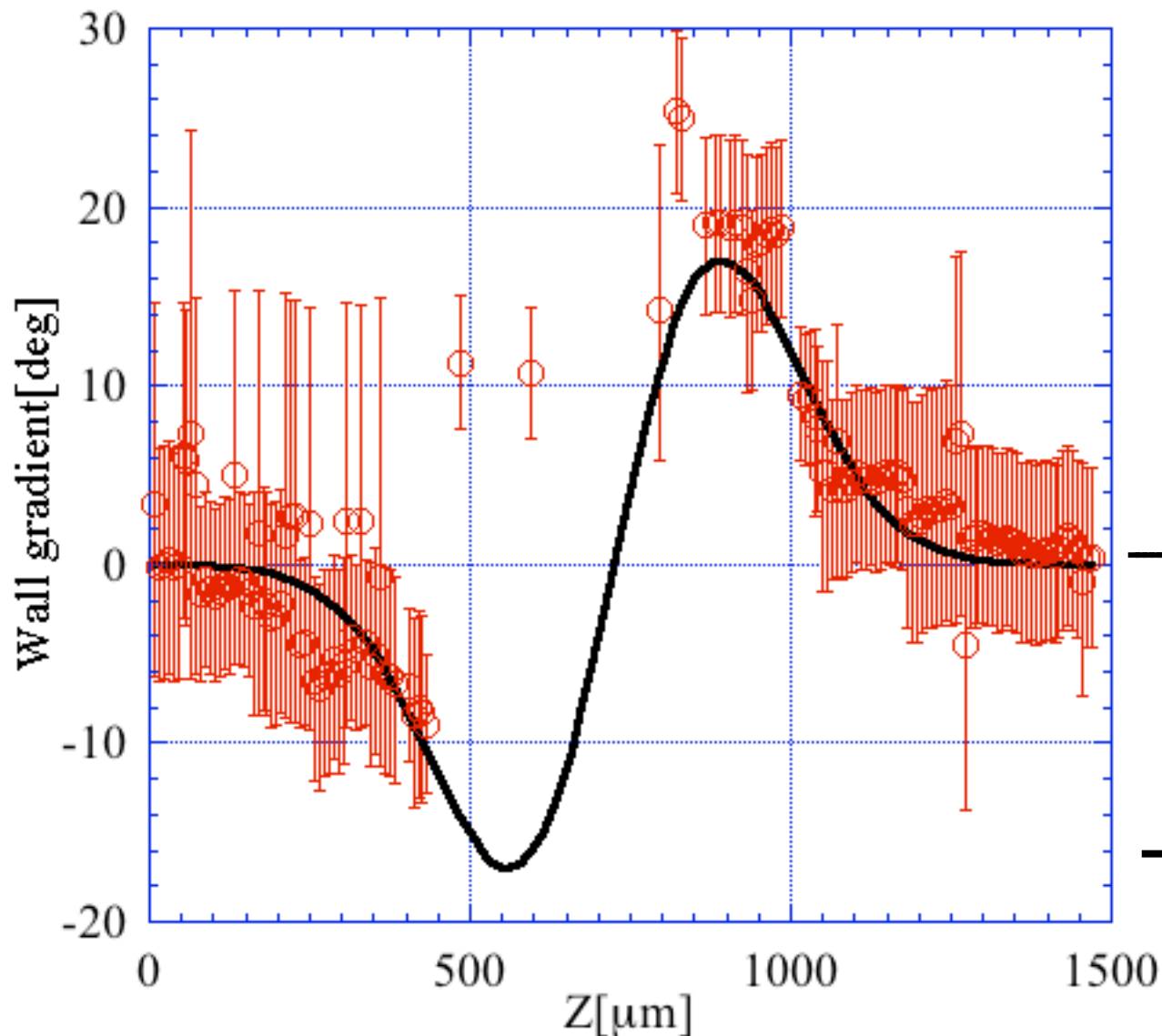


The center spot move left to right

Wall Gradient Measurement



Wall Gradient of spot at #3 cell 168°



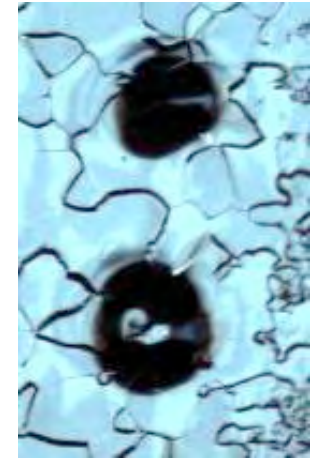
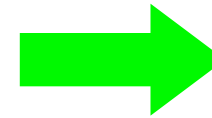
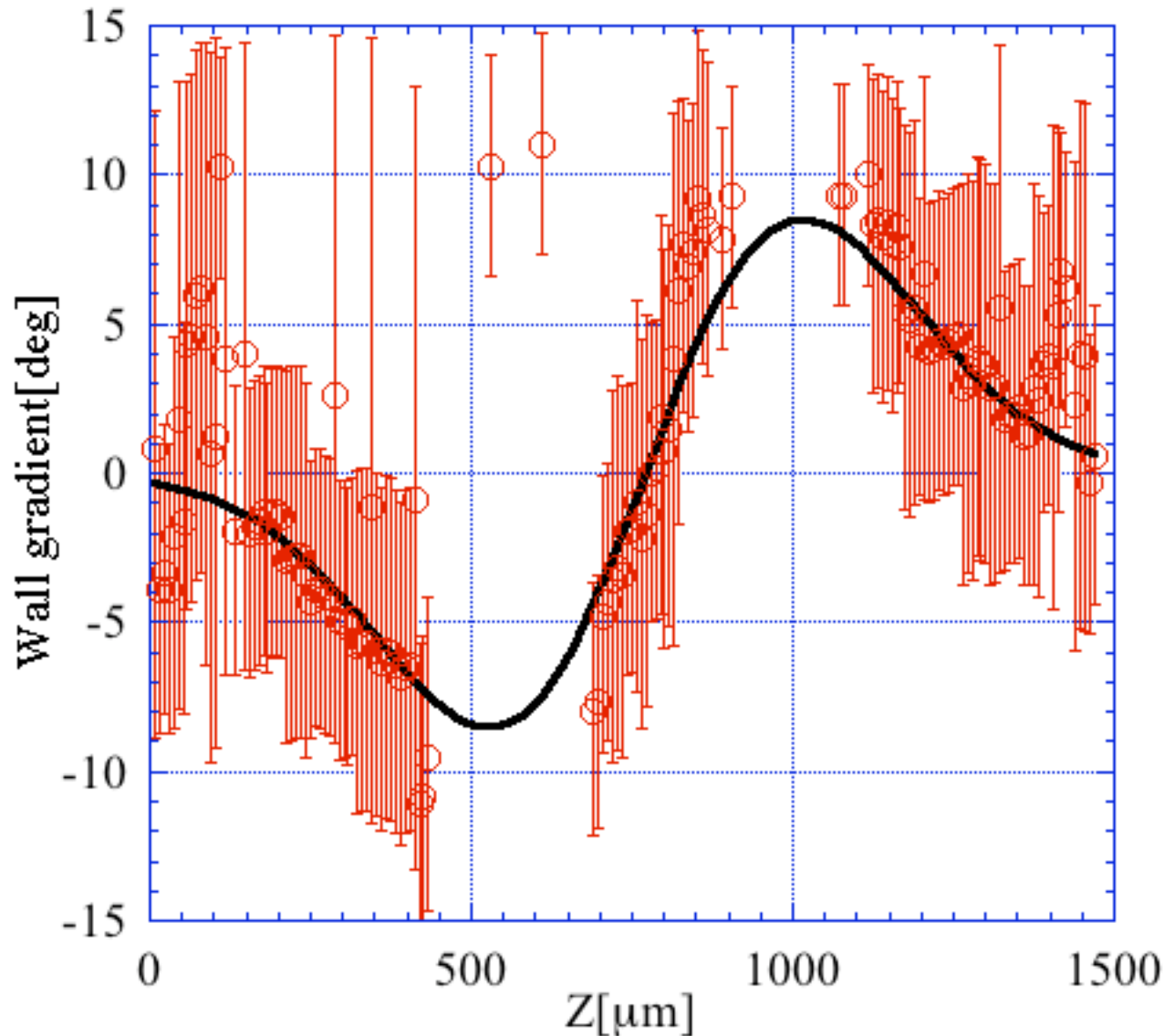
Left: Measured gradients and a fitted differential gaussian.

Right: Schematic drawing of the integral of the fitted curve in the left.

This data shows that the spot is a convex(ball).

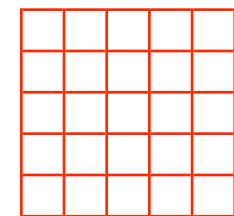
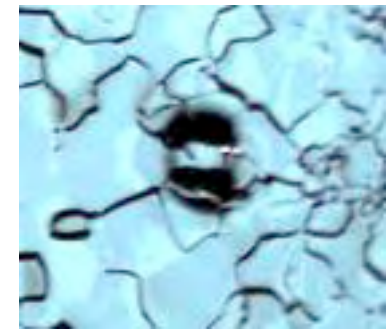
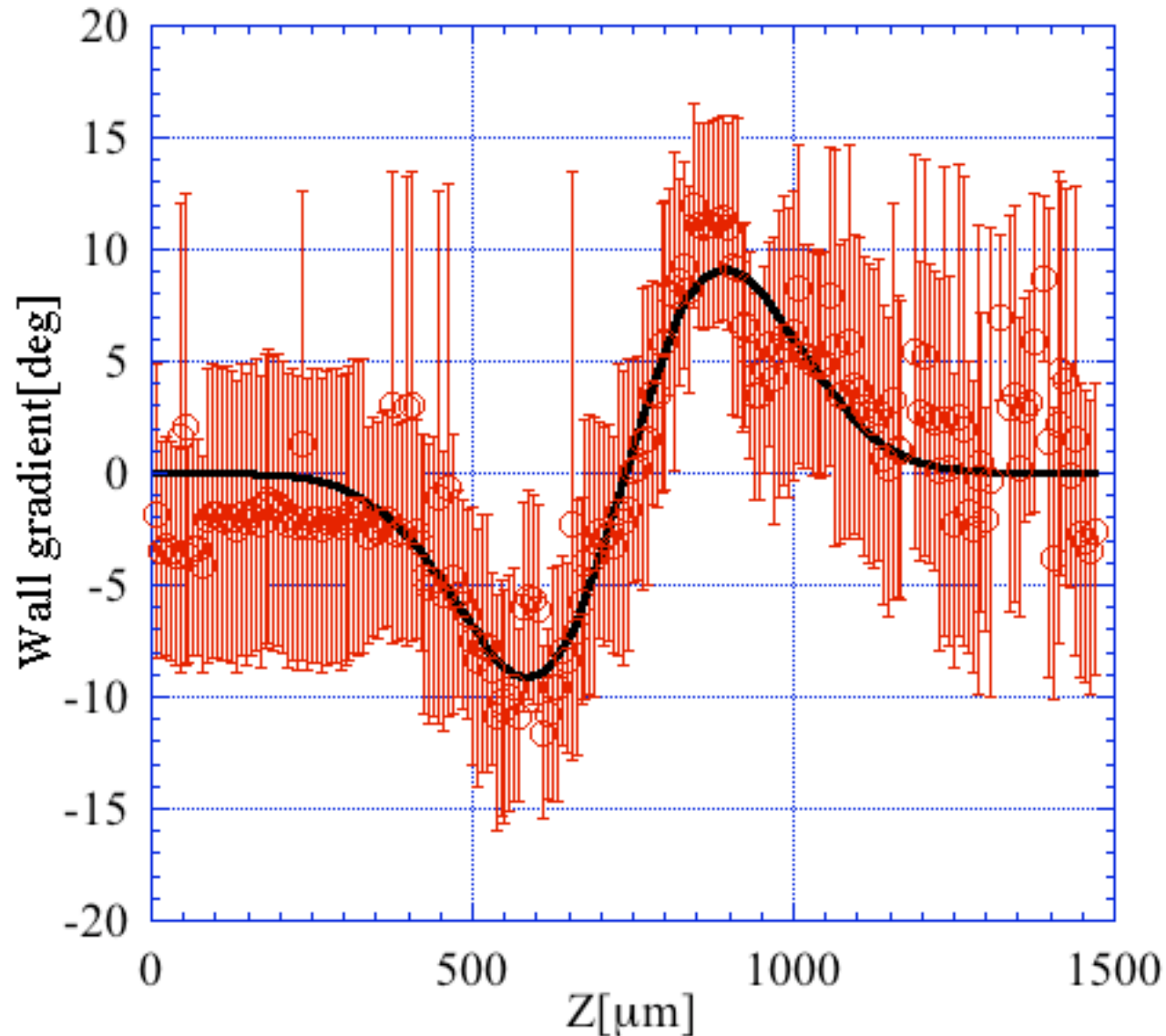
From the fitted differential gaussian, the height is 84 μ m.

Wall Gradient of spot at #3 cell 169°



This data shows that the spot is a convex(ball).
From the fitted differential gaussian, the height is $60\mu\text{m}$.

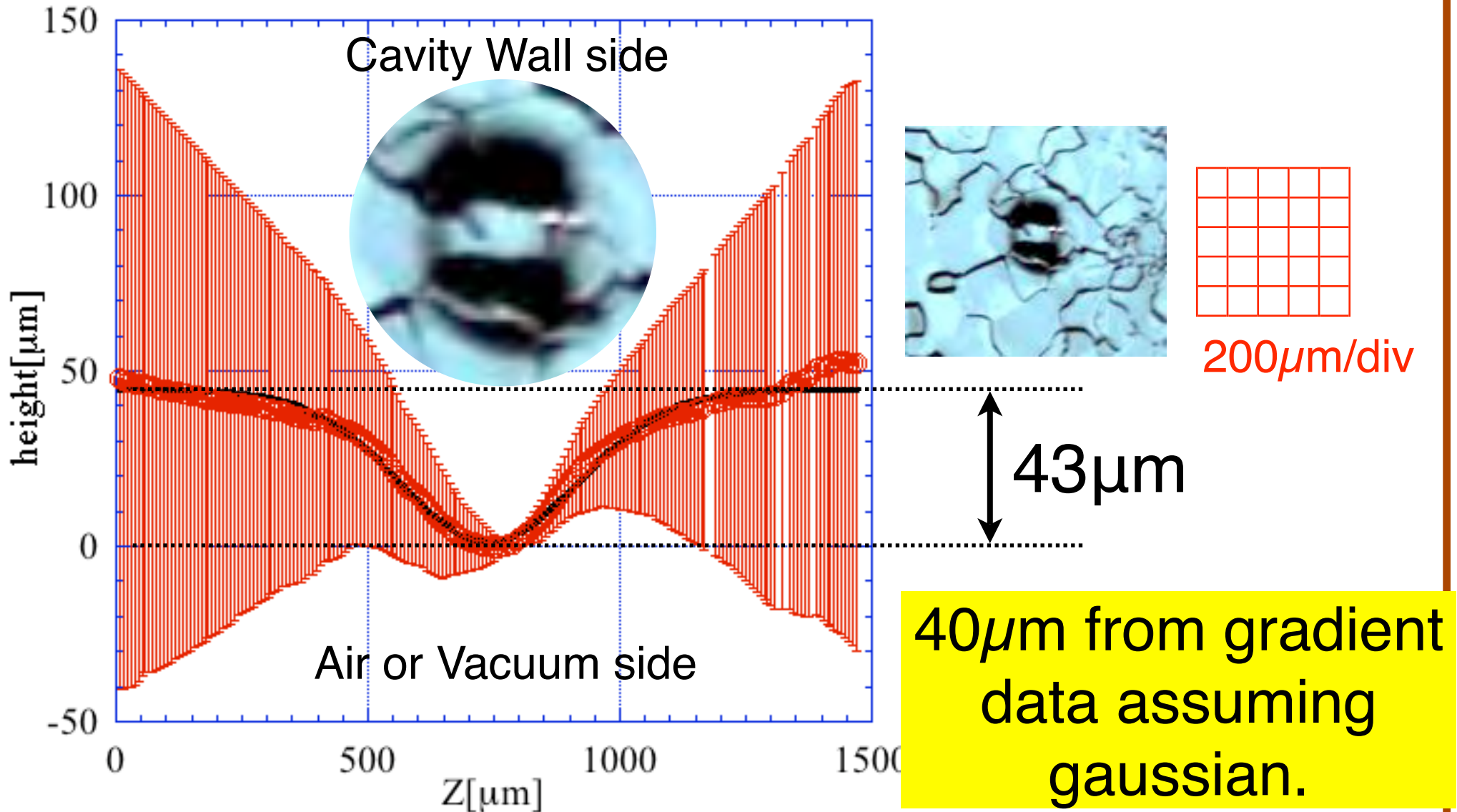
Wall Gradient of spot at #3 cell 181°



200μm/div

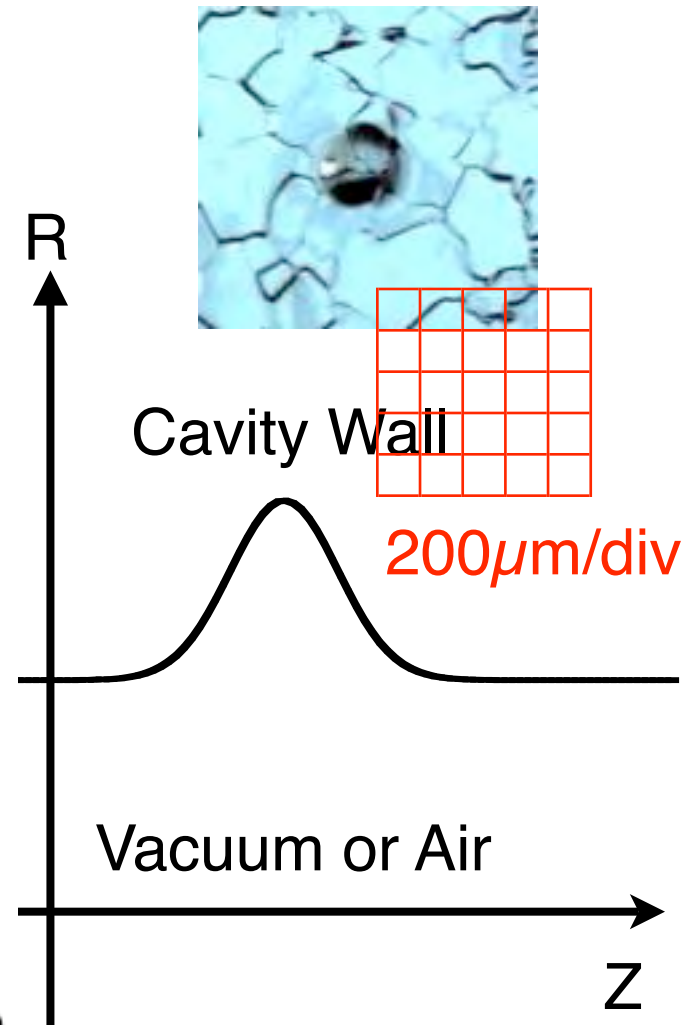
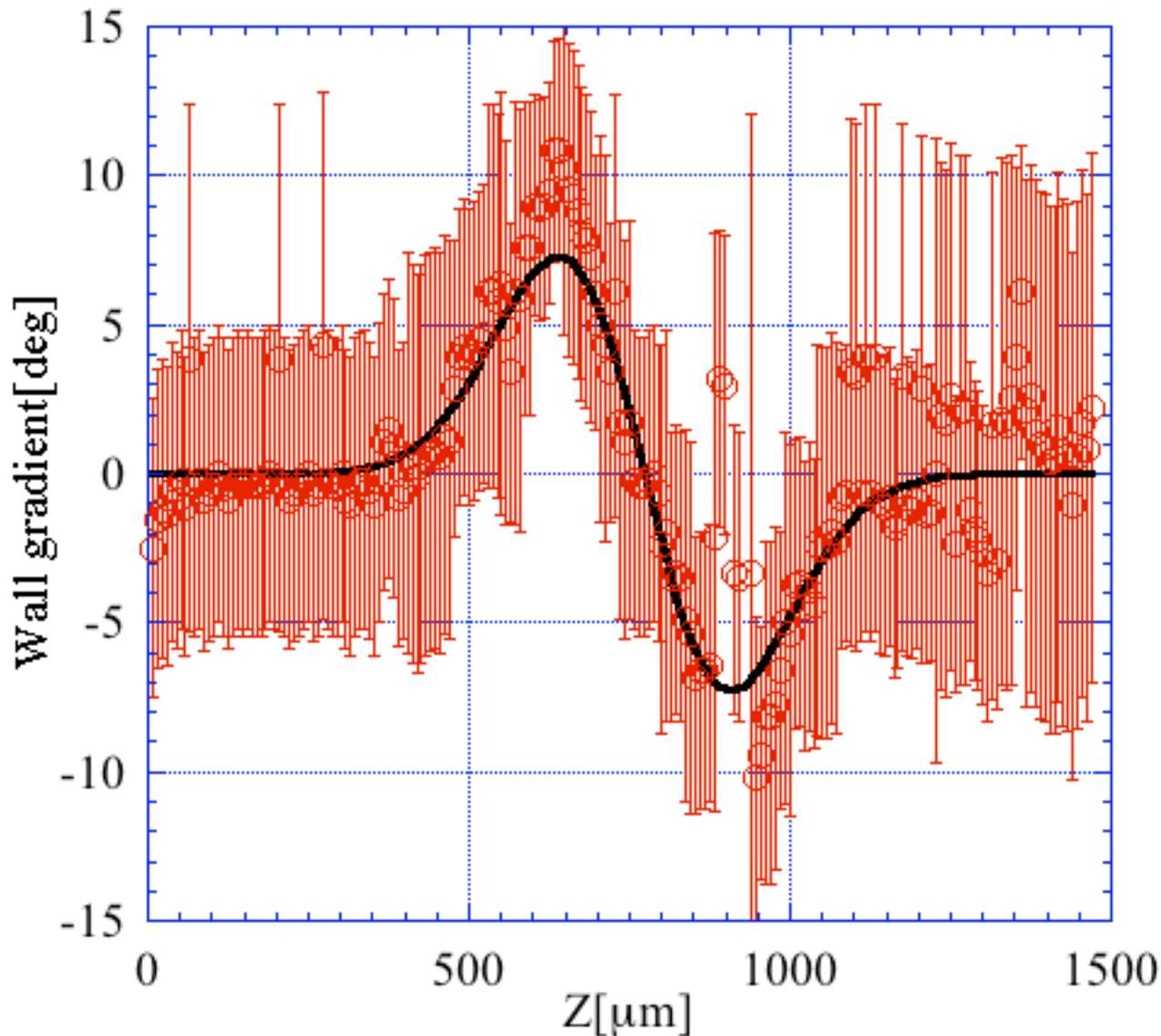
- This data shows that the spot is a convex(ball).
- Because of the continuity of the measured gradient, we can integrate the gradient to estimate the height of the spot.

Height of spot at #3 cell 181°



Black curve is a fitted gaussian.

Wall Gradient of spot at #7 cell 325°

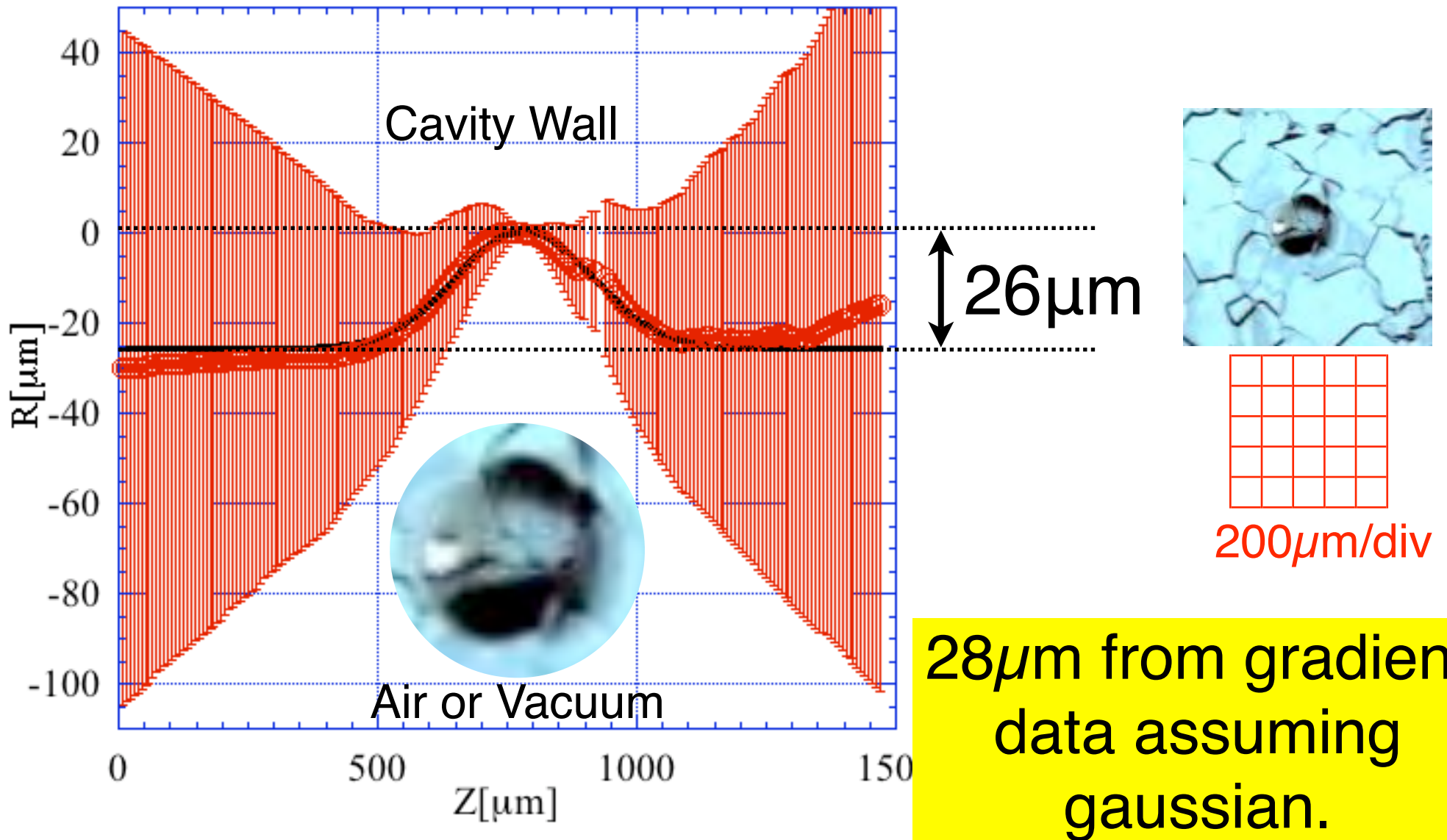


Left: Measured gradients and a fitted differential gaussian.

Right: Schematic drawing of the integral of the fitted curve in the left.

This data shows that the spot is a concave(pit).

Height of spot at #7 cell 325deg



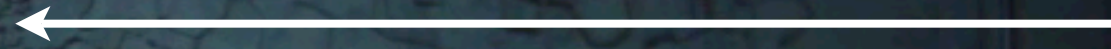
Black curve is a fitted gaussian.

Observation of AES001

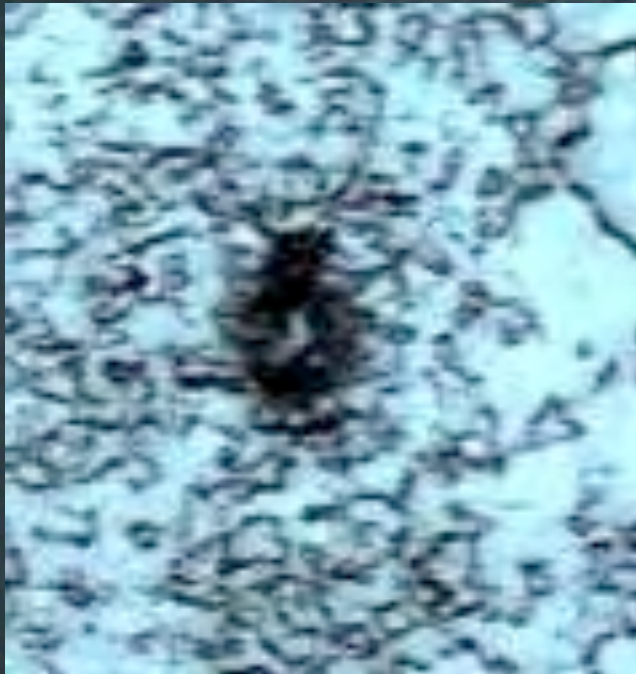
- Mainly the equator and the iris regions of all the cells were observed.(about 30mm width)
- Three spots in the equator region of #3 cell were found.
- One spot in the equator region of #7 cell were found.
- These two results seems to be correlated with the pass-band mode measurements.
- The azimuthal positions of the three spots found in #3 cell were 168, 169 and 181deg:
- This result seems to be correlated with the result of CERNOX measurements. (We think that in the CERNOX measurements, the first two spots were observed as one hot spot, because of the position resolution.)

Appendix

AES001 #1 cell 252°



EBW seam



stain?



to Equator
and #2 cell

The result of SI measurements
shows that this spot is flat.

1mm



Appendix

AES001 #2-3 iris 212°

back side of EL

to Equator
of #3 cell

← iris →

←
to Equator
of #2 cell

↗
arc scar?

back side of EL



The result of SI measurements shows that this spot is flat. This spots looks like a sign of Field Emission or Arcing. Many spots like this were observed.

1mm ←→

Appendix

AES001 #4-5 iris 233°

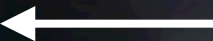


back side of EL

back side of EL

bright belt

to Equator
of #4 cell



to Equator
of #5 cell



All the Iris regions are **yellowish**.
This spot is locally bright.
It may be caused by EP?

1mm



Appendix

AES001 #4-5 iris 136°

iris



back side of EL

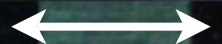
back side of EL

← to Equator
of #4 cell

to Equator
of #5 cell →

Dropped coffee
smear?

1mm



Appendix

AES001 #7-8 iris 279°



← to Equator
of #7 cell

scar?

Dropped
coffee
smear?

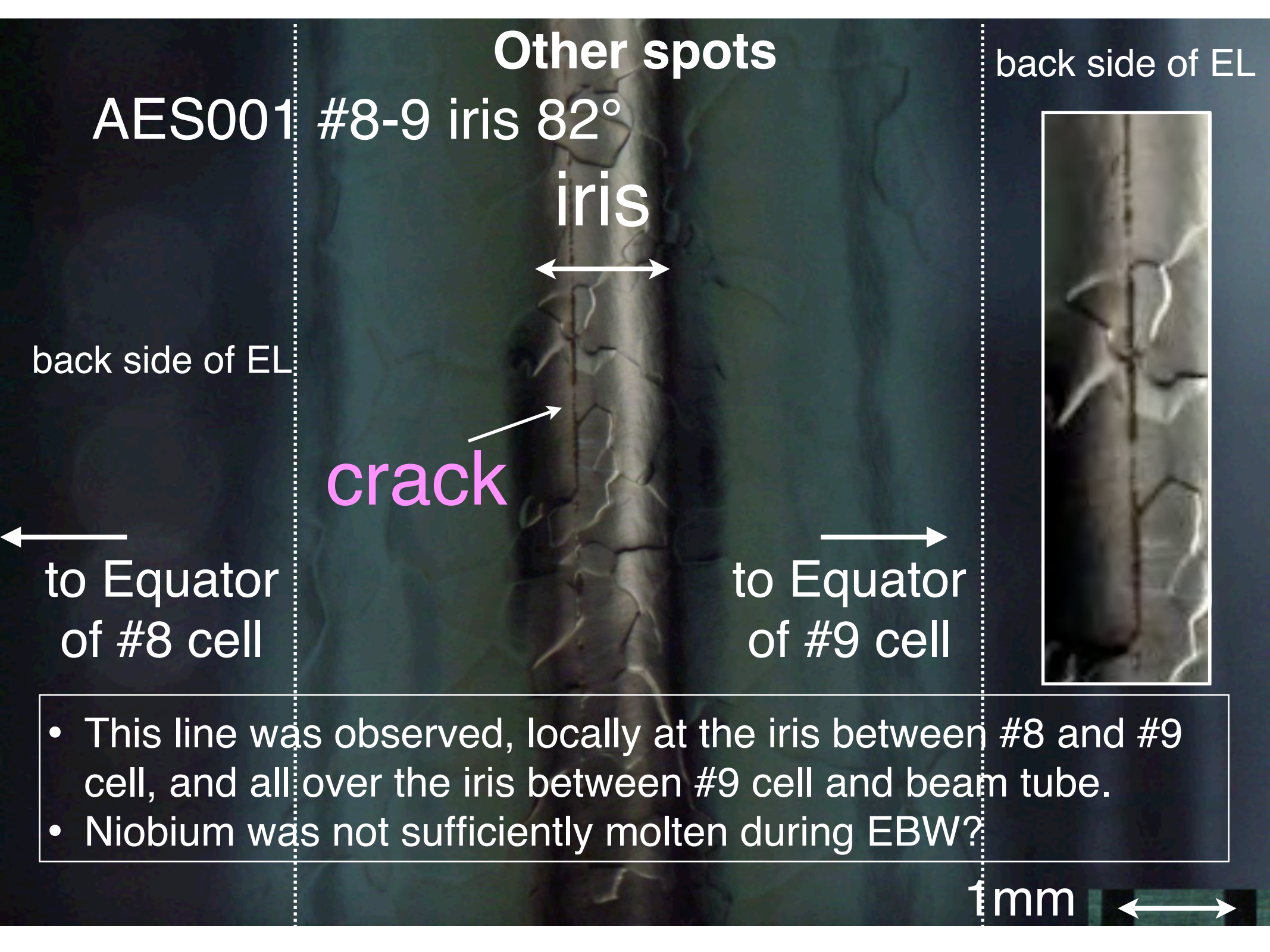
→ to Equator
of #8 cell

back side of EL

back side of EL

iris
↔

1mm ↔



AES001

#8-9 iris 82°

Other spots

back side of EL

iris

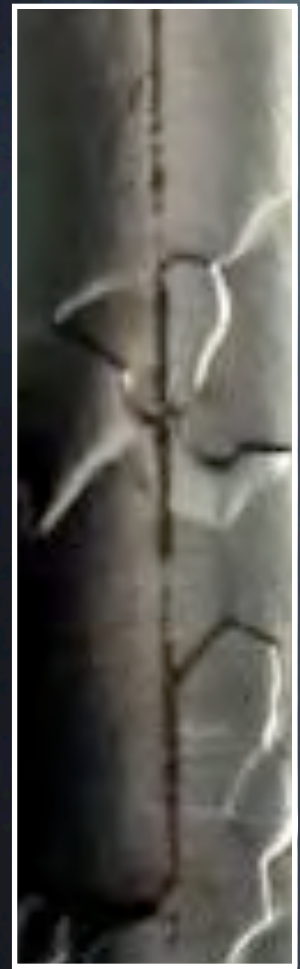


crack



to Equator of #8 cell

to Equator of #9 cell



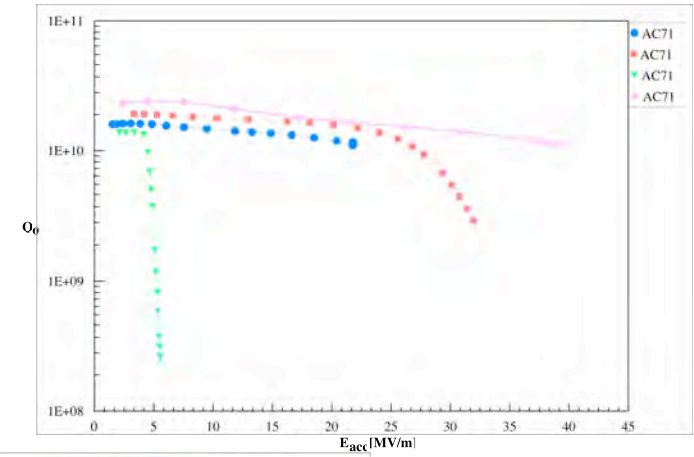
- This line was observed, locally at the iris between #8 and #9 cell, and all over the iris between #9 cell and beam tube.
- Niobium was not sufficiently molten during EBW?

1mm

DESY cavities
(AC71, AC74, AC80)
surface inspection

Preliminary preview!

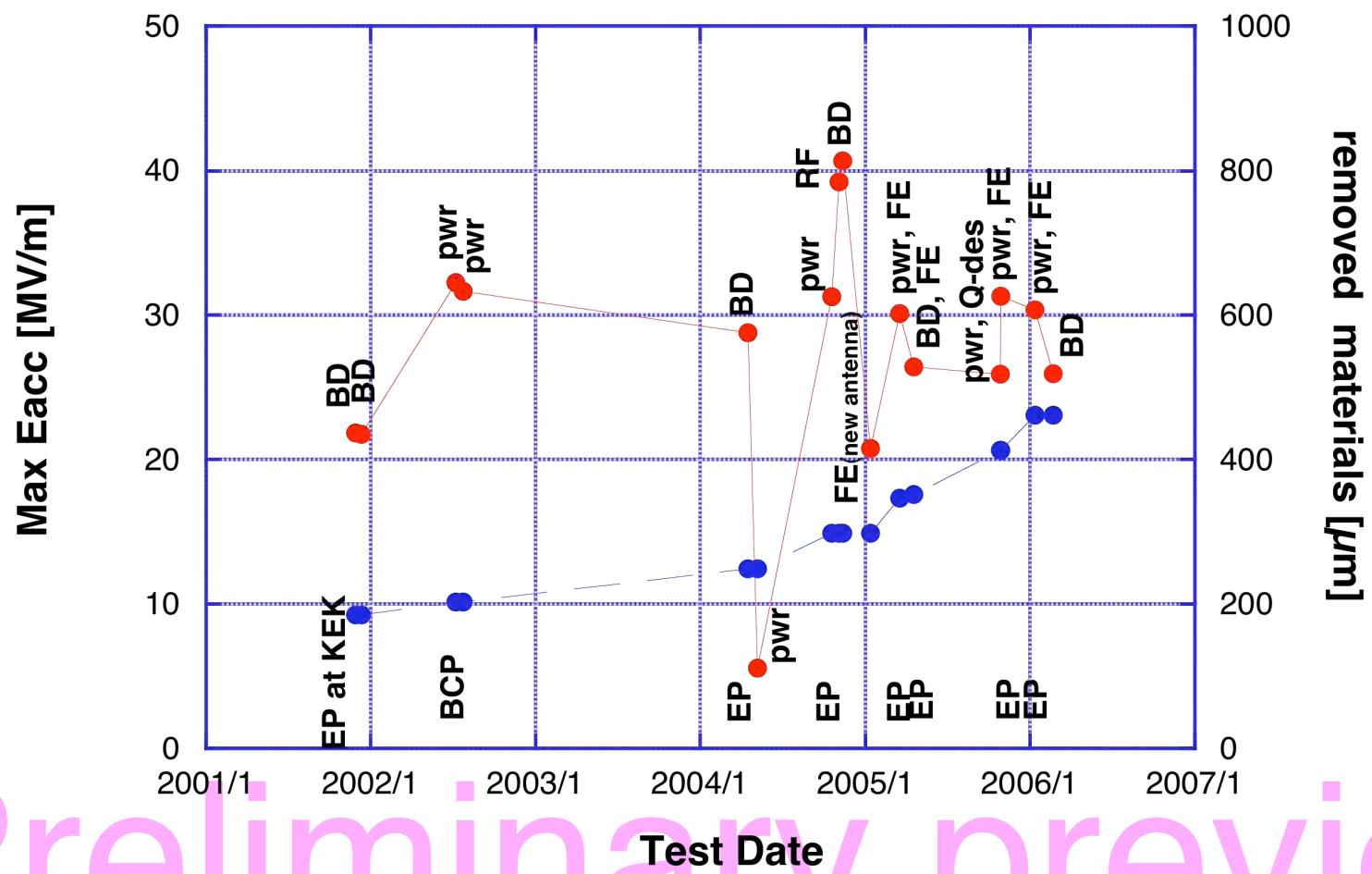
AC71



● Max Eacc [MV/m]

● removed materials [μm]

AC71



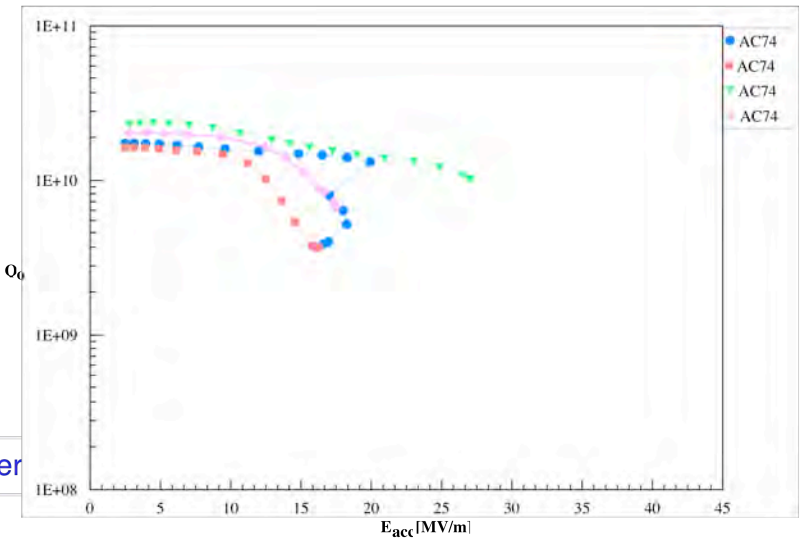
Preliminary preview!

AC71

RF trouble, FE etc. after 40MV/m
no significant mark in the cavity!

Preliminary preview!

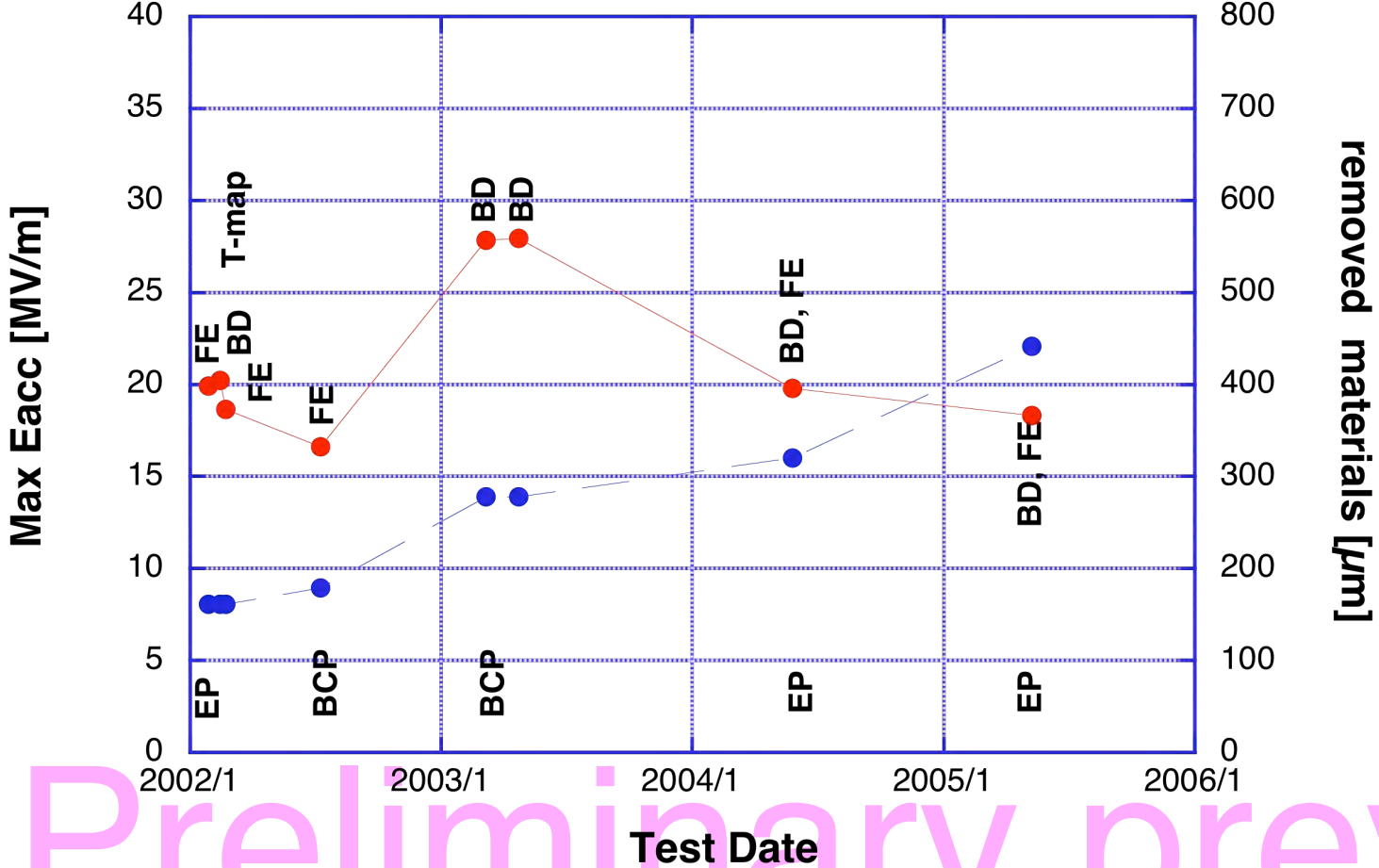
AC74



● Max Eacc [MV/m]

● removed mater

AC74



Preliminary preview!

AC#74

Field Emission

Found many small pits on Iris

T-map indicate;

Found small balls

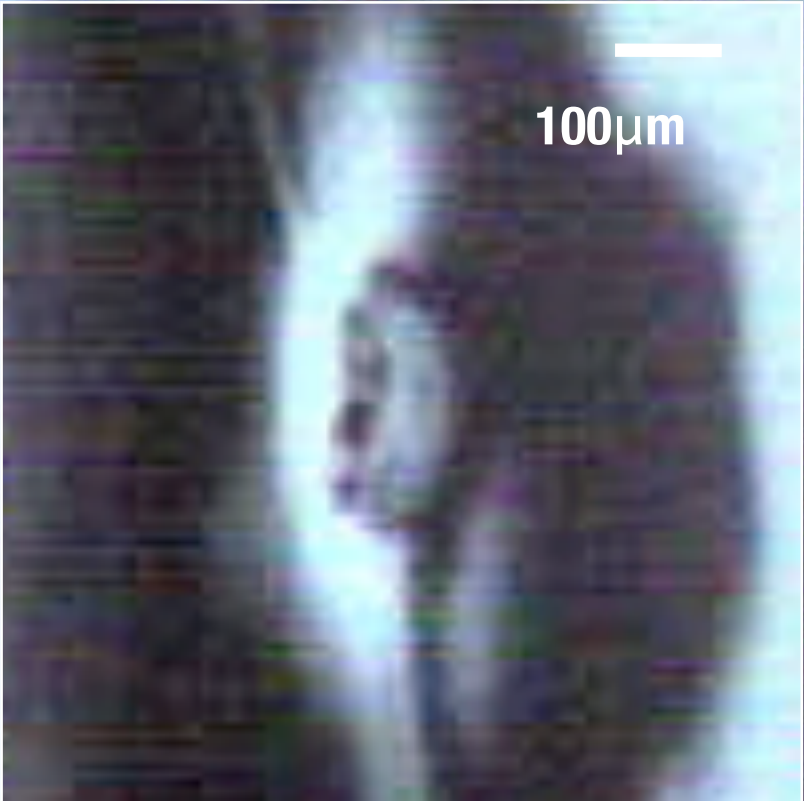
hot spot at cell#4 near Iris,
at cell #2 between Iris & Equator

Nothing Found

Preliminary preview!

AC74: hot spot1 95°

Cell #4



1mm



AC74: hot spot2 141°

Cell #4



1mm



Spot location

#3 ←

Cell #4

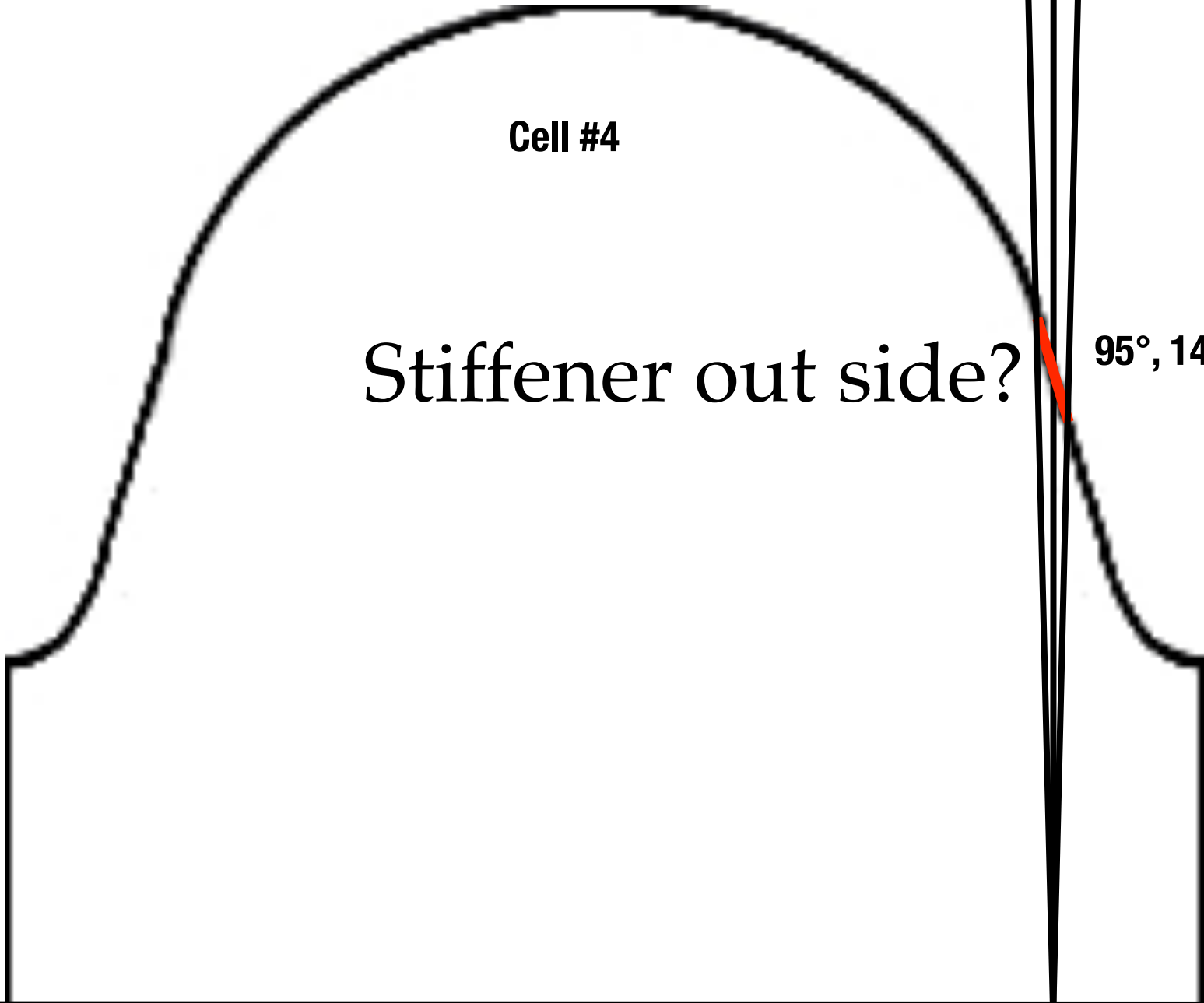
→ #5

Stiffener out side?

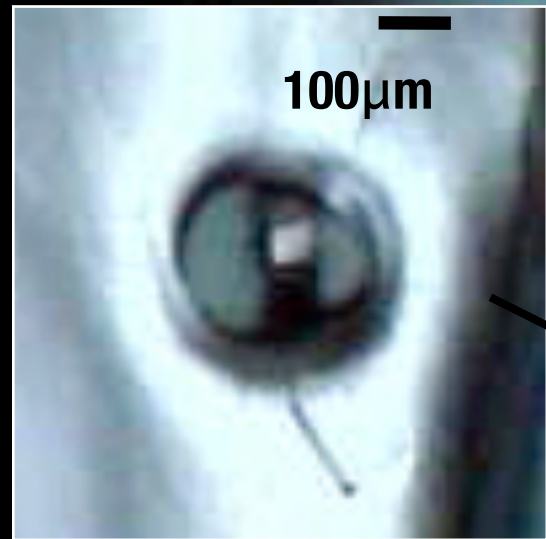
95°, 141°

*No mark on Cell#1-2

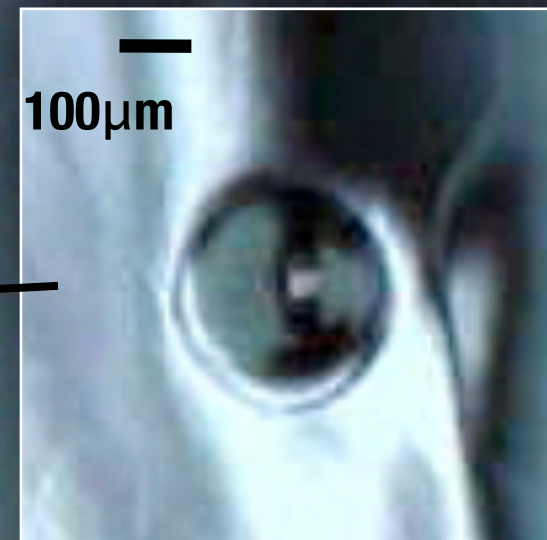
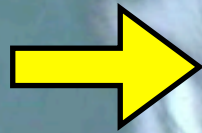
Preliminary preview!



AC74: iris between cell#1 and #2



$\theta=296^\circ$



$\theta=298^\circ$



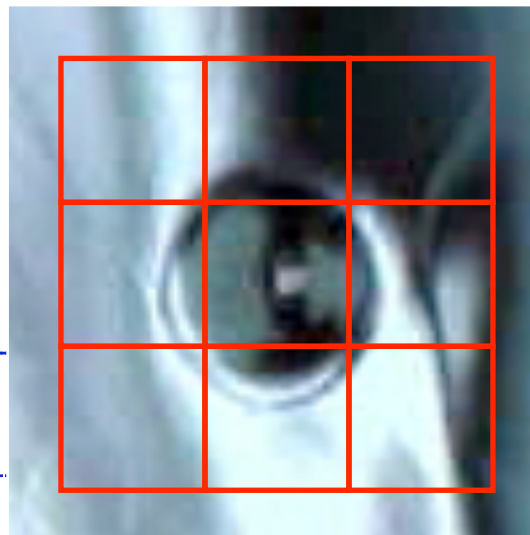
$\theta=302^\circ$



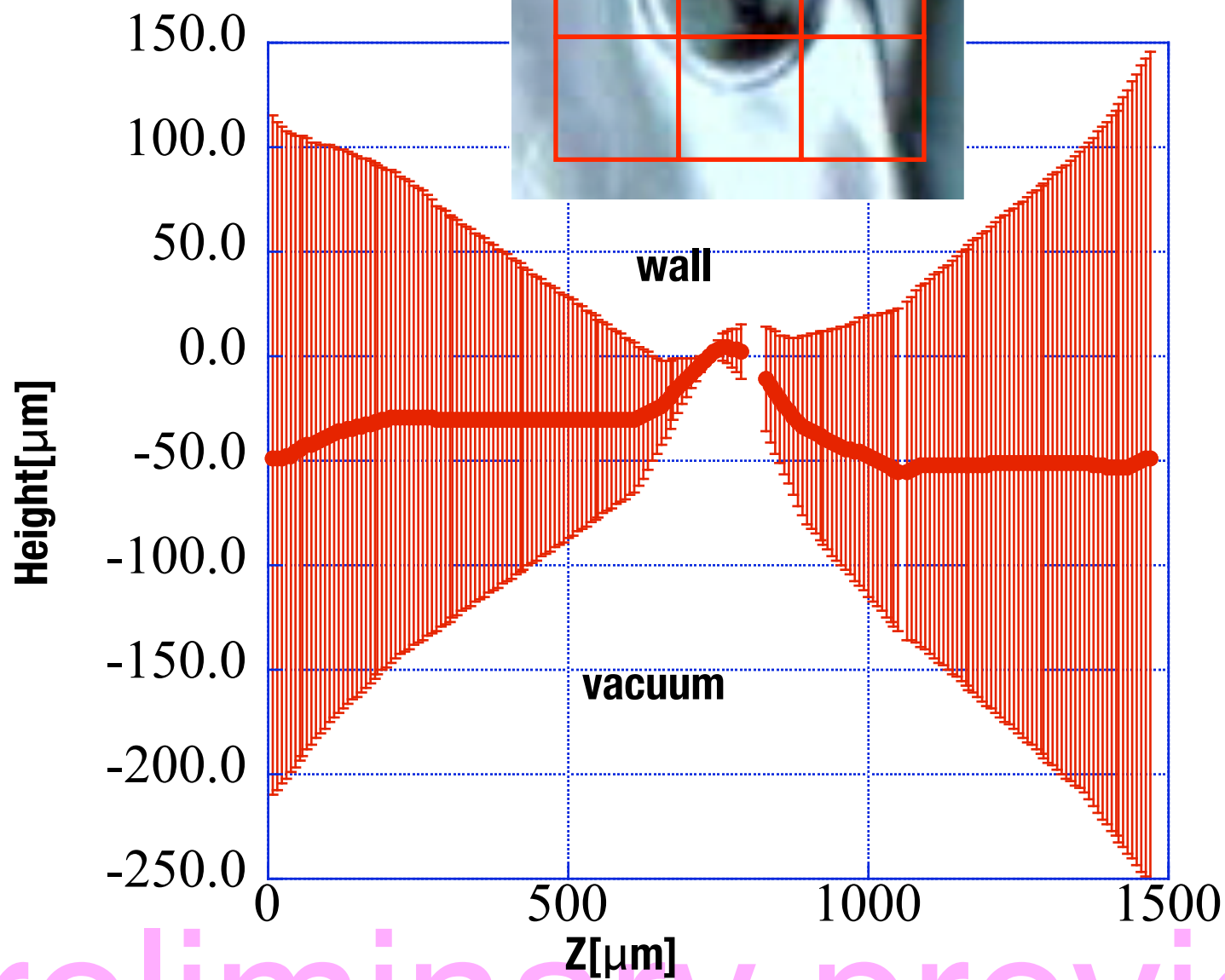
1mm

A white scale bar located in the bottom right corner of the main image.

AC74: iris#1-2, 296°

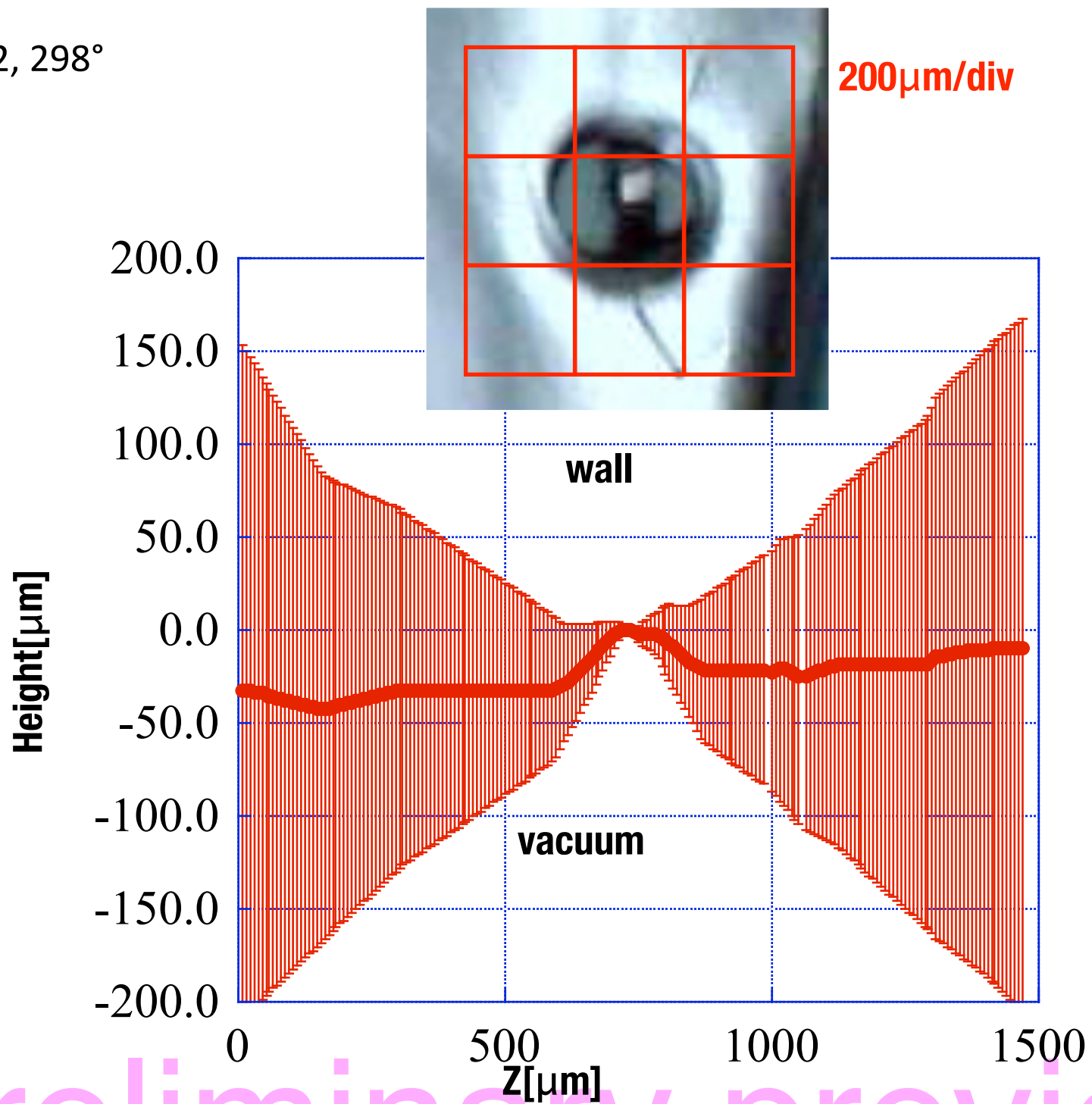


200μm/div



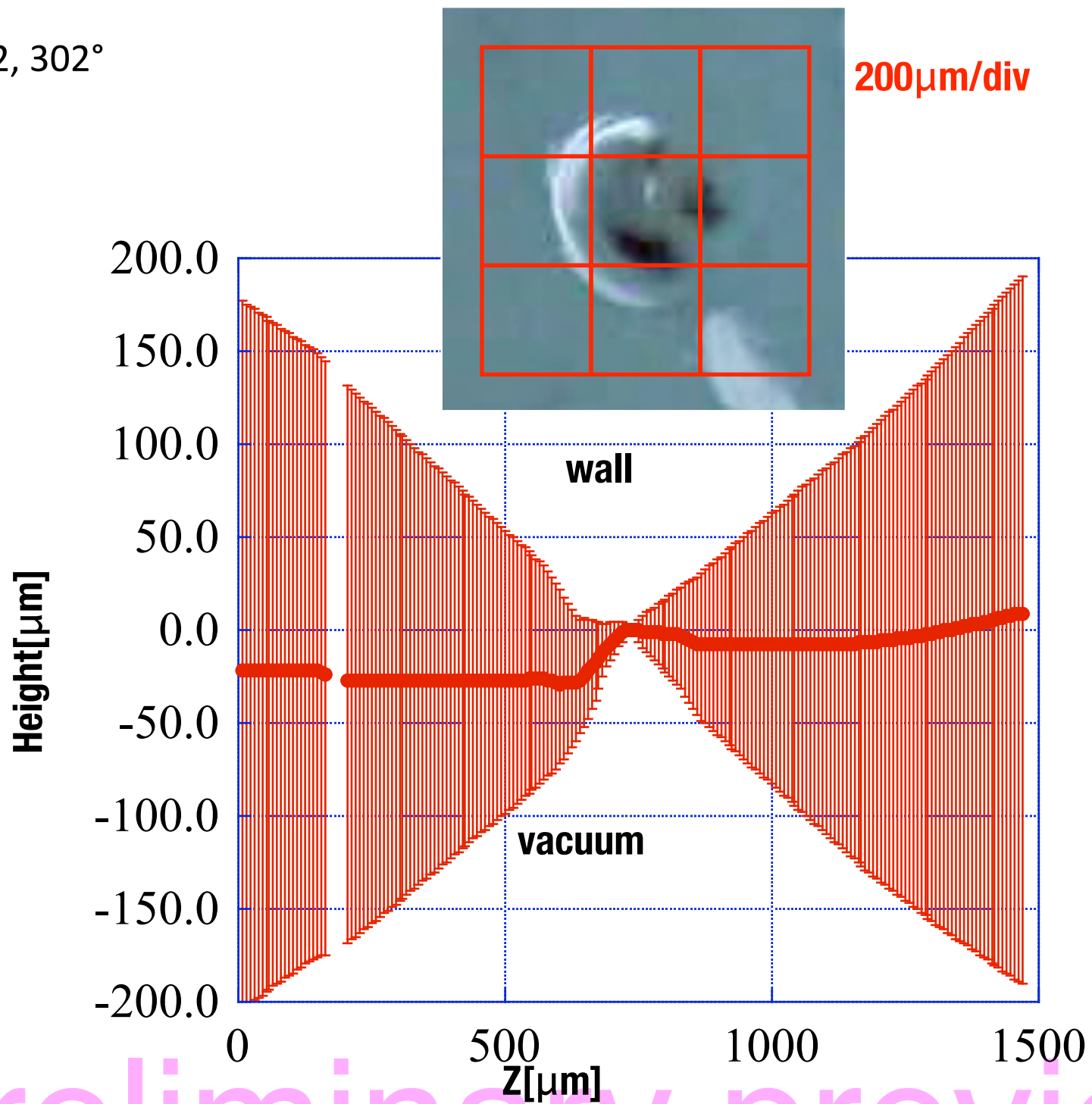
Preliminary preview!

AC74: iris#1-2, 298°



Preliminary preview!

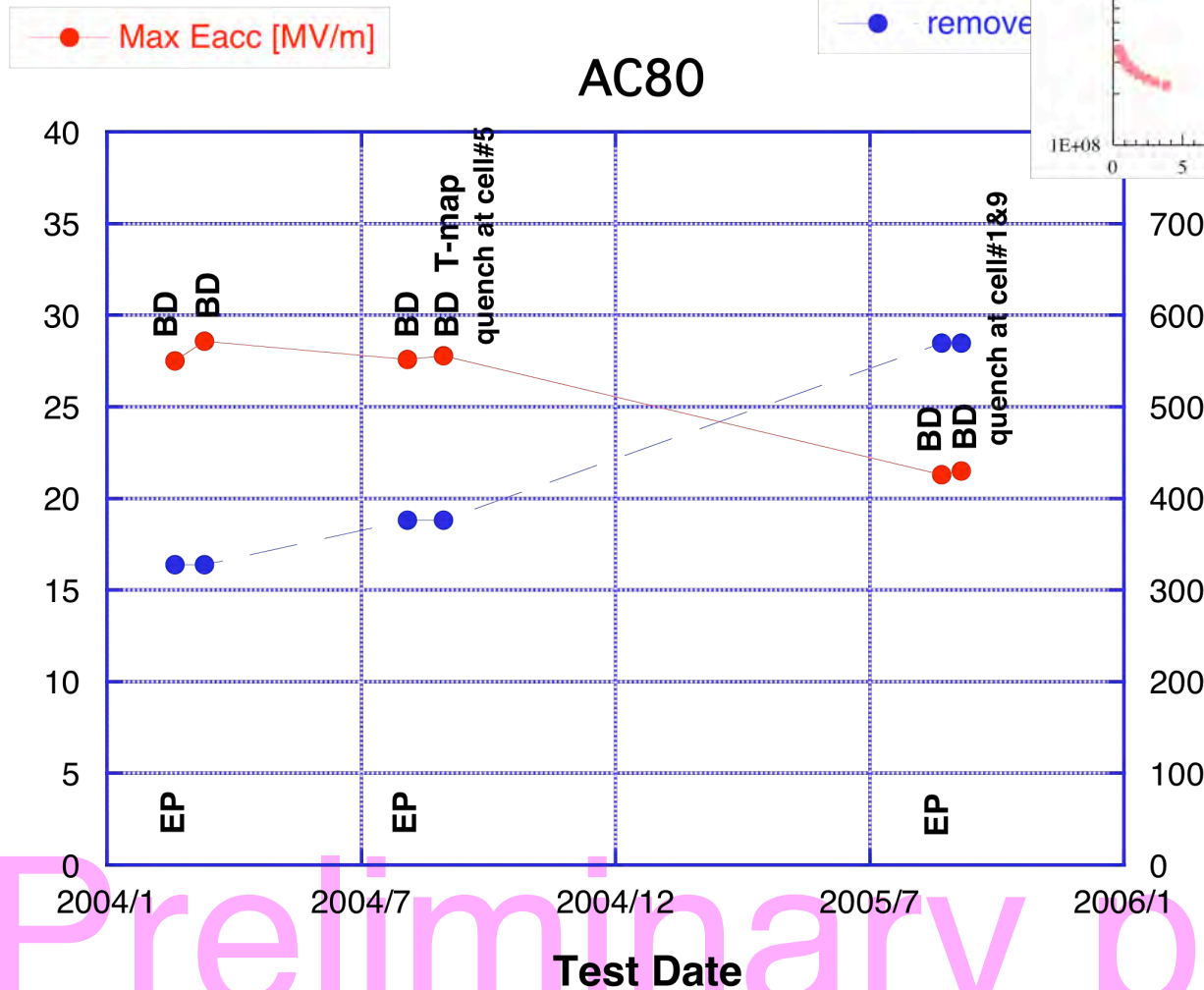
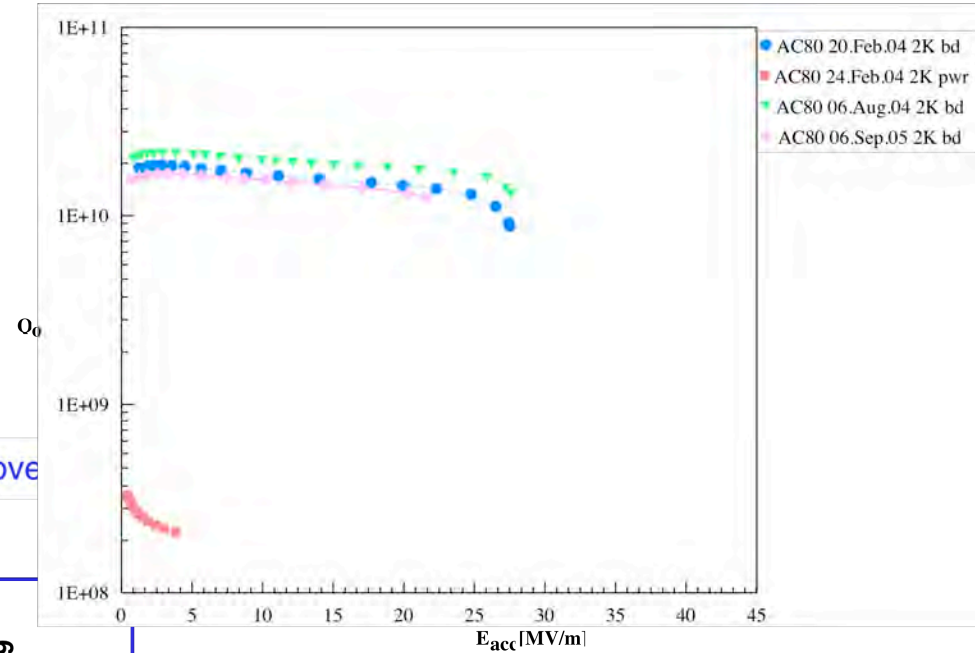
AC74: iris#1-2, 302°



Preliminary preview!

AC80

Vertical Test Results



Preliminary preview!

AC#80

Quench at cell #5, cell #1 or 9

T-map indicate;
hot spot at cell#5 equator



Found small pits, however not match to T-map
Need check again.

Preliminary preview!

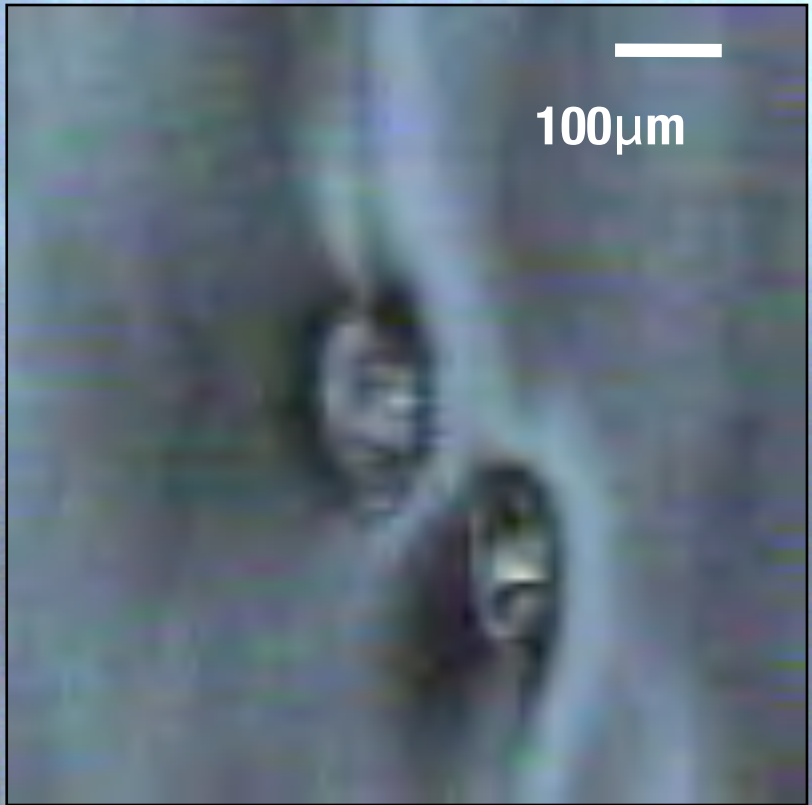
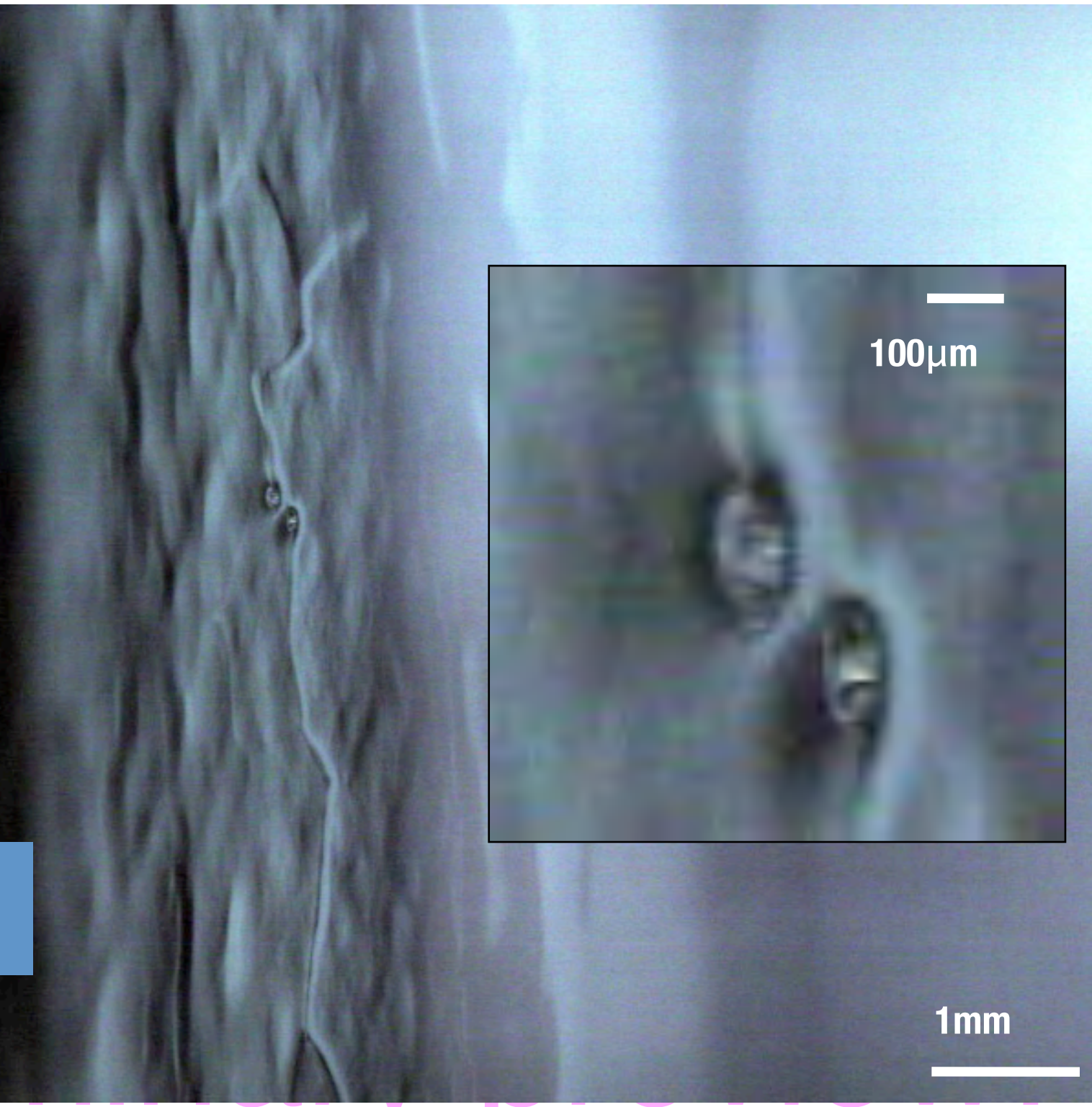
AC80: bubble sign@equator

Bubble sign exist on cell #1,2,3 equator.
Reduce it for #4,5,6..., Nothing in cell
#9. .

1mm



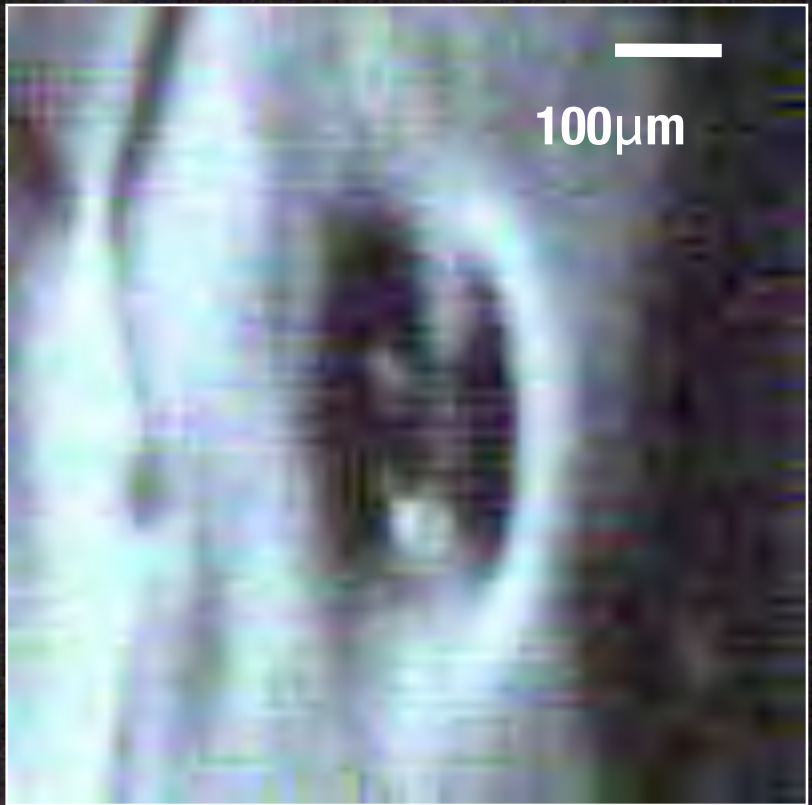
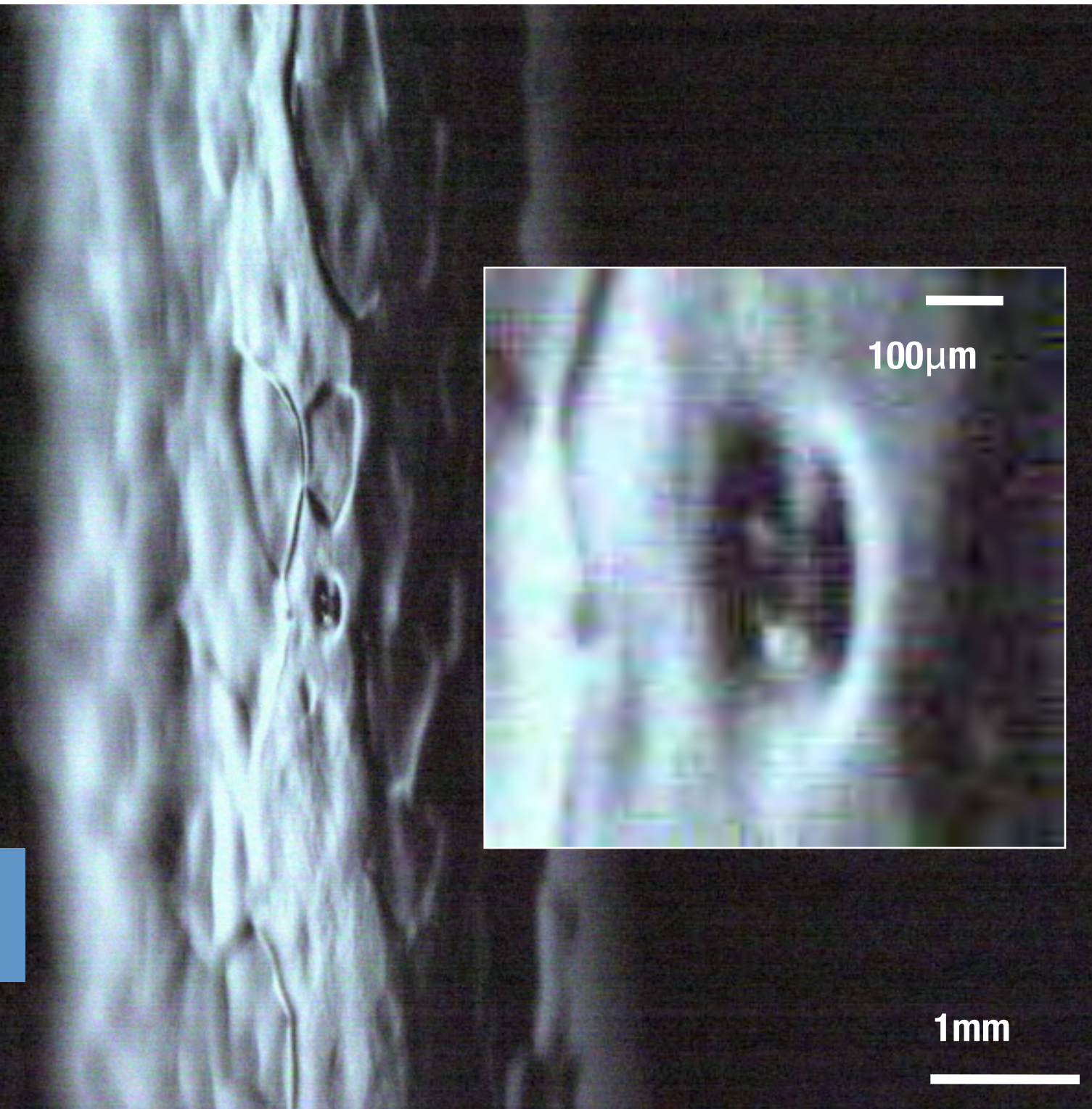
AC80: hot spot1



Cell #5.

1mm

AC80: hot spot2



Cell #5.

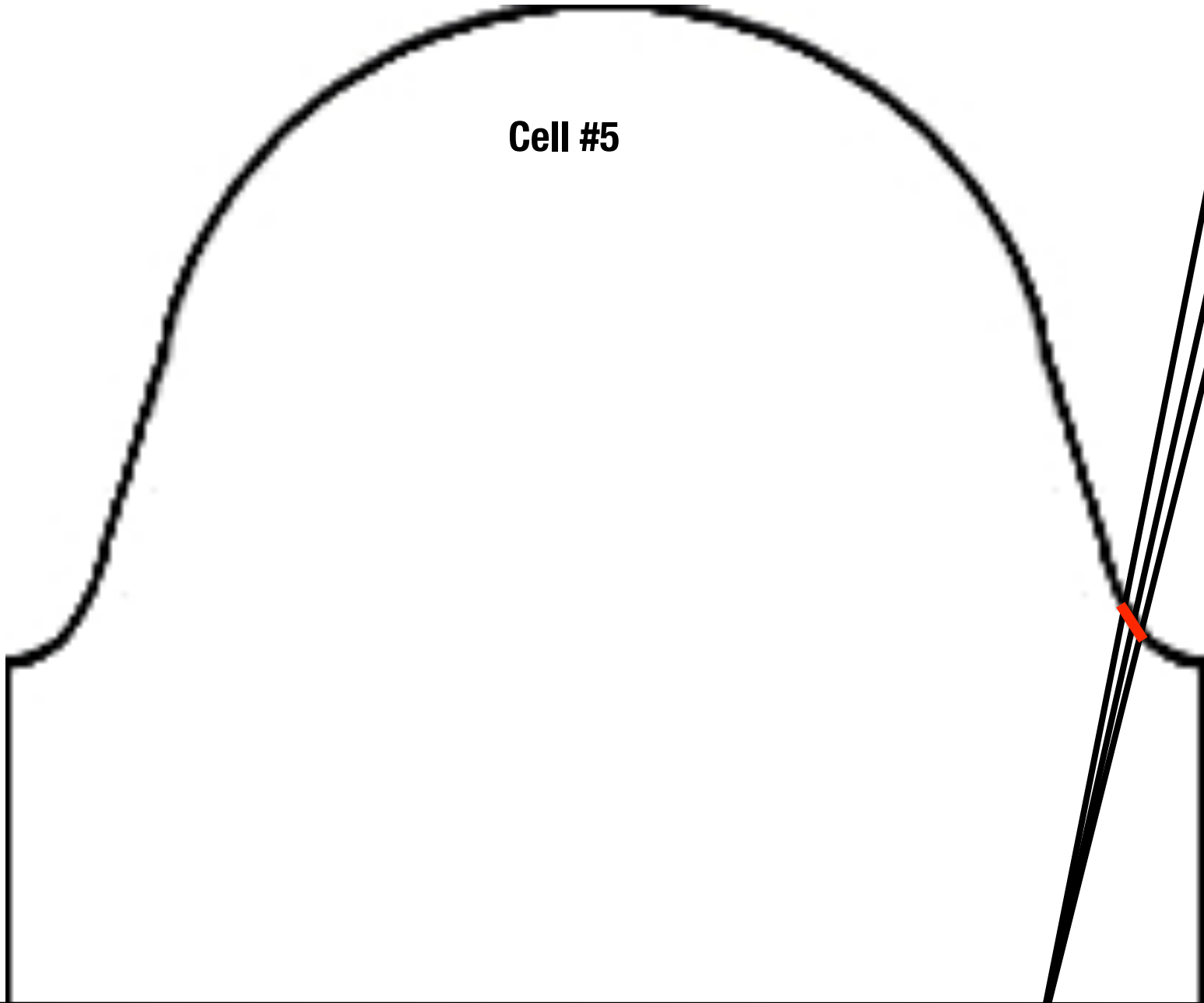
Spot location

#4 ←

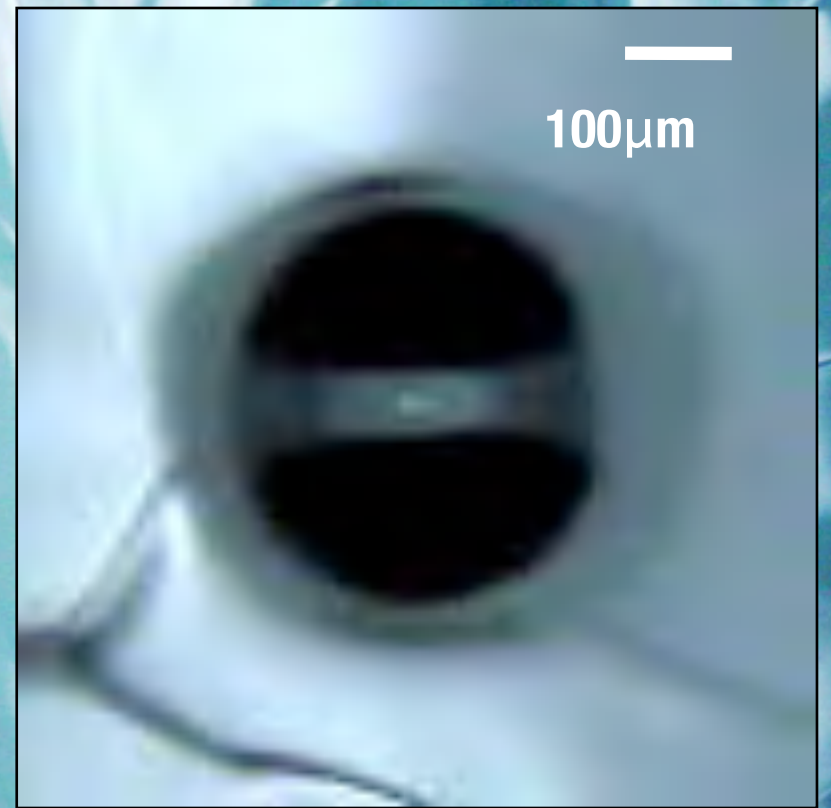
Cell #5

→ #6

Preliminary preview!



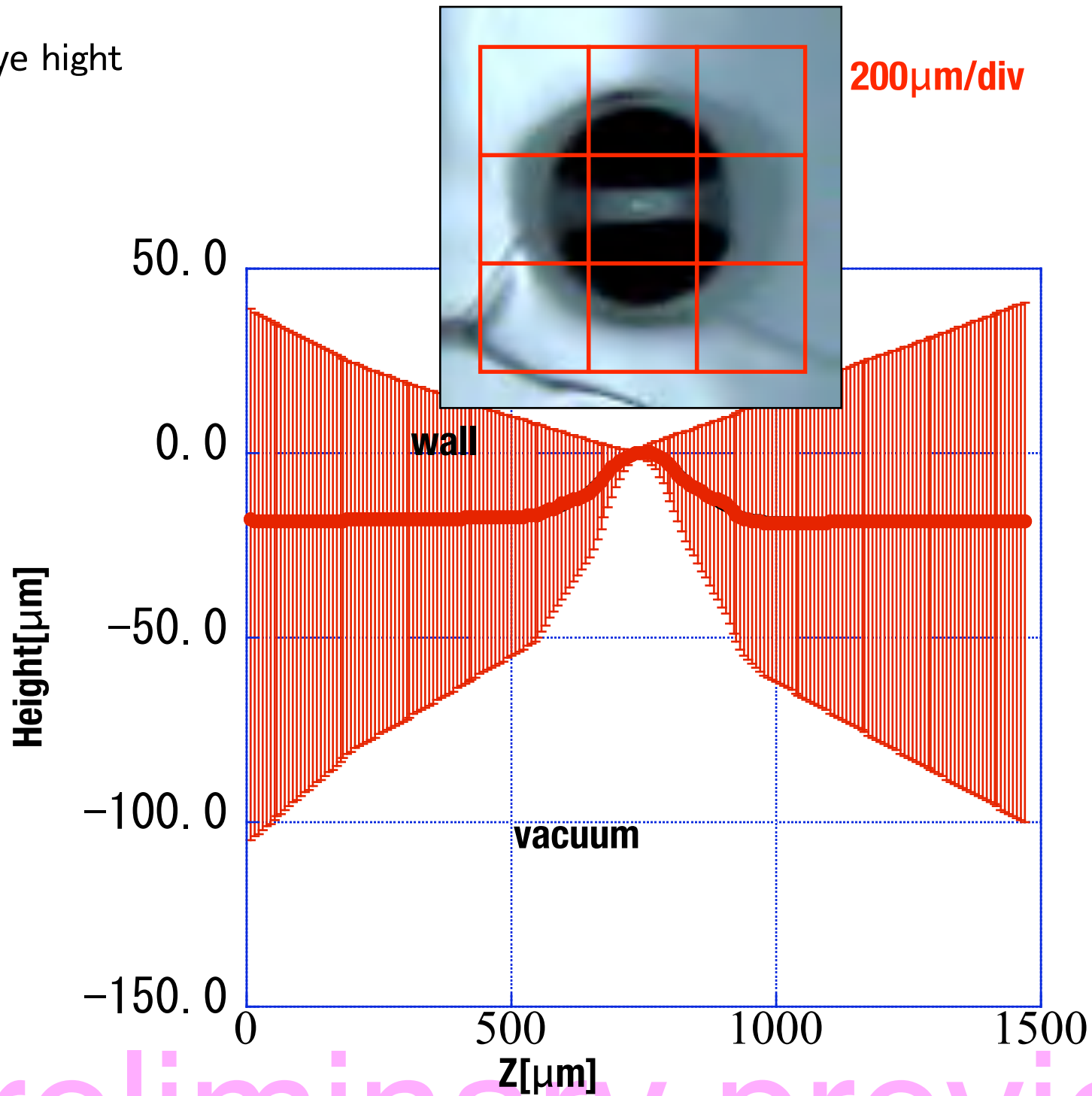
AC80: cat's eye
@cell#5_equator



This does not match to T-map hot spot. Need to check again.

1mm

AC80: cat's eye hight



Preliminary preview!

Summary

- I. Z84 had 28 spots with more than $100\mu\text{m}$ radii; they were all input coupler side.
- II. The resolution of $7.4\mu\text{m}$ is achieved; it is limited by the working distance of the lens.
- III. AES1 had four spots; their locations agree with the results from passband mode and thermometry measurements.
- IV. The wall height/depth can be estimated by integrating the measured gradient.
- V. Preview of DESY cavities (AC71,74,80)